AD-A079 856 AIR FORCE INST OF TECH WRIGHT-PATTERSON AFB OH SCHOO--ETC F/G 20/4
THE PREDICTION OF MASS LOADED NATURAL FREQUENCIES AND FORCED RE--ETC(U)
DEC 79 L B GLENESK
UNCLASSIFIED AFIT/GAE/AA/79D-5 NL

1 OF 2
AD A079856

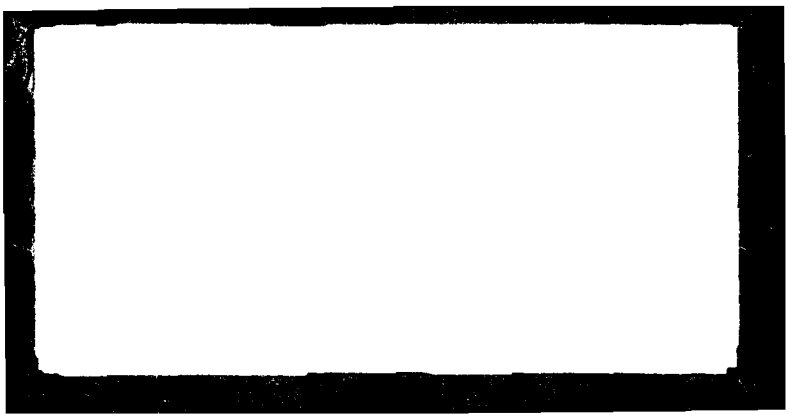

Graduate Thesis

(10) Larry Blake Glenesk

THE PREDICTION OF MASS LOADED NATURAL FREQUENCIES AND FORCED RESPONSE OF COMPLEX, RIB-STIFFENED STRUCTURES.

THESIS

AFIT/GAE/AA/79D-5

Larry B. Glenesk
Captain, CAF

(11) Dec 79

(12) 147

AFIT/GAE/AA/79D-5

THE PREDICATION OF MASS LOADED NATURAL FREQUENCIES AND FORCED RESPONSE OF COMPLEX, RIB-STIFFENED STRUCTURES

THESIS

Presented to the Faculty of the School of Engineering

of the Air Force Institute of Technology

Air University

in Partial Fulfillment of the

Requirements for the Degree of

Master of Science

by

Larry B. Glenesk, B.S.E.E.

Captain CAF

Graduate Aeronautical Engineering

December 1979

Approved for Public Release; Distribution Unlimited.

Acknowledgements

An individual faced with the task of conducting an independent study, cannot hope to bring it to a successful completion (conclusion) without the aid and guidance of his thesis advisor, and the numerous others involved during the course of the study. It is with this thought in mind that I wish to express my gratitude to Capt. Wayne Whaley my thesis sponsor for his time and effort throughout the study. I also sincerely thank Mr. Charlie Thomas for the use of the test facilities of the Air Force Flight Dynamics Laboratory, Mr. Dick Talmadge for his guidance and expertise both in setting up the test systems and during the latter phases of the study, and Mr. Dansen Brown for his time spent digitizing and processing data. Finally, I wish to extend my thanks to the numerous technicians at the Air Force Flight Dynamics Laboratory for their aid in acquisition, calibration, and trouble-shooting all the required experimental apparatus.

Table of Contents

List of Figures

List of Tables

List of Symbols

Symbol	Definition
A_n	Stable average after n inputs
a	Plate width
b	Plate length
E	Young's modulus
E{}	Expected value - ensemble average
$H(\omega)$	System transfer function
h	Plate thickness
I_n	n^{th} input
K_i	Generalized stiffness
M_i	Generalized mass
M_o	Added lumped mass
n	Number of inputs (n = 1,2,...15)
Q_i	Generalized force
q_i	Generalized coordinates
R_x	Radius of gyration about x-axis
R_y	Radius of gyration about y-axis
$R_{xy}(\tau)$	Cross correlation
$S_{rr}(\omega)$	Auto power spectrum
$S_{yr}(\omega)$	Cross power spectrum
T	Kinetic energy
V	Strain energy
X_o	x coordinate of the added mass

Symbol	Definition
Y_o	y coordinate of the added mass
υ	Poisson's ratio
ϕ	Mode shape
ρ	Plate mass density
ω_i	Natural frequencies

Abstract

An experimental investigation was conducted to determine the validity of an algorithm developed by Whaley (Ref 14) to approximate the natural frequencies of a complex structure under arbitrary mass loading conditions, when only the unloaded natural frequency and mode shape data is known. The chosen test specimen was a curved, rib-stiffened panel from a C-141 Starlifter, aircraft. The panel was suspended from the ceiling by bungy cords and tested in an unloaded configuration and nine separate mass loaded configurations. Then using only unloaded data the generalized mass and generalized stiffness for each mass loaded configuration were computed, and the natural frequencies for each configuration were computationally predicted using the aforementioned algorithm. The theoretical and experimental results were then compared to determine the amount of error incurred in the approximation technique. The theory of how to ultimately determine the overall forced response of the specimen was discussed and an error model was developed to enable an examination of the reliability of the algorithm in predicting forced response. Recommendations concerning future test procedures, areas requiring further study, and the use of the algorithm were made.

THE PREDICTION OF MASS LOADED NATURAL FREQUENCIES AND FORCED RESPONSE OF COMPLEX, RIB-STIFFENED STRUCTURES

I Introduction

Background

The thrust of this study is aimed at the ever-increasing need for better performance in the field of vibration control methods for airborne electro-optical systems. In order to yield acceptable performance levels in such a scheme, the designer must be provided with an accurate description of the vibration characteristics of the airframe. Also, these vibration characteristics may change markedly due to the additional mass of the electro-optical system. This, due to the sensitivity of the electro-optical system to airframe vibration disturbances, may cause serious degradation of system accuracy. Therefore, one would also like to be able to predict how the vibration characteristics are altered due to arbitrary mass loading conditions. In an effort to make this possible, several approximate methods for prediction of the modified characteristics have been developed. Some of these are discussed later in this chapter. The method considered in this study was developed by Whaley (Ref 14). The algorithm he developed will be derived later in this study. It allows a designer, given the unloaded natural frequencies and mode shapes of a particular structure, to predict the change in the natural frequencies due to any arbitrary mass loading conditions. Tests have been conducted on a cantilevered uniform flat plate to determine the validity of the algorithm, Henderson (Ref 3). Favorable results were realized, as the first eight (8) modes for eleven (11) mass loading configurations were predicted to within a small margin of error for

virtually every case. All but nine cases yielded errors of less than 10%, and those other nine were all less than 20%. Whaley (Ref 14).

Purpose

Even though this technique has proven itself acceptable in the cases of beams and flat plates, further validation is required in the specific area of built-up aircraft structures. Since this methodology was originally developed with these types of structures in mind, it is necessary to determine whether this theory holds valid for a structure of much greater complexity than those previously tested, one typical of what can be found on today's aircraft. For this purpose, a curved, rib-stiffened panel from a cargo aircraft was selected for experimental validation. The structure has two longitudinal stiffeners, and five lateral stiffeners. A complete modal survey was conducted to determine the first several natural frequencies and their respective mode shapes. The selected number of modes to be included in the analysis will be discussed in Chapter II along with the reasons for chosing it. The modal analysis will be done for the panel in its unloaded configuration, and nine separate mass loaded configurations.

Following completion of the above experimental testing, the unloaded modal data was utilized in the algorithm to predict the natural frequencies for each mass loading configuration. The experimentally determined values will then be compared to the predicted ones to find the percent error, and ultimately the validity of the algorithm. After it was determined that these results were favorable, the system forced response was evaluated for each mass loaded configuration. These will then be compared to the experimentally determined values, to ultimately discover the accuracy of this prediction method when it is applied

to complex structures.

Previous Mass Loading Techniques

There presently exist a number of techniques for modeling various types of structures with an added mass load. Several of these are discussed briefly by Whaley (Ref 14). Those most closely related to the technique used in this study, are that of Weissenburger (Ref 12), and Pomazal and Snyder (Ref 6). Weissenburger expresses the natural frequencies of the loaded structure in terms of those of the unloaded structure which results in the need for solving a transendental equation (in matrix form). Pomazal and Snyder basically employ Weissenburger's technique, but utilize a Newton-Raphson matrix interaction technique to solve for the modified eigenvalues. The technique utilized in this study differs in that the eigenvalue problem is posed in terms of measured, unmodified natural frequencies and mode shapes. The complexity of the problem is directly dependent on the desired number of natural frequencies and/or mode shapes.

II Background Theory

The derivation of the algorithm to be used in this study has been reported by Whaley (Ref 14) and is discussed in detail below. By expressing the response of a continuous structure in terms of its normal modes, it is possible to transform the governing partial differential equation for the structure into an infinite set of uncoupled ordinary different equations in terms of the generalized coordinates. Lagrange's equation is:

$$\frac{d}{dt}\frac{\partial T}{\partial q_i} + \frac{\partial V}{\partial q_i} = Q_i \tag{1}$$

for a flat plate:

$$T = \tfrac{1}{2}\int_0^b\int_0^a \rho h \left(\frac{\partial W}{\partial T}\right)^2 dxdy \tag{2}$$

$$V = \tfrac{1}{2}\int_0^b\int_0^a \frac{Eh^3}{12(1-\nu^2)}\left(\left(\frac{\partial^2 W}{\partial x^2}\right)^2 + \left(\frac{\partial^2 w}{\partial y^2}\right)^2 + 2\nu\frac{\partial^2 w}{\partial x^2}\frac{\partial^2 w}{\partial y^2} + 2(1-\nu)\left(\frac{\partial^2 w}{\partial x \partial y}\right)^2\right) dxdy \tag{3}$$

where:

$$W(x,y,t) = \sum_{i=1}^{\infty} \phi_i(x,y)\, q_i(t) \tag{4}$$

Define δP = Virtual work of applied inertial loads.

$$\delta P = F(x_o,y_o,t)\,\delta W(x_o,y_o,t) + M(x_o,y_o,t)\,\delta W(x_o,y_o,t)$$

Therefore the generalized force may be expressed as:

$$Q_i = \frac{\delta P}{\partial q_i} = -M_o\ \phi_i(x_o,y_o)\ \sum_{j=1}^{\infty}\phi_j(x_o,y_o)\ \frac{d^2q_i}{dt^2}$$

$$- M_o\ R_x^2\ \frac{\partial\phi_i}{\partial x}\ (x_o,y_o)\ \sum_{j=1}^{\infty}\ \frac{\partial\phi_j}{\partial x}(x_o,y_o)\ \frac{d^2q_j}{dt^2}$$

$$- M_o\ R_y^2\ \frac{\partial\phi_i}{\partial y}\ (x_o,y_o)\ \sum_{j=1}^{\infty}\ \frac{\partial\phi_j}{\partial y}\ (x_o,y_o)\ \frac{d^2q_j}{dt^2} \qquad (5)$$

Combining Eqs (1) through (5) yields an infinite set of equations, the i^{th} one of which will be:

$$M_i\ \ddot{q}_i + K_i\ q_i = Q_i \qquad (6)$$

where the following definitions hold:

$$\underline{\text{Generalized Mass}} = M_i = \int_o^b\int_o^a \rho h\ \phi_i^2\ (x,y)\ dxdy \qquad (7a)$$

$$\underline{\text{Generalized Stiffness}} = K_i = \int_o^b\int_o^a \{\frac{Eh^3}{12(1-\nu^2)}((\frac{\partial^2\phi_i}{\partial x^2})^2 + (\frac{\partial^2\phi_i}{\partial y^2})^2$$

$$+ 2\nu\ \frac{\partial^2\phi_i}{\partial x^2}\ \frac{\partial^2\phi_i}{\partial y^2} + 2(1-\nu)(\frac{\partial^2\phi_i}{\partial x\partial y})^2\ dxdy \qquad (7b)$$

Now, we can avoid the necessity of solving transcendental equations or using an extremely complex finite element modelling technique, if we can truncate our infinite set of Eqs (6) to a sufficiently small finite number. One can accomplish this by assuming that a reliable result can be achieved by considering only the first "n" modes. Then Eqs (6) can be written in matrix form as follows:

$$[A]\ \{\ddot{q}_i\} + [K]\ \{q\} = \{o\} \qquad (8)$$

where (K) is a diagonal matrix made up of the generalized stiffness elements determined from Eq (7b), and [A] is made up of the following elements:

$$Amm = Mm + Mo\ \phi^2_m(x_o,y_o) + Mo\ R_x^2\ \left(\frac{\partial \phi_m}{\partial x}\ (x_o,y_o)\right)^2 + Mo\ R_y{}^2\left(\frac{\partial \phi_m}{\partial y}(x_o,y_o)\right)^2 \tag{8a}$$

$$Amn = M_o\phi_m(x_o,y_o)\,\phi_n\ (x_o,y_o) + M_o\ R_x^2\ \left(\frac{\partial \phi_n}{\partial x}\ (x_o,y_o)\right) \tag{8b}$$

$$+ M_oR_y^2\ \left(\frac{\partial \phi_m}{\partial y}\ (x_o,y_o)\ \frac{\partial \phi_n}{\partial y}\ (x_o,y_o)\right)\ m \neq n$$

If one now assumes simple harmonic motion (i.e., $q = \hat{q}e^{iwt}$), and premultiplies Eq (8) by $[K]^{-1}$, a standard eigenvalue problem of dimensions n by n results:

$$\left\{\frac{1}{\omega^2}[I] - [K]^{-1}\ [A]\right\}\ \{\hat{q}\} = \{0\} \tag{9}$$

The frequency ω can be found by setting the determinant of the above matrix to zero.

Thus, one is faced with a problem which requires a great deal less computational effort than if it were necessary to derive a detailed model for the structure. For the complex structures that are typically found on aircraft, the various stiffeners, spars, ribs, and curved panels make a continuous model out of the question. Therefore, the most common approach to this type of structure has been to formulate a finite element model. The finite element analysis is, however, much more complex, requires a great deal more modelling and programming effort, and utilizes more expensive computer time than solving Eq (9) for the loaded frequencies.

In summary, to utilize this algorithm, one requires only knowledge

of the unloaded natural frequencies and mode shapes (descrete representations), and the magnitude, location and radii of gyration of the added mass.

III Experimental Procedure

Experimental testing was conducted to determine the natural frequencies and discrete mode shapes of the unloaded panel. These data were required by the prediction algorithm to approximate the loaded natural frequencies. The natural frequencies of the panel in each of its mass loaded configurations also had to be experimentally determined to enable comparison between the actual and predicted natural frequencies. In this manner, the validity of the algorithm for the chosen complex structure could be determined. All testing was conducted at the Air Force Flight Dynamics Laboratory (AFFDL). All equipment that was required is listed in Table 1. Due to problems in acquisition and processing of data which will be discussed below, three separate test methods were attempted. The third one of these was the only one to yield acceptable data. All three of these methods are discussed in this chapter in some detail. This is done with the goal of familiarizing the reader with the three methods, the aspects in which each did or did not fail, and the reasons for their respective failures or alternatively their successes. Armed with this knowledge, persons conducting future testing in this area will be able to avoid problems similar to those encountered by the author in the course of this study.

The panel was suspended in a horizontal position from the ceiling by bungy cords attached to each corner. This allowed freedom of motion of the entire panel in any direction (termed a FREE - FREE mode). A grid of accelerometer locations was then laid out on the panel surface as shown in Fig 1. Three different masses were chosen as mass loads.

TABLE I EXPERIMENTAL APPARATUS

APPARATUS	MANUFACTURER	MODEL	COMMENTS
Accelerometer Calibrator	Bruel and Kjaer	B&K 4291	1 g peak
Fourier Spectrum Analyzer	Hewlett-Packard	HP 5451B	
25 lb. Shaker	Ling Electronics		
Random Noise Generator	Hewlett-Packard	HP 3722A	flat spectrum
Accelerometers (6)	Vibrametrics	1000 A	
Force Gauge	Vibrametrics	208 A03	1 mV/lb force
Amplifiers (6)	Intech	A-2318	Variable gain
Oscilloscope (2)	Hewlett-Packard	HP 1707B	
Universal Filter	General - Radio		Bandpass 50-1000 Hz
Terminal	Tektronix	TEK 4014-1	
Copier	Xerox	Versatek	Hard copies from terminal
FM Recorder	LAR	LAR 7400	
Voltmeter	NLS	LX-2	
Power Supply	AFFDL/FBG		$\pm$ 15V DC
Strobe	Strobex	121 A	
Force Gauge Power Unit	Piezotronics	480 A	
Low Frequency Oscillator	Electrodyne	N 300	

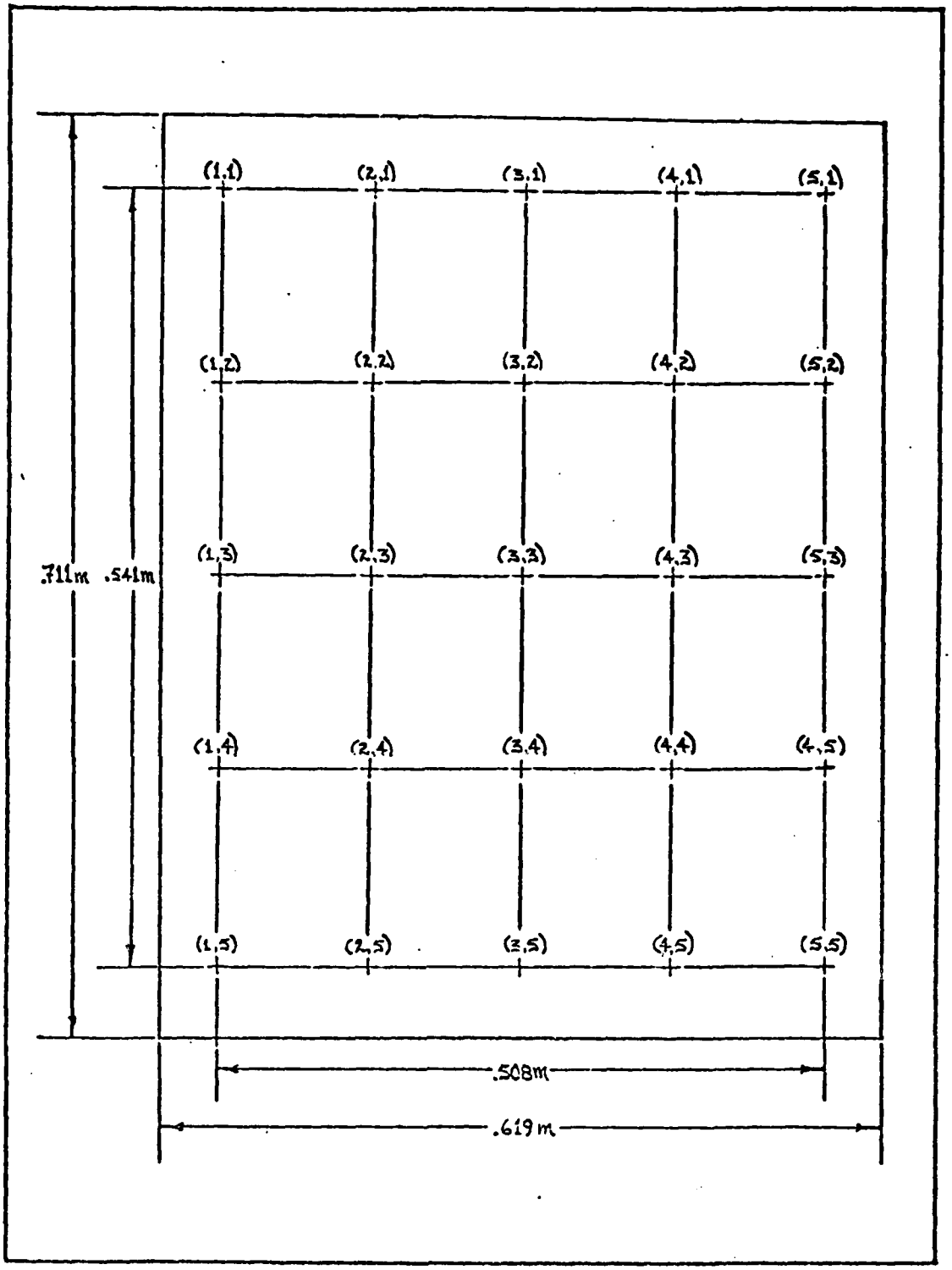

Fig. 1 Grid Layout on Panel Surface

The isometric views of these three masses are shown in Figures 2, 3, and 4. Then, three arbitrary mass loading locations were chosen as shown in Fig 5. Utilizing each mass in all three locations yielded a total of nine mass loaded configurations. The pertinent data for all nine of these is given in Table II. In each of the three separate testing procedures all of the above-mentioned conditions remained the same. Briefly, the three methods employed were:

1. Single point excitation using a continuous, random noise input to the 25 lb. shaker. All accelerometer data was recorded on FM tape, along with the force input (from a force gauge). The recorded data was then digitized and processed to yield Power Spectral Density and Transfer Function plots.

2. The force input to the panel was the same as above, but all data processing was done by the HP5451B Fourier Spectrum Analyzer.

3. The input excitation was 15 impulse inputs at random locations. Data processing was done by the HP5451B, and all response data was an average of the responses to each of the 15 inputs. These three methods are described in detail below.

Test Method 1

The panel was set up as was previously discussed. A 25 lb. Ling Shaker was attached to one of the two longitudinal stiffeners which ran the length of the panel, almost directly below the first column of accelerometers, and was slightly off center from the middle lateral stiffener. The input signal to the shaker was a continuous, broadband, random noise signal. A force gauge was placed between the shaker and the panel. Due primarily to a software problem which rendered the Hewlett-Packard Fourier Spectrum Analyzer unavailable when testing was begun, an

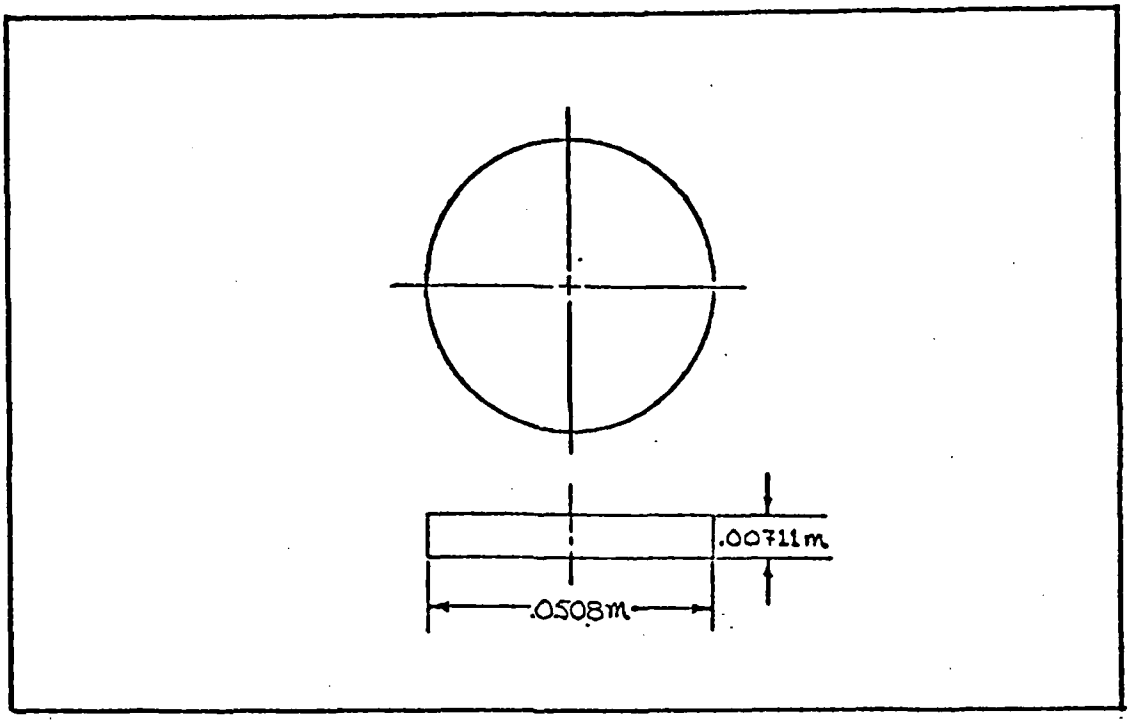

Fig. 2 Isometric Views of Mass #1

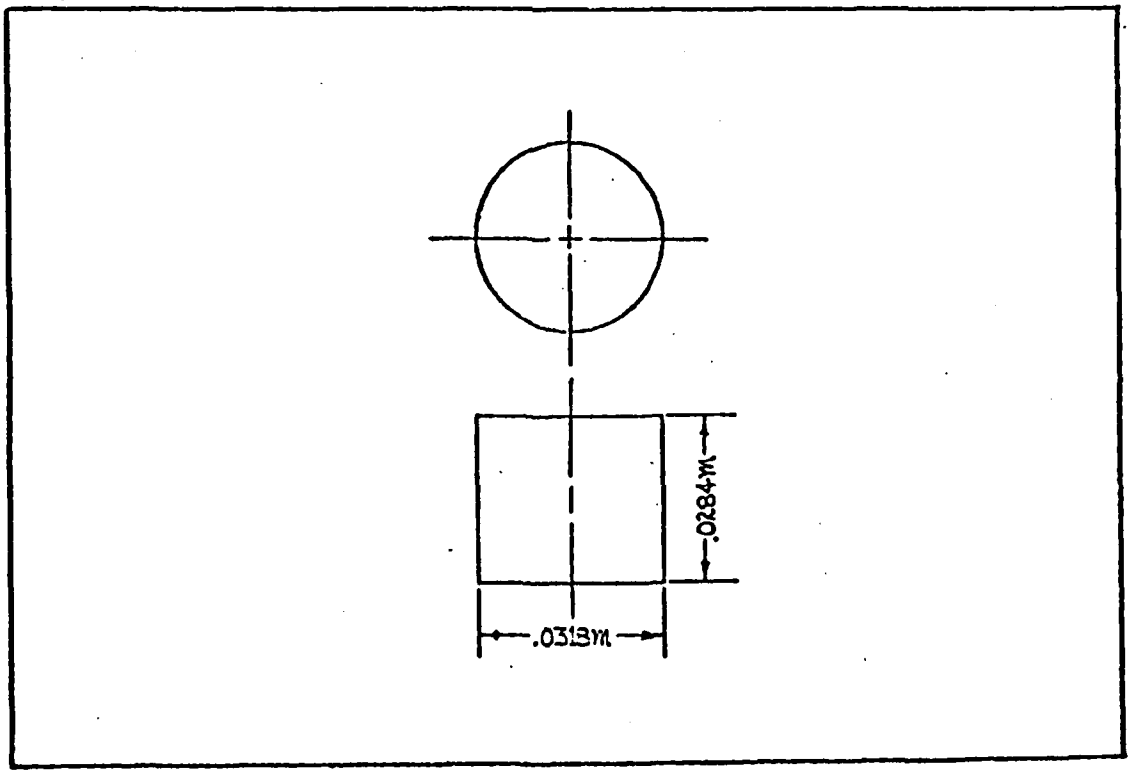

Fig. 3 Isometric Views of Mass #2

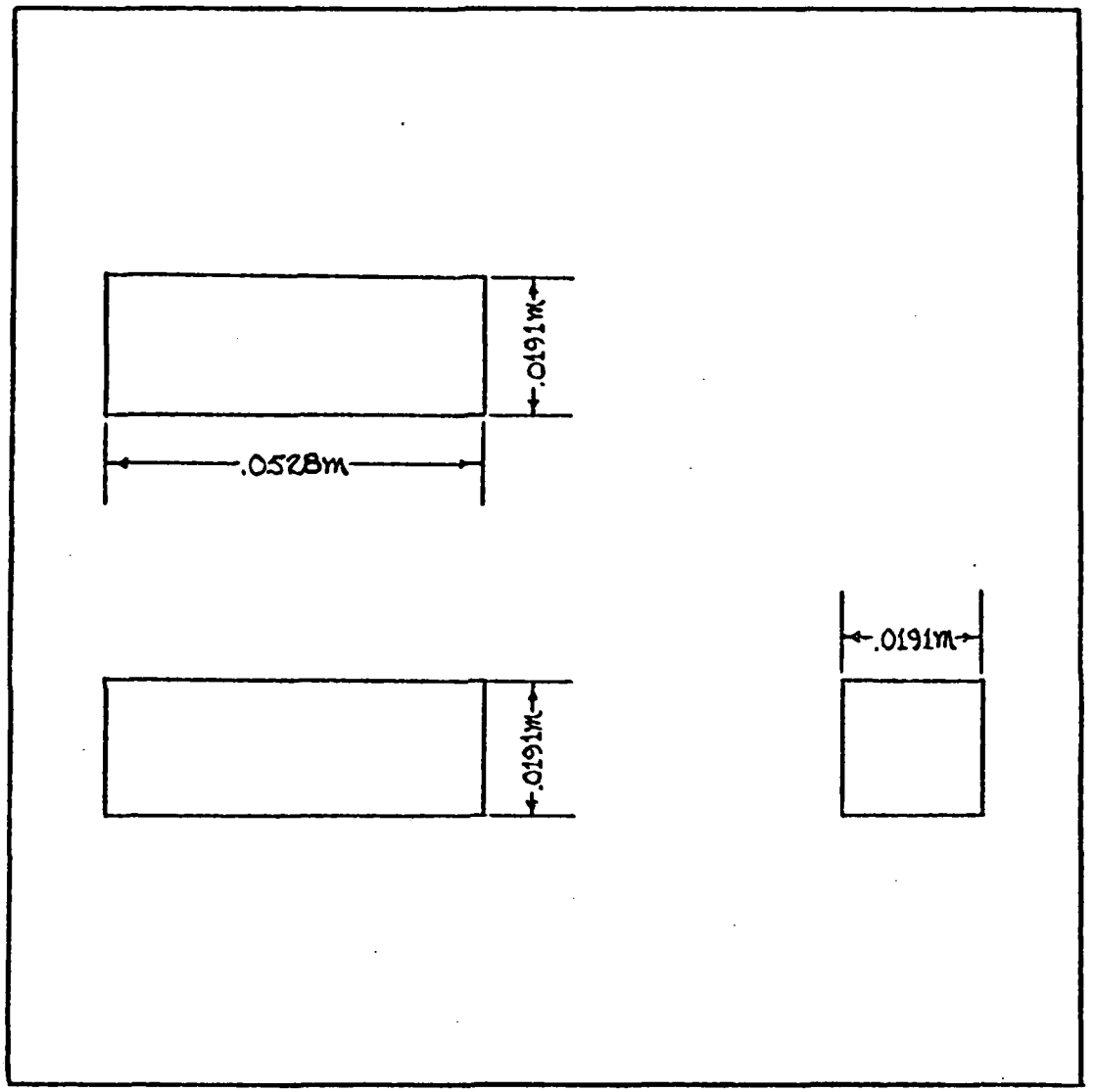

Fig. 4 Isometric Views of Mass #3

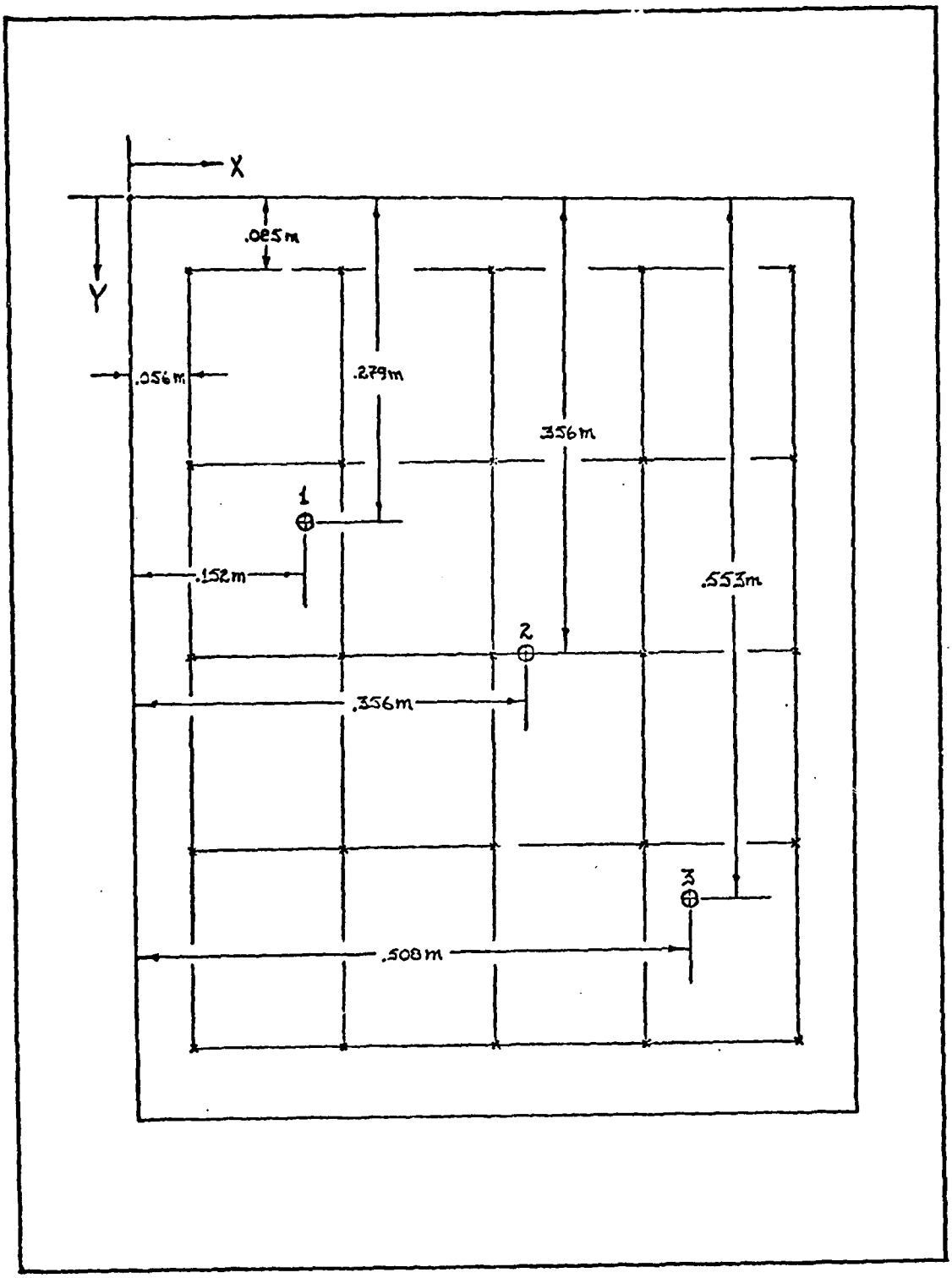

Fig. 5 Mass Loading Locations

Table II MASS LOADING CONFIGURATION DATA

Configuration Number	Mass Number	Mass (Kg)	R_x (m)	R_y (m)	X_o (m)	Y_o (m)
1	1	0.110	0.0129	0.0129	0.152	0.279
2	1	0.110	0.0129	0.0129	0.356	0.356
3	1	0.110	0.0129	0.0129	0.508	0.533
4	2	0.189	0.0142	0.0142	0.152	0.279
5	2	0.189	0.0142	0.0142	0.356	0.356
6	2	0.189	0.0142	0.0142	0.508	0.533
7	3	0.052	0.0123	0.0188	0.152	0.279
8	3	0.052	0.0123	0.0188	0.356	0.356
9	3	0.052	0.0188	0.0123	0.508	0.533

older, more conventional method was utilized. The response data was collected from five (5) accelerometers (one column) at a time (i.e., accelerometers were placed first on points (1,1), (1,2), (1,3), (1,4), (1,5), then moved to (2,1), (2,2), (2,3), (2,4), (2,5), and so on). These points were as depicted in Fig 1 and the output of the force guage and all five accelerometers were amplified and recorded on FM tape. See Fig 6 for a complete wiring diagram. Upon completion of thirty (30) seconds of recorded data, the accelerometers were moved to columns 2, 3, 4, and 5 in succession, repeating the above procedure each time. This FM tape was then digitized and processed to yield Power Spectral Density (PSD) and Transfer Function Plots. See Appendix E for a sample of the Transfer Function Magnitude and Phase Plots that resulted. From these it was possible to determine the frequency band of interest, as it was desirable to confine the analysis to approximately the first ten (10)* modes, which covered a frequency band of 50 - 500 Hz (the lower limit avoids some very low frequency modes of the suspension system which were found by doing a frequency sine sweep). In addition to the Transfer Function Plots, tabular listings were printed for both the magnitude and phase of the Transfer Function values for intervals of 0.5 Hz. From these, the natural frequencies and a discrete representation of each mode shape was determined. This procedure was carried out for the panel in an unloaded configuration and each of the nine mass loaded configurations.

At this stage, a serious problem arose in that the phase information proved to be erroneous. Theoretically, the phase angle between the input force and an output acceleration should always be $\pm 90^{\circ}$. This, however, was not the case. In fact, at every frequency that had consistently yielded

* Ten was chosen because it is small enough that the eigenvalue problem does not become too unwieldly, but as outlined in Whaley (Ref 5) this is a sufficient number of terms to provide a good approximation of forced response.

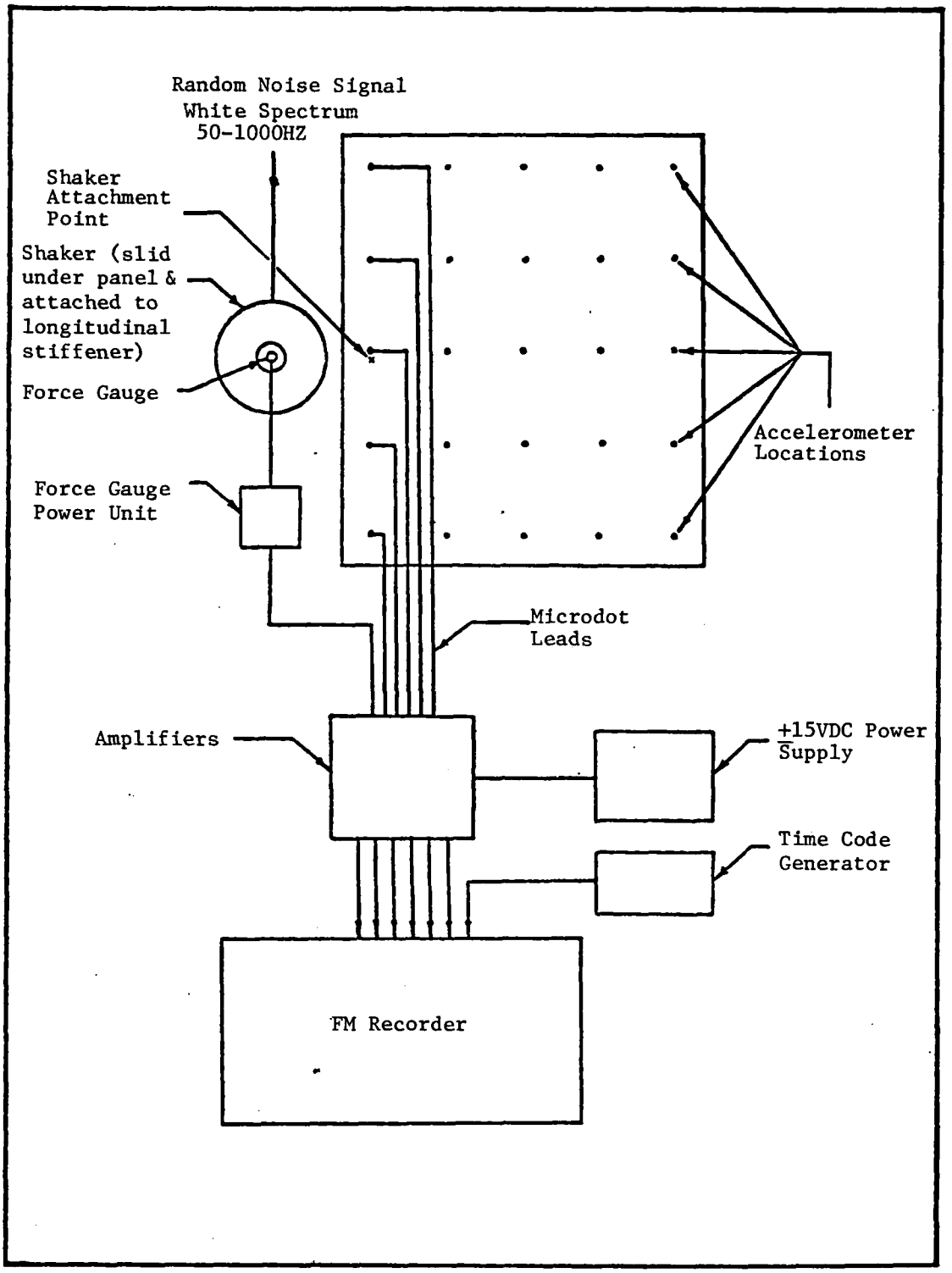

Fig. 6 Wiring Diagram - Test Method 1

a local peak in the Transfer Function plots, and was therefore thought to be a natural frequency, there were many points at which the phase angle was as much as 40° away from $\pm 90^{\circ}$. Because of this discrepancy, coherence function plots were examined, which are in essence a measure of the reliability of the data. The coherence function is defined in Richardson (Ref 9) as follows:

$$2 = \frac{|\bar{S}_{yx}(\omega)|^2 *}{\bar{S}_{xx}(\omega)\bar{S}_{yy}(\omega)} \qquad (10)$$

where: Input Power Spectrum = $S_{xx}(\omega) = X(\omega)X^*(\omega)$ (11)

Output Power Spectrum = $S_{yy}(\omega) = Y(\omega)Y^*(\omega)$ (12)

Cross Power Spectrum = $S_{xy}(\omega) = Y(\omega)X^*(\omega)$ (13)

Representing the system in block form:

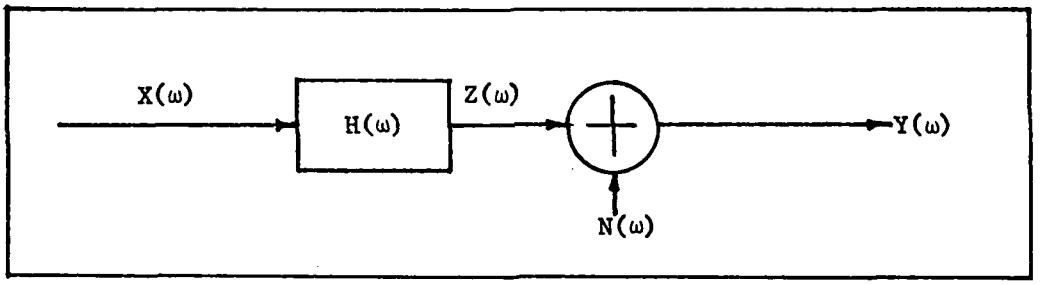

Fig. 7 Block Diagram of Test Station

$X(\omega)$ = Fourier Transform of input signal

$H(\omega)$ = System Transfer Function

$Z(\omega)$ = Fourier Transform of desired output signal

$N(\omega)$ = Fourier Transform of extraneous noise (thermal noise, 60-cycle, etc.)

$Y(\omega)$ = Fourier Transform of actual measured output signal

* Bar denotes algebraic average of the number of measurements taken.

$$Y(\omega) = H(\omega) + N(\omega) \tag{14}$$

$$S_{xy}(\omega) = Y(\omega)X^*(\omega) = H(s)X(\omega) + N(\omega)\ X^*(\omega)$$

$$S_{xy}(\omega) = H(\omega)\ S_{xx}(\omega) + N(\omega)X^*(\omega) \tag{15}$$

$$S_{yy}(\omega) = (H(\omega)X(\omega) + N(\omega))(H(\omega)X(\omega) + N(\omega))^*$$

$$S_{yy}(\omega) = |H(\omega)|^2\ S_{xx}(\omega) + H^*(\omega)S_{nx}(\omega) + H(\omega)S_{xn}(\omega) + S_{nn}(\omega) \tag{16}$$

$$S_{zz}(\omega) = (H(\omega)X(\omega))(H(\omega)X(\omega))^*$$

$$S_{xx}(\omega) = |H(\omega)|^2\ S_{xx}(\omega) \tag{17}$$

From Eqs (10), (15) and (16) it can be seen that when measured response power is equal to measured input power, $\gamma^2 = 1$, and the noise power, $N(\omega)$, has no effect on $H(\omega)$. However, when measured response power is greater than measured input power because of the contribution of some extraneous noise sources, $\gamma^2 < 1$, for all those frequencies where the noise adds power to the response signal. Therefore, the coherence function can be used to indicate the degree of noise contamination in Transfer Function measurements. Since the additive noise can be modelled as a zero mean random process, its effect on the Transfer Function results can be reduced by averaging results of several responses together (i.e., ensemble averaging).

When the coherence function plots for each grid point were generated, it was found that for everyone of them in all configurations, the coherence was dropping almost to zero at several frequencies indicating that the measurements had been contaminated by a great deal of extraneous noise (See Fig 8). To alleviate this problem, a couple of alterations to parameters in the data processing method were tried: 1) increasing the frequency resolution and therefore the transform time, and 2) increasing the number of transforms in the averaging process. These both improved the resulting data, but the coherence function plots still indicated that a great deal of unwanted noise

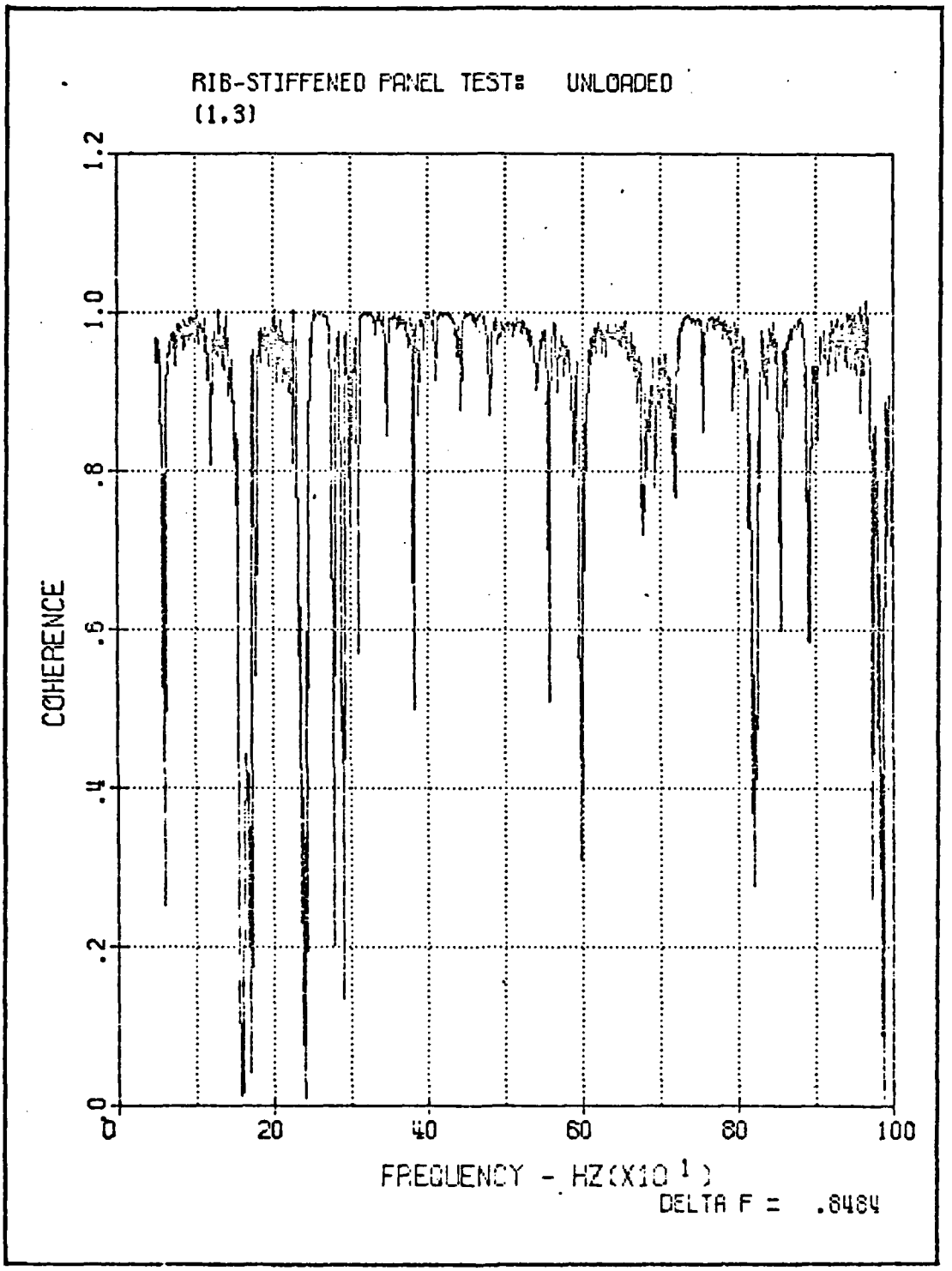

Fig. 8 Sample Coherence Function Plot Showing How it Drops Off at Numerous Places

was present in the system.

The author and some engineers at the Air Force Flight Dynamics Laboratory (AFFDL) formulated the following hypothesis as to the cause of the problem: the unacceptably large amount of noise contamination was the result of a combination of two factors - the amplitude of the input excitation force, and the extremely low structural damping factor of the test specimen. As a result, an input to the panel at, say, T = 0, would not be damped out for a long period of time. To understand fully how this becomes a problem, one must know how data processing for continuous inputs is accomplished. In the case of thirty (30) second runs of recorded data, and using the maximum frequency resolution (.4242 Hz) attainable on the processing equipment at AFFDL, means that Fourier Transforms will be taken over 1/.4242 = 2.357 seconds intervals and twelve (12) transforms can be taken. These twelve transforms can then be averaged to reduce the effect of extraneous noise on the results. To yield the desired output, artificial damping is introduced onto the recorded data in the form of a "Hanning Window". (See Fig 9) In this manner, one can look at the panel response over a given "time window" (2.357 seconds) in the 30 second sample, then take the Fourier Transforms of the input and the output at a given point, and generate the Power Spectral Density or Transfer Function plots for that particular point. A similar process must be carried out for all twenty-five (25) points. What actually happens in the case of such a lightly damped structure is that any transient response which is due to inputs prior to the beginning of any given "time window", enter that window as noise. Note that this effect would be absent if one could compute an "exact" Fourier Transform (over an infinite time interval). The reliability of all the data is extremely dependent upon the Signal-to-Noise Ratio (SNR) being sufficiently high to yield good data.

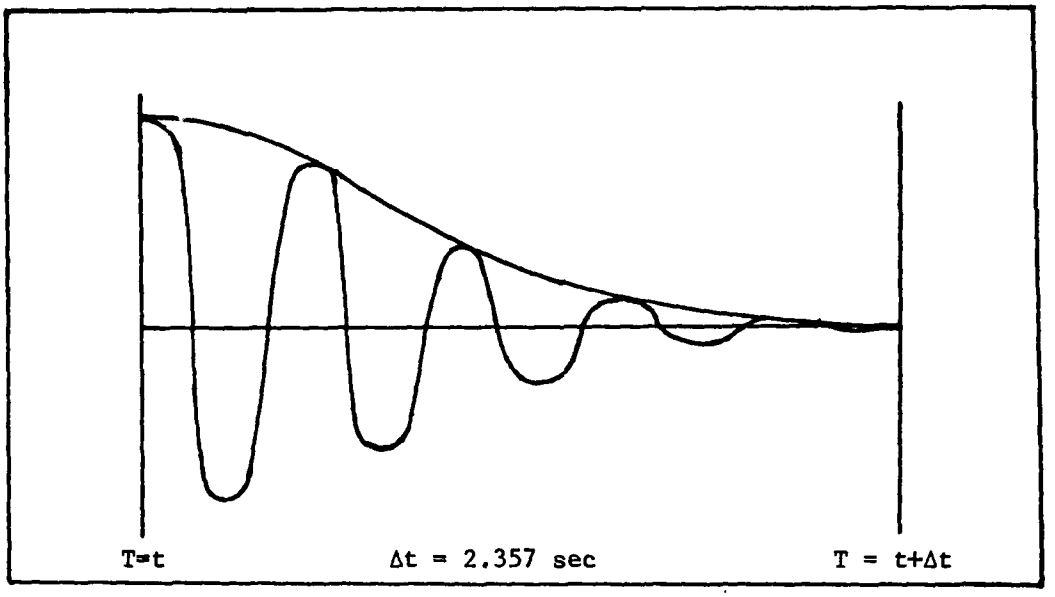

Fig. 9 Hanning Window artificially damping response to zero

Therefore, as more and more prior response enters each successive window as noise, the SNR becomes worse and worse, and so does the data. The problem could not be resolved using the best possible values of total data time, frequency resolution, and number of transforms in the averaging process that AFFDL's data processing unit had to offer.

In summary, this first test method failed because the extremely low structural damping factor of the panel resulted in its responding to a given input for a long period of time. This combined with the inability of the data processing method to allow sufficient time for the panel responses to damp out caused the SNR to grow worse with each successive Fourier Transform taken. This in turn caused the data taken to become worse and worse with the result that the gathered data could not be considered reliable. Therefore, a new test method was sought.

Test Method 2

By this point in time the HP5451B, Fourier Analyzer, Hewlett-Packard (Ref 4),

was ready for use. This device utilizes Fast Fourier Transform and Ensemble Averaging Techniques to calculate Power Spectral Densities and Transfer Functions very rapidly. The test set up was still exactly the same as in Fig 6, with the exception that because the Fourier Analyzer could perform all data processing, the FM Recorder was no longer required. The two inputs to the analyzer were the output of the force gauge (always), and the output of each one of the twenty-five accelerometers in succession. The panel was still driven by the twenty-five lb shaker excited by broadband random noise. The HP5451B was capable of achieving better limits of the performance parameters: longer transform time and therefore better frequency resolution, and greater numbers of transforms to be used in the averaging process. It was hoped that this improved performance would solve the problem, and yield some reliable data. It was also thought that although it would not improve the coherence at any given point, the removal of any bay modes from the analysis would simplify the task of forming the discrete mode shapes. Bay modes are modes which occur in only one or more, but not all, of the bays created by the isolating effect of the stiffeners. Since the author was interested only in global modes, or modes of the entire panel, eliminating bay modes from the analysis altogether at the beginning of testing, would save a great deal of time during the data reduction process. To this end, a high frequency strobe was obtained. The intention was to do a sine sweep throughout the frequency band of interest, tune to each harmonic, and view the panel with the strobe to determine whether the mode was a global one, or just a mode of one or more bays. However, the amplitude of panel motion was very small and therefore it was extremely difficult to view the panel modes. The strobe was, as a result, ineffective. The Fourier Analyzer was also incapable of resolving the problems of unreliable data. This was once again determined by examining the coherence

function plots. The Fourier Analyzer was capable of computing these using Eq (10), and then plotting them. These revealed the same problem as was experienced earlier. The noise power at several frequencies was so high that the coherence dropped off very nearly to zero at some, and to as low as 0.5 at many others. Therefore it was concluded that the data was not reliable and could not be used. As a result, a third experimental procedure was required.

Test Method 3

This third method, in which the method of data analysis was developed by Brown (Ref 7) proved to be effective, and was the one finally used. First, a location for a "reference accelerometer" was chosen. This location remained the same throughout all testing. It was discovered that an accelerometer location near the center of the panel yielded better results than a location close to an edge. The amplified output from this reference accelerometer was one of the inputs to the Fourier Analyzer. The other input was the amplified output of an accelerometer at one of the twenty-five data points on the grid (Fig 1). A complete wiring diagram of this experimental set up is shown in Fig 10.

The panel was then excited by tapping (impulse input) the surface once at each of fifteen (15) arbitrary locations. After each individual impulse, sufficient time was allowed for the panel response to dampen out (an indicator light on the Spectrum Analyzer notified the tester when the response had decreased to a negligible level). For each excitation the Fourier Analyzer was used to compute the Auto Power Spectrum of the response at the reference point, the Auto Power Spectrum of the response at a given point, and the Cross Power Spectrum between the two. A stable average of each was then computed over the fifteen inputs. The computed parameters are

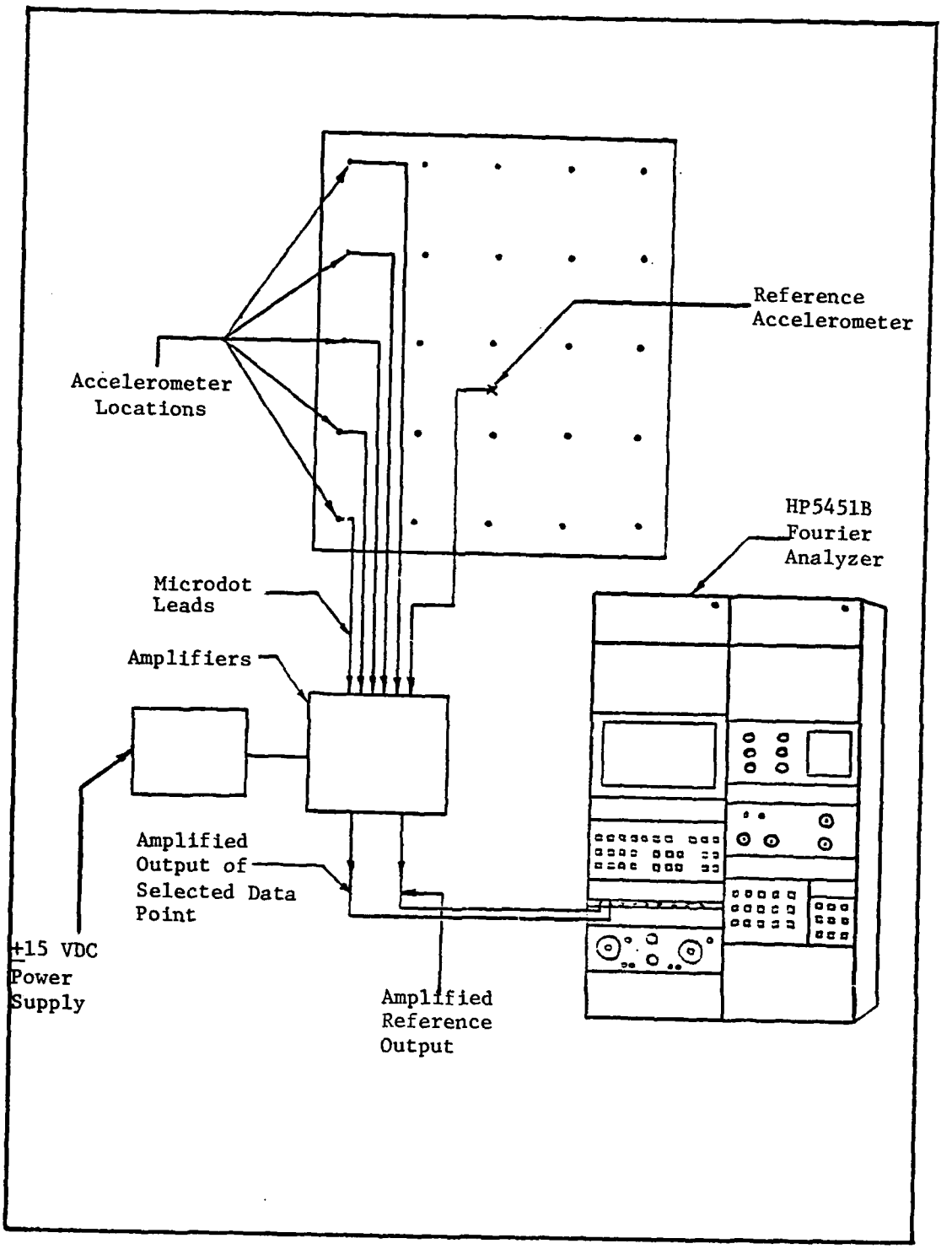

Fig. 10 Wiring Diagram - Test Method 3

defined as follows:

Output Auto Power Spectrum of Reference = $Srr(\omega) = R(\omega)R^*(\omega)$ (18)

Output Auto Power Spectrum of Data Point = $Syy(\omega) = Y(\omega)Y^*(\omega)$ (19)

Cross Power Spectrum = $Syr(\omega) = R(\omega)Y^*(\omega)$ (20)

Stable Average = $A_n = A_{n-1} + \frac{I_n A_{n-1}}{n}$ (21)

Then, at the end of the fifteen excitations a Modal Assurance Criteria (MAC) function (Brown), was computed which is defined as follows:

$$MAC = \frac{|\bar{S}_{yr}(\omega)|^{2*}}{\bar{S}_{rr}(\omega)\bar{S}_{yy}(\omega)} \quad (22)$$

The difference between this function, and the coherence function defined in Eq (10) is that both auto spectrums are of responses at two points (there is no power spectrum of the force input), and the cross power spectrum is that between two output responses instead of between a force input and an ouput excitation as in Eq (10). At all natural frequencies, the magnitude and phase relationships between the responses at any two points on the panel surface will be the same, as for a given natural frequency there is a corresponding mode shape. Therefore, at these modal frequencies, the magnitude of the Cross Power Spectrum squared will be equal to the product of the individual Auto Spectra. It follows that at these frequencies the value of the MAC function will be 1.0. Now, at all non-modal frequencies the relationship between the responses at any two points on the surface of the panel, is a zero mean random process (Brown). Therefore, for each of the fifteen excitations, the relationship between the Reference and a given point will be different, and the average of the Cross Power Spectrum over those fifteen will be small compared to 1. Thus, the value of the MAC function at all frequencies that are not natural frequencies will be small.

* Bar (-) over values in Eq (22) denotes stable average of those parameters.

(See Fig 11 for a sample MAC function). Also computed at the completion of the fifteen impulse inputs, was the Transfer Function. In the case of this type of testing, this Transfer Function was not defined in the sense of a classical system Transfer Function (which is output response divided by input response), but was defined as follows:

$$H(\omega) = \frac{\bar{S}_{yr}(\omega)}{\bar{S}_{rr}(\omega)} \qquad (23)$$

This is a measure of the relative response at a given point as compared with the response at the Reference point.

In accordance with the programming for this overall process, once all computations had been completed, the Fourier Analyzer displayed the MAC Function plot. By viewing this, the user could determine whether or not the data taken was acceptable. If the MAC function was a "clean" one as shown in Figure 11, i.e. MAC = 1.0 at the natural frequencies and zero elsewhere, the data was good. Whereas, if there were many values between zero and 1.0, and the value remained at 0.0 very seldom, the data was considered erroneous. When it was decided that the data was good, the user gave the "CONTINUE" command, and the Power Spectral Density (PSD) plot (a measure of the relative power in each frequency throughout the band of interest), and the tabulated values of the MAC and Transfer Functions were outputted to the TEK 4014-1 scope in succession, and sent to the Versatek hard copier. See Figures 12, 13, and 14 for samples of each. This process had to be repeated for all twenty-five accelerometer locations, for each of the ten separate configurations. The PSD plots for each data point of the unloaded configuration are included in Appendix A. Using this procedure the author was able to generate the required two hundred fifty sets of

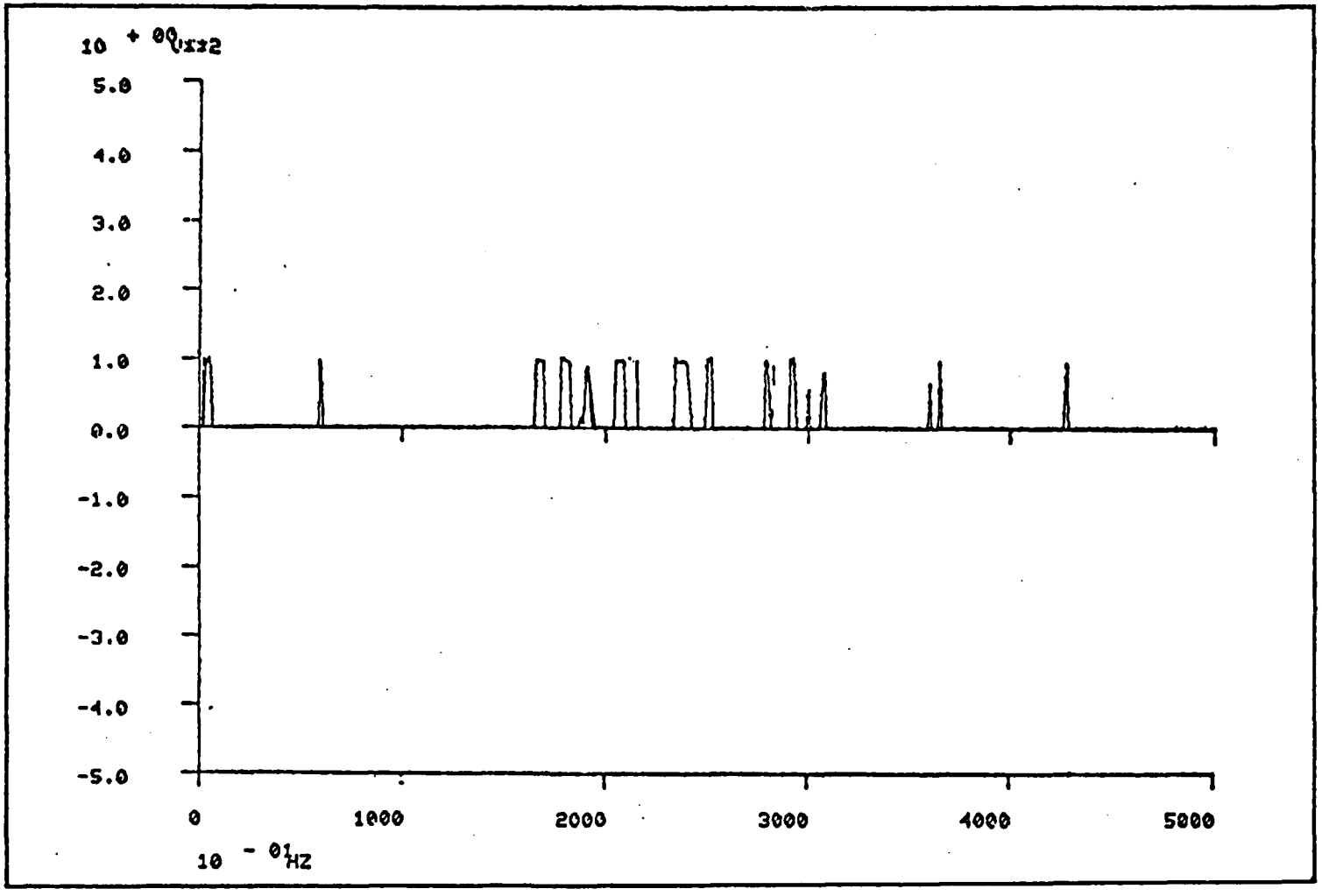

Fig. 11 Sample MAC Function Plot

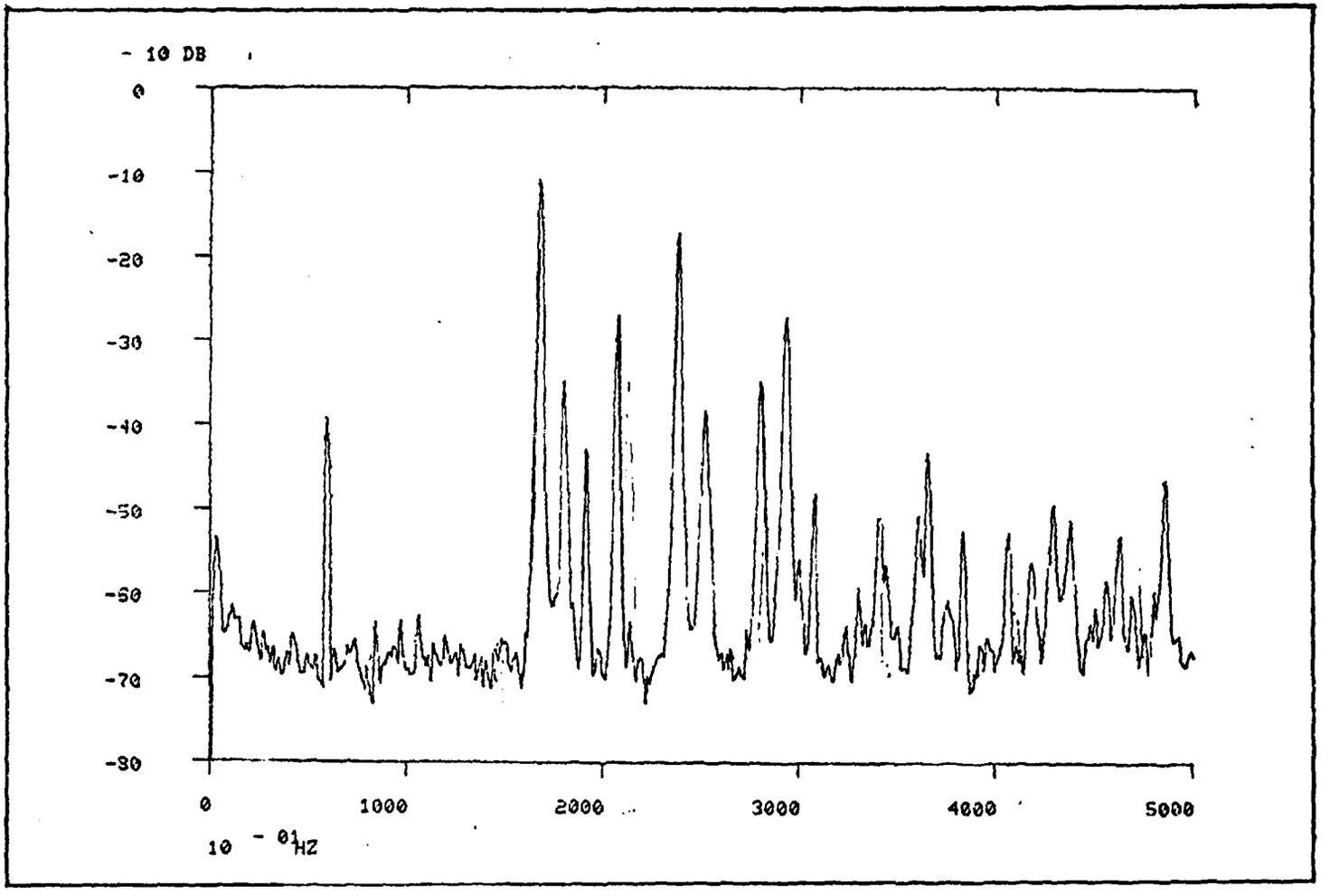

Fig. 12 Power Spectral Density

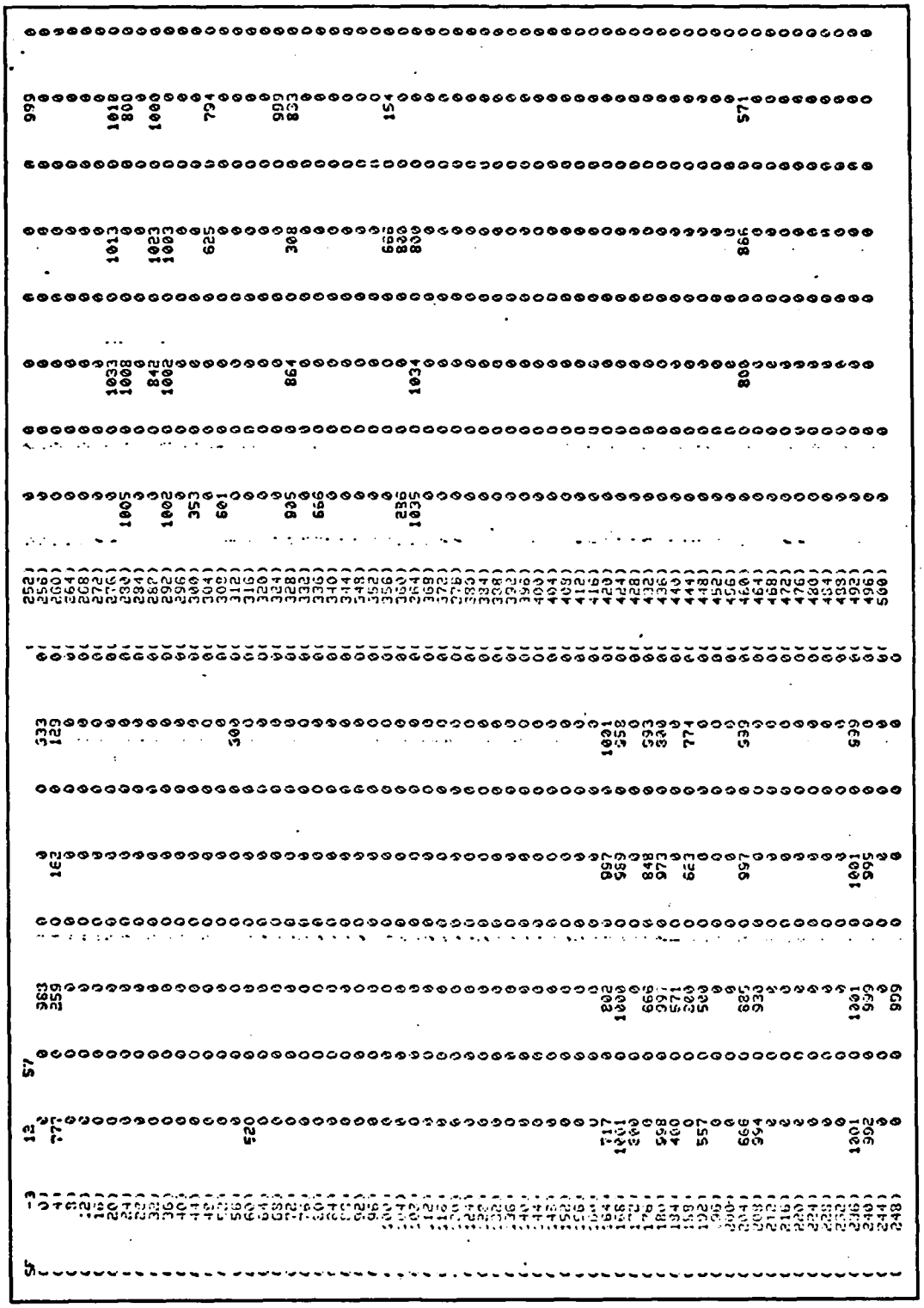

Fig. 13 MAC Values

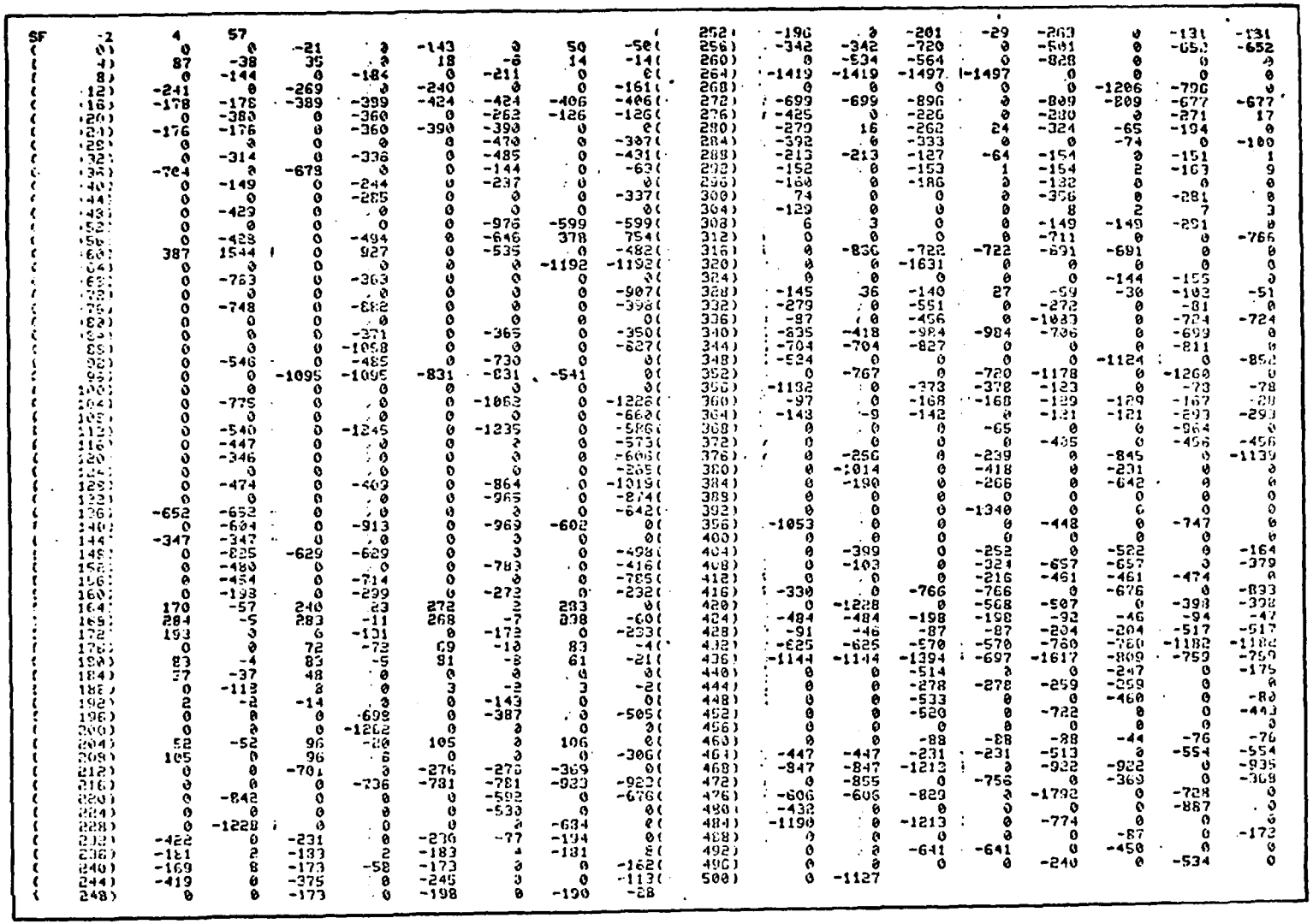

SF	-2	4	57														
(0)	0	0	-21	0	-143	0	50	-50	(252)	-196	0	-201	-29	-269	0	-131	-131
(4)	87	-38	35	0	18	-6	14	-14	(256)	-342	-342	-720	0	-501	0	-652	-652
(8)	0	-144	0	-184	0	-211	0	0	(260)	0	0	-534	-564	0	-828	0	0	0
(12)	-241	0	-269	0	-240	0	0	-161	(264)	-1419	-1419	-1497	-1497	0	0	0	0
(16)	-178	-178	-389	-399	-424	-424	-406	-406	(268)	0	0	0	0	0	-1206	-796	0
(20)	0	-383	0	-360	0	-262	-126	-126	(272)	-699	-699	-896	0	-809	-809	-677	-677
(24)	-176	-176	0	-360	-390	-390	0	0	(276)	-425	0	-226	0	-280	0	-271	17
(28)	0	0	0	0	0	-470	0	-307	(280)	-279	16	-262	24	-324	-65	-194	0
(32)	0	-314	0	-336	0	-485	0	-431	(284)	-392	6	-333	0	0	-74	0	-100
(36)	-764	0	-679	0	0	-144	0	-63	(288)	-213	-213	-127	-64	-154	0	-151	1
(40)	0	-149	0	-244	0	-237	0	0	(292)	-152	0	-153	1	-154	2	-169	9
(44)	0	0	0	-285	0	0	0	-337	(296)	-160	0	-186	0	-182	0	0	0
(48)	0	-429	0	0	0	0	0	0	(300)	74	0	0	0	-356	0	-281	0
(52)	0	0	0	0	0	-976	-599	-599	(304)	-129	0	0	0	8	2	7	3
(56)	0	-428	0	-494	0	-646	378	754	(308)	6	3	0	0	-149	-149	-291	0
(60)	387	1544	0	927	0	-535	0	-482	(312)	0	0	0	0	-711	0	0	-766
(64)	0	0	0	0	0	0	-1192	-1192	(316)	0	0	-836	-722	-691	-691	0	0
(68)	0	-783	0	-363	0	0	0	0	(320)	0	0	0	-1631	0	0	0	0
(72)	0	0	0	0	0	0	0	-907	(324)	0	0	0	0	0	-144	-155	0
(76)	0	-748	0	-882	0	0	0	-398	(328)	-145	36	-140	27	-59	-38	-102	-51
(80)	0	0	0	0	0	0	0	0	(332)	-279	0	-551	0	-272	0	-81	0
(84)	0	0	0	-371	0	-365	0	-350	(336)	-87	0	-456	0	-1080	0	-724	-724
(88)	0	0	0	-1068	0	0	0	-827	(340)	-835	-418	-984	-984	-706	0	-699	0
(92)	0	-546	0	-485	0	-730	0	0	(344)	-704	-704	-827	0	0	0	-811	0
(96)	0	0	-1095	-1095	-831	-831	-541	0	(348)	-524	0	0	0	0	-1124	0	-852
(100)	0	0	0	0	0	0	0	0	(352)	0	-767	0	-720	-1178	0	-1260	0
(104)	0	-775	0	0	0	-1063	0	-1228	(356)	-1132	0	-373	-378	-123	0	-78	-78
(108)	0	0	0	0	0	0	0	0	(360)	-97	0	-168	-168	-129	-129	-167	-20
(112)	0	-540	0	-1245	0	-1235	0	-586	(364)	-143	-9	-142	0	-121	-121	-293	-293
(116)	0	-447	0	0	0	0	0	-573	(368)	0	0	0	-65	0	0	-964	0
(120)	0	-346	0	0	0	0	0	-606	(372)	0	0	0	0	-485	0	-456	-456
(124)	0	0	0	0	0	0	0	-265	(376)	0	-256	0	-239	0	-845	0	-1139
(128)	0	-474	0	-469	0	-864	0	-1019	(380)	0	-1014	0	-418	0	-231	0	0
(132)	0	0	0	0	0	-965	0	-874	(384)	0	-190	0	-266	0	-642	0	0
(136)	-652	-652	0	0	0	0	0	-642	(388)	0	0	0	0	0	0	0	0
(140)	0	-604	0	-913	0	-969	-602	0	(392)	0	0	0	-1340	0	0	0	0
(144)	-347	-347	0	0	0	0	0	0	(396)	-1053	0	0	0	-448	0	-747	0
(148)	0	-825	-629	-629	0	0	0	-498	(400)	0	0	0	0	0	0	0	0
(152)	0	-480	0	0	0	-783	0	-416	(404)	0	-399	0	-252	0	-522	0	-164
(156)	0	-454	0	-714	0	0	0	-785	(408)	0	-103	0	-324	-657	-657	0	-379
(160)	0	-198	0	-299	0	-273	0	-232	(412)	0	0	0	-216	-461	-461	-474	0
(164)	170	-57	240	23	272	0	283	0	(416)	-330	0	-766	-766	0	-676	0	-833
(168)	284	-5	283	-11	268	-7	308	-60	(420)	0	-1228	0	-568	-507	0	-398	-398
(172)	193	0	6	-101	0	-172	0	-233	(424)	-484	-484	-198	-198	-92	-46	-94	-47
(176)	0	0	72	-72	69	-10	83	-4	(428)	-91	-46	-87	-87	-204	-204	-517	-517
(180)	83	-4	83	-5	81	-8	61	-21	(432)	-625	-625	-570	-570	-760	-760	-1182	-1182
(184)	37	-37	48	0	0	0	0	0	(436)	-1144	-1144	-1394	-697	-1617	-809	-759	-759
(188)	0	-113	8	0	3	-2	3	-2	(440)	0	0	-514	0	0	-247	0	-175
(192)	2	-2	-14	0	0	-143	0	0	(444)	0	0	-278	-278	-259	-259	0	0
(196)	0	0	0	-698	0	-387	0	-505	(448)	0	0	-533	0	0	-460	0	-80
(200)	0	0	0	-1262	0	0	0	0	(452)	0	0	-520	0	-722	0	0	-443
(204)	52	-52	96	-20	105	0	106	0	(456)	0	0	0	0	0	0	0	0
(208)	105	0	96	-6	0	0	0	-306	(460)	0	0	-88	-88	-88	-44	-76	-76
(212)	0	0	-701	0	-276	-276	-369	0	(464)	-447	-447	-231	-231	-513	0	-554	-554
(216)	0	0	0	-736	-781	-781	-933	-922	(468)	-847	-847	-1212	0	-922	-922	0	-935
(220)	0	-842	0	0	0	-592	0	-676	(472)	0	-855	0	-756	0	-369	0	-369
(224)	0	0	0	0	0	-530	0	0	(476)	-606	-606	-829	0	-1792	0	-728	0
(228)	0	-1228	0	0	0	0	-634	0	(480)	-432	0	0	0	0	0	-887	0
(232)	-422	0	-231	0	-236	-77	-194	0	(484)	-1190	0	-1213	0	-774	0	0	0
(236)	-181	2	-183	2	-183	4	-181	8	(488)	0	0	0	0	0	-87	0	-172
(240)	-169	8	-173	-58	-173	0	0	-162	(492)	0	0	-641	-641	0	-458	0	0
(244)	-419	0	-375	0	-245	0	0	-113	(496)	0	0	0	0	-240	0	-534	0
(248)	0	0	-173	0	-198	0	-190	-88	(500)	0	-1127						

Fig. 14 Transfer Function (Real and Imaginary)

data, all were determined to be reliable on the basis of the MAC function. It should be noted here that acquiring reliable data required re-testing at some points where the MAC function indicated that the data was not good. This bad data could have been caused by several factors; allowing insufficient time for panel response to damp out between impulse excitations, causing a system overload by striking the panel too hard on one or more of the 15 excitations during one test run, or double-tapping - mistakenly striking the panel twice on a single impulse input. From this, it is necessary to realize that extreme care must be exercised when taking data, if one expects even this method to yield reliable results.

In summary, after determining that data processing limitations precluded the use of a broad-band random force input, a method using 15 discrete impulse inputs was used. An HP5451B Fourier Analyzer, Hewlett-Packard (Ref 4) was used to perform all data processing. Using a reference accelerometer which remained in a constant location and an accelerometer at one of the 25 data points as the inputs to the Fourier Analyzer, the individual Power Spectra and the Transfer Function were computed. From these, the natural frequencies and a discrete representation of the mode shapes were determined utilizing the procedure outlined in the section that follows.

IV Computational Procedure

ta Reduction

This section contains a description of the procedure that was employed extract the required natural frequencies and mode shapes from all of the ta that was collected. To yield this needed information one must pick out e location of modes in the frequency domain, and then find the relative gnitudes and phase of the displacement of each point, at each mode. This t be done for all ten configurations. By examining the tabulated values the MAC function for a particular point and for a given configuration, it possible to locate the natural frequencies with relative ease, as they indicated by the occurrence of several consecutive values of the MAC ng equal to or very close to one (see Fig 13, as an example of how the MAC ction indicates a mode check frequencies close to 168Hz and it can be n that there are 6 consecutive values all approximately = 1). Then by king the corresponding frequencies at the tabulated Transfer Function es, it was possible to pinpoint the natural frequency. This was done amining the listed values in the vicinity of a chosen frequency, which given in terms of real and imaginary components. By realizing that the e angle between the two acceleration responses (reference and test t) at a mode must be either 0^{o} or 180^{o}, it was necessary only to find frequency where the imaginary component was zero or closest to zero. e this was done, the relative position of that point, in the positive or tive direction was given by the real component of the transfer function e at the determined frequency. This procedure was carried out for all nty-five points for each configuration. This yielded the natural uencies and a discrete representation of the corresponding mode shapes

for the first nine (9) modes (all the modes that existed between 0 and 500 Hz) for all 10 configurations.

An example of the discrete mode shape plots is shown in Fig 15, and the plots for the first nine modes of the unloaded configurations are included in Appendix B.

Description of Computer Programs

General

Since both Eq (9) and the computation of the generalized elements required derivatives of the mode shapes, continuous representations of the discrete mode shapes previously formed, must somehow be generated. This was accomplished using a bi-cubic spline curve fitting approach. The bi-cubic spline is a mathematical algorithm which fits a cubic polynomial between sets of discrete data points, and yields continuous first and second-order derivatives at these data points. Also required for the computation of the Generalized Masses were the thickness and mass density of the panel. Since one of the objectives of this prediction technique was to enable analysis of a complex structure in a relatively simple manner, without having to utilize a complex model for the structure (i.e., finite element approach), the specimen was modelled as a uniform panel for computational purposes. A geometric averaging approach was used to take the stiffeners into account. The surface area of the stiffeners was averaged over the surface area of the panel to yield a constant thickness which was somewhat greater than that of the panel surface alone. The mass of the stiffeners was also taken into account by then calculating an effective panel mass density using the known overall panel mass, surface area, and the averaged thickness.

Once this was done, the generalized mass and stiffness were computed for each mode of each configuration, using Program 1 described below. These

CONFIGURATION # 0 MODE # 1 FREQUENCY 167.8

VECTORS:

1	1.000	6	.048	11	.035	16	.048	21	-.095
2	-1.650	7	-.089	12	-.066	17	-.089	22	-.093
3	.069	8	.068	13	.035	18	.068	23	.051
4	-.582	9	-.015	14	-.011	19	-.015	24	.224
5	.259	10	-.038	15	-.027	20	-.038	25	.221

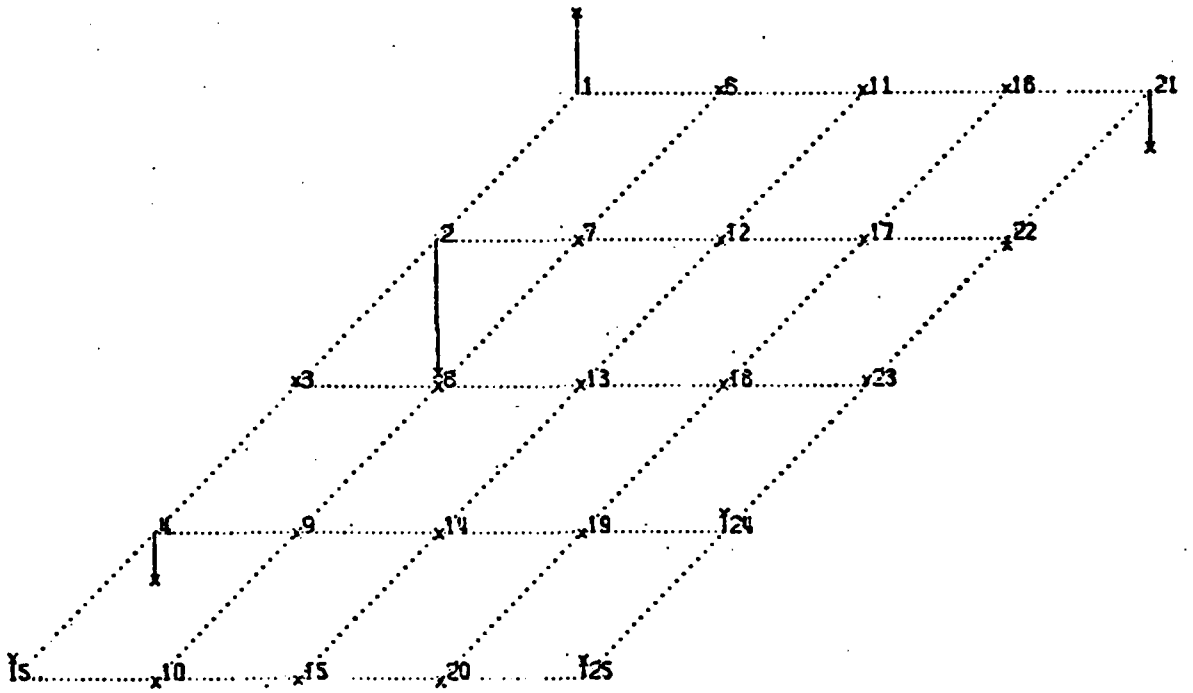

Fig. 15 Discrete Mode Shape Plot

These values were then used in Eq (9), to solve for the predicted natural frequencies (of each mass loaded configuration), using Program 2 described below.

Program 1

This program had been largely developed previously, but was adapted and improved for the purpose of this study. A complete listing of this computer program may be found in Appendix D. Utilizing only unloaded natural frequency and discrete mode shape data, this program made use of existing International Mathematical and Statistical Libraries (IMSL) subroutines to compute a bicubic spline approximation to curve-fit a continuous mode shape to the discrete data. The user controls the accuracy of this approximation by chosing the number of points in both the X and Y direction at which he wishes the values to be computed. In the case of this study, the author chose to divide the total length in the X and Y directions into forty (40) parts. This means that the value of each mode shape was computed at a total of 1600 points. Obviously, the finer one chooses the mesh size for these computations, the more accurate will be the approximation of the continuous mode shape, but the computer time and therefore expense also increases drastically. Therefore, a certain amount of engineering judgement was required in the determination of the desired mesh size. Once the continuous mode shape approximations had been computed, they were used in Eq (7a), and two separate integral equations were solved, one for the surface of the specimen itself, and one for the discrete mass load. The two results were then summed to yield the Generalized Mass values for each of the first nine modes, for each one of the nine mass loading configurations. The Generalized Stiffness values were then computed using the following formula:

$$K_{ij} = M_{ij}\omega_i^2 \qquad (24)$$

Where the ω_i's are the unloaded natural frequencies. The "j" subscript represents the configuration number. Note that Eq (7b) was not used to compute the Generalized Stiffness values due to the large errors that result from squaring the second derivative of the approximated mode shapes. A complete listing of the Generalized Mass and Stiffness values computed by this program are included in Appendix D.

Program 2

Again, much of this program had been previously written by Whaley (Ref 3) for the test conducted on the flat plate. However, it was necessary to adapt and improve it due to the greater complexity and scope of this study. This program solves Eq (9) for the predicted mass-loaded natural frequencies. As can be seen from Eqs (8a) and (8b), aside from the nine (9) Generalized Mass and Stiffness Values for each configuration (from Program 1) other data values were required as inputs to this program. These were, the value of the added mass (Kg), the location of the added mass, (Xo,Yo), as shown in Fig 5, and the radii of gyration of the added mass, (Rx,Ry). See Table II for all this data. A sample calculation of the radii of gyration for one of the masses loads used is shown in Appendix E. A complete listing of this program is included in Appendix D and the outputs showing the predicted loaded natural frequencies (as percentages of the unloaded ones) are included at Appendix D.

Program 3

This program is really Program 1 with a couple of deletions, and a large addition written by the author which allows the user to output three-dimensional plots of as many of the continuous mode shapes as is desired. This was used

largely to clear up any ambiguities that arose when deciding which of the experimentally determined mode shapes for all of the mass loading configurations matched up with those from the unloaded case. Due to some modes being very close to one another and some being shifted upwards in frequency, it was necessary to plot the mode shapes and compare them to the unloaded ones. In this manner, it was possible to determine the correspondence between the loaded modes shapes and the unloaded ones, where any doubt had previously existed. As one example of this, a mode existed at 238.22 Hz in configuration 6. This is at a slightly higher frequency than the nearest mode in the unloaded case (237.74 Hz). The mode shapes are almost exactly the same leaving no question that they were the same mode. A second example, is that a mode was found at 257.5 Hz in configuration 7, and here again, matching up the mode shapes confirmed this mode was indeed the same as the one at 252.10 Hz in the unloaded case. In each case, two views of the same mode shape were generated. Examples of these plots are shown in Figures 16 and 17. A complete listing of the program used to make these plots is included in Appendix D. The two views plotted of the first nine mode shapes for the unloaded configuration plus those from the two examples mentioned above, are included in Appendix C.

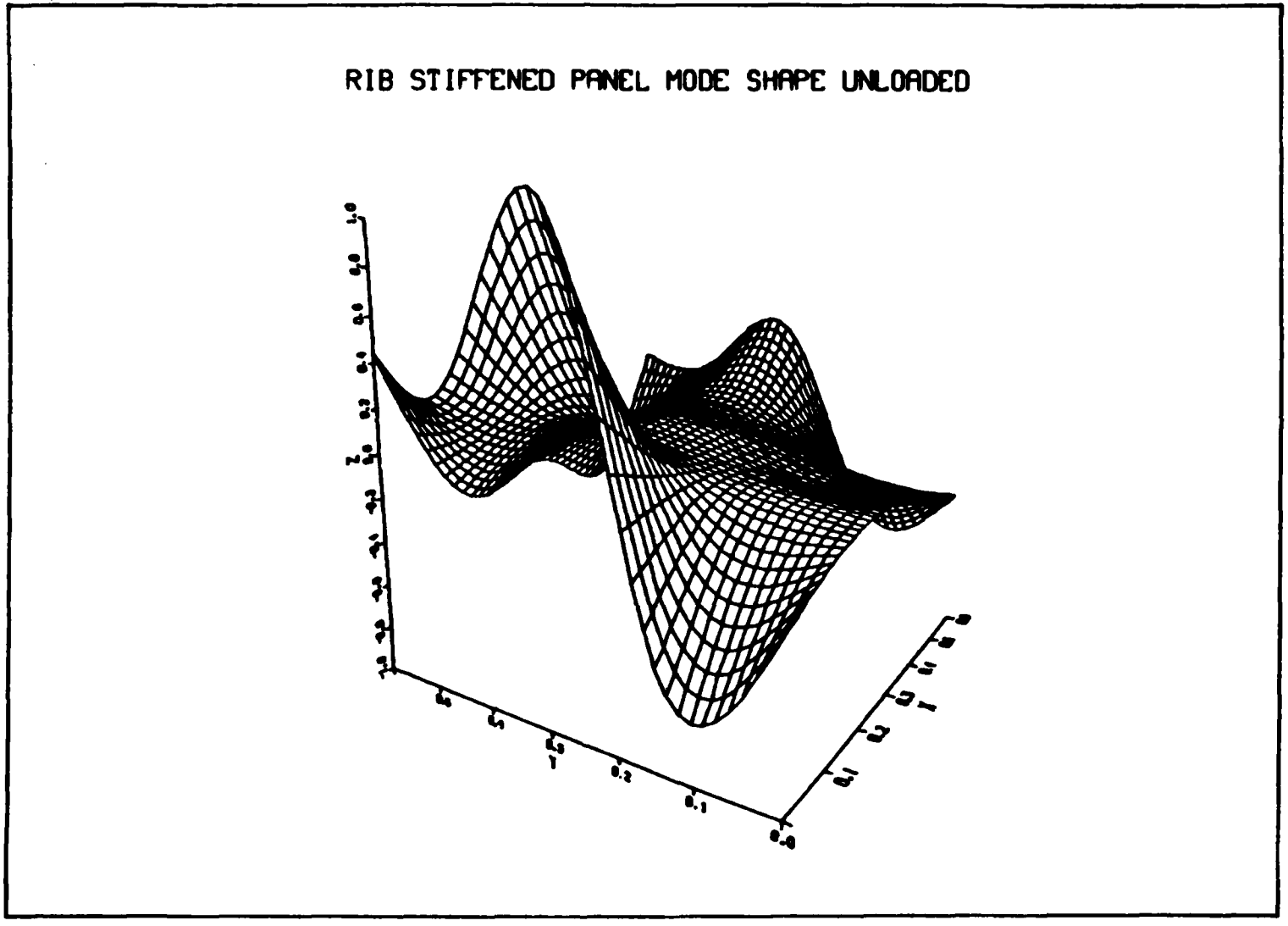

Fig. 16 View 1 - 4th Mode - Unloaded Configuration

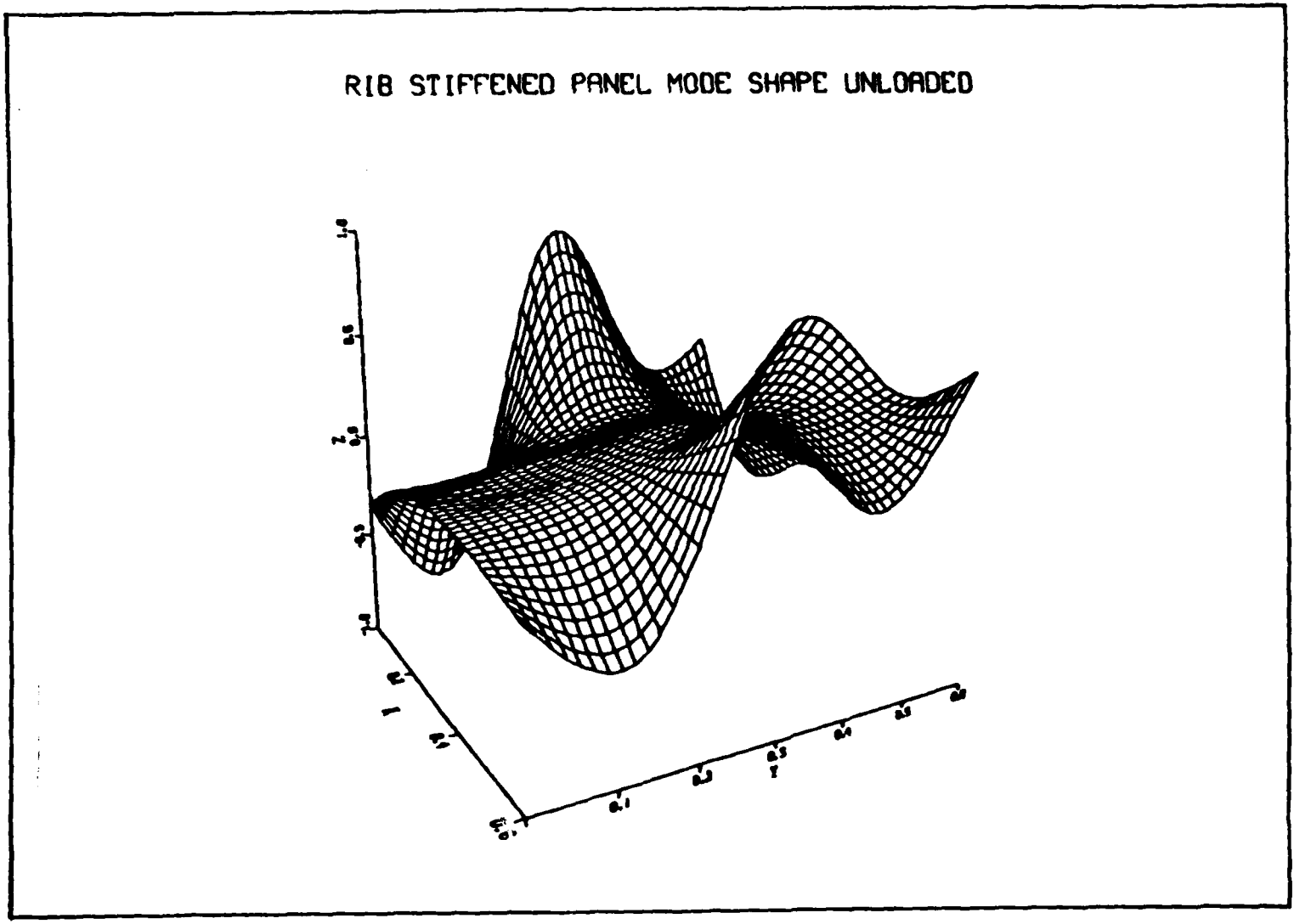

Fig. 17 View 2 - 4th Mode - Unloaded Configuration

V Results

A summary of the test results and significant findings is presented in this section. Table III gives all the experimentally determined natural frequencies for the unloaded and loaded configurations. Some very interesting results were immediately noticeable. The first mode at 167.93 Hz in the unloaded case was suppressed (did not show up at all) in the case of configurations 1, 2, 3, and 4 which, because it is the first mode, should have a significant impact on the forced response, and on the error incurred in the forced response predictions. This was confirmed by plotting the first two or three mode shapes in each case, and matching them up with those for the unloaded case. Also, since there was a chance, albeit remote, that the referenced accelerometer had been placed on a node of the first mode for each configuration, which would cause the mode to seem to disappear, the panel was re-tested in these four configurations with a new reference location. However, the results were unchanged. Also interesting was the fact that for some configurations, some modes were actually shifted upward somewhat infrequency. Modes 5 and 6 of configuration 7 are examples of this. Again, these results were confirmed by plotting these particular mode shapes and comparing them to the corresponding unloaded shapes. In each case, there was no question that the modes matched up as they are shown in Table III. This second phenomenon seems counter intuitive but a possible explanation for it is offered here. It has been found, Talmadge (Ref 8), that in the case of structures such as the panel used in this study that for a given global mode, the individual bays (formed by the stiffeners) often do not all vibrate at exactly the same frequency or amplitude. One of the bay frequencies could be predominant in the unloaded case, but the location of the mass load makes one of the other

Table III NATURAL FREQUENCIES - EXPERIMENTAL

Configuration Number	MODE NUMBER								
	1	2	3	4	5	6	7	8	9
0	167.93	180.50	191.22	207.31	237.74	252.12	280.02	292.83	365.00
1		173.83	184.23	201.05	237.52	253.09	279.79	292.77	364.89
2		174.08	187.62	204.00	225.31	243.32	263.80	282.45	363.08
3		171.40	181.42	210.80	240.70	251.08	280.00	292.22	340.95
4		173.90	183.10	211.50	237.11	252.53	279.63	291.88	341.60
5	167.70	179.53	187.14	202.58	223.92	246.32	273.65	291.19	362.81
6	169.71	180.72	199.30	208.27	238.22	252.20	279.95	292.20	360.20
7	143.10	175.09	184.83	204.30	238.22	257.50	279.88	292.76	361.71
8	153.70	177.02	189.63	205.21	230.94	245.82	273.73	281.02	362.84
9	162.02	177.43	182.71	205.64	237.22	251.43	279.51	292.29	361.48

bays the dominant one. Since it is not unusual for the bay frequencies to be 4 or 5 Hz apart it is very possible to find a loaded mode that is a few Hz higher in frequency than the corresponding unloaded one. The phenomenon of modal suppression however, could not be theoretically explained by the author or any of the test engineers at AFFDL, although it had been encountered in previous testing there. In spite of this, due to two factors, the data was considered to be correct. (1) Since there had been so little previous testing in this area with a structure as complex, and therefore so little knowledge, exactly what to expect is an unknown parameter. (2) Since such care had been taken in gathering the data, and the indications from the MAC functions were that the data was good, the author was confident that the data was reliable.

Tables IV through XII show the comparison between the experimentally determined and the predicted natural frequencies, along with the resulting per cent error of each predicted value. This is shown separately for each configuration. Excluding the four occurrences of complete modal suppression, in all but one case the per cent error was well below 10% and the one case where this is not so, the error is well below 20%. Note that in Table VI (configuration 3) and in Table IX (configuration 6) the predicted natural frequencies for modes 7 and 8 are reversed in order. That is, the predictions reflect that the 8th mode is actually shifted below the 7th mode in frequency. This is not what happens in reality and therefore, the prediction of the eighth natural frequency in both of these cases is considered a major failure on the part of the algorithm, even though the per cent errors in these cases are still only 5.50% and 7.21% respectively. Another interesting phenomenon occurred that should be noted here: that was the occurrence of modes in some mass loaded

Table IV DATA RESULTS - CONFIGURATION 1

MODE	ACTUAL FREQUENCY	PREDICTED FREQUENCY	PERCENT ERROR
1	( )	167.67	( )
2	173.83	179.16	3.07
3	184.23	190.94	3.64
4	201.05	206.88	2.90
5	237.52	237.09	- 0.18
6	253.09	246.89	- 2.45
7	279.79	276.23	- 1.27
8	292,77	292.14	- 0.22
9	364.89	364.18	- 0.19

Table V DATA RESULTS - CONFIGURATION 2

MODE	ACTUAL FREQUENCY	PREDICTED FREQUENCY	PERCENT ERROR
1	( )	167.79	( )
2	174.08	180.15	3.49
3	187.62	191.13	1.87
4	204.00	206.43	1.19
5	225.31	237.37	5.35
6	243.32	251.86	3.51
7	263.80	279.61	5.99
8	282.45	291.95	3.36
9	363.08	362.76	- 0.09

Table VI DATA RESULTS - CONFIGURATION 3

MODE	ACTUAL FREQUENCY	PREDICTED FREQUENCY	PERCENT ERROR
1	( )	166.46	( )
2	171.40	176.36	2.89
3	181.42	191.25	5.42
4	210.80	206.10	- 2.23
5	240.70	235.81	- 0.69
6	251.08	251.51	0.17
7	280.00	278.95	- 0.38
8	292.22	276.16	- 5.50
9	340.95	344.80	1.13

Table VII DATA RESULTS - CONFIGURATION 4

MODE	ACTUAL FREQUENCY	PREDICTED FREQUENCY	PERCENT ERROR
1	( )	167.69	( )
2	173.90	179.03	2.95
3	183.10	190.83	4.22
4	211.50	206.69	- 2.27
5	237.11	236.83	- 0.11
6	252.53	245.04	- 2.97
7	279.63	274.65	- 1.78
8	291.88	292.03	0.05
9	341.60	363.76	6.49

Table VIII DATA RESULTS - CONFIGURATION 5

MODE	ACTUAL FREQUENCY	PREDICTED FREQUENCY	PERCENT ERROR
1	167.70	167.79	0.054
2	179.53	180.10	0.56
3	187.14	190.01	1.53
4	202.58	207.20	2.31
5	223.92	237.32	5.98
6	246.32	251.79	2.22
7	273.65	279.44	2.12
8	291.19	291.77	0.20
9	362.81	361.34	- 0.41

Table IX DATA RESULTS - CONFIGURATION 6

MODE	ACTUAL FREQUENCY	PREDICTED FREQUENCY	PERCENT ERROR
1	169.71	166.22	- 2.06
2	180.72	175.34	- 2.98
3	199.30	191.23	- 4.05
4	208.27	205.63	- 1.27
5	238.22	235.20	- 1.27
6	252.20	251.18	- 0.40
7	279.95	278.44	- 0.54
8	292.20	271.14	- 7.21
9	360.20	338.70	- 6.11

Table X DATA RESULTS - CONFIGURATION 7

MODE	ACTUAL FREQUENCY	PREDICTED FREQUENCY	PERCENT ERROR
1	143.10	167.77	17.24
2	175.09	180.20	2.91
3	184.83	191.16	3.44
4	204.30	206.98	1.31
5	238.22	237.33	- 0.37
6	257.50	250.45	- 2.73
7	279.88	278.70	- 0.42
8	292.76	292.48	- 0.096
9	361.71	364.39	0.74

Table XI DATA RESULTS - CONFIGURATION 8

MODE	ACTUAL FREQUENCY	PREDICTED FREQUENCY	PERCENT ERROR
1	153.70	167.80	9.17
2	177.02	180.41	1.93
3	189.63	191.23	0.86
4	205.21	206.86	0.81
5	230.94	237.50	2.85
6	245.82	251.99	2.52
7	273.73	279.88	2.26
8	281.02	292.36	4.04
9	362.84	363.69	0.25

Table XII DATA RESULTS - CONFIGURATION 9

MODE	ACTUAL FREQUENCY	PREDICTED FREQUENCY	PERCENT ERROR
1	162.02	166.73	2.92
2	177.43	177.77	0.21
3	182.71	191.27	4.69
4	205.64	206.53	0.45
5	237.22	236.48	0.30
6	251.43	251.51	0.044
7	279.51	279.43	- 0.025
8	292.29	281.42	- 3.72
9	361.48	351.59	- 2.74

configurations, that did not show up at all in the unloaded case. For example, there was a mode at 202.7 Hz in configuration 3 and one at 201.0 Hz in configuration 4. However, the author offers the following possible explanation of this phenomenon: the "extra" mode would have been there in the unloaded case, but was so close (in frequency) to another mode that they appeared as one. But these two particular mass loading configurations simply caused them to be shifted apart sufficiently to make one distinguishable from the other. This phenomenon is discussed in Richardson (Ref 9) and it was determined that this is a frequent occurrence in testing of this kind, in a private conversation with the chief test engineer at the Air Force Flight Dynamics Laboratory Talmadge (Ref 8). Therefore, the fact that there was no predicted counterpart for these "extra" modes was not considered an error on the part of the prediction algorithm.

In summary, the algorithm predicted the mass-loaded natural frequencies to within a very small amount of error, excluding those unexplainable occurrences of modal suppression. So, with the exception of those four cases, the results were quite favorable.

VI Discussion

General

In 74 of 81 cases the natural frequencies of the panel were predicted with less than 10% error, and one other was less than 20% error. Of the remaining six cases, four were the occurrences of complete modal suppression which the algorithm has no way of predicting. This would become an obvious shortcoming in the event that this phenomenon occurred on a large number of occasions for one particular structure. But based on the fact that in the case of this particular structure it only happened a total of four times and never occurred more than once for a given mass loaded configuration, the event of numerous such occurrences is unlikely. The last two cases were those of the modal "flip-flopping" in configurations 3 and 6, discussed in the previous chapter. These errors were more than likely due to three factors:

1. For the purposes of the prediction program, the panel was modelled as a flat plate of uniform thickness and density, which was the result of the geometric smearing of the stiffeners discussed earlier.

2. The bi-cubic approximation of the continuous mode shapes were computed only over the surface area covered by the grid, and not the entire surface area of the panel. This was due to the fact that only some and not all of the subroutines employed in this process were capable of approximating values beyond the boundaries of the gathered data.

3. Addition of the point mass loads caused warping of the mode shapes. The loaded mode shapes are not exactly the same as the unloaded ones, and since the unloaded mode shapes are used in the prediction calculations, some error naturally arises.

The first nine natural frequencies were predicted under nine different mass loading conditions. Therefore, a broad array of loading conditions was examined. There does, however, remain some doubt in the author's mind that this spectrum of mass loading conditions was broad enough to conclude with any certainty that this method is effective for all arbitrary mass loading configurations. A careful examination of Table III reveals that the largest change in any of the loaded natural frequencies was only 18.7%. (Coincidentally, this was the case with the largest error between measured and predicted which was equal to 17.24%.) Most of the loaded natural frequencies were altered by only 5% or less from their unloaded counterparts. In light of this, the error margins shown in Tables IV through XII may not be quite as impressive as they look at first glance. It is suspected that if the unloaded frequencies were changed by a significantly greater amount, that these error margins may worsen in direct proportion. The fact that the loaded frequencies were changed by the small amount mentioned is directly attributable to the size of the mass loads used. In defense of this, fairly small mass loads were chosen for two reasons:

1. The panel was suspended from the ceiling by bungy cords in a configuration somewhere between FREE - FREE and SIMPLY SUPPORTED. Due to this, it was thought that it would not require large mass loads to alter the vibration characteristics by an easily measurable amount.

2. On the recommendation of the chief test engineer at AFFDL, who thought that even the largest mass used in this study might be too large, the heavier masses that the author originally planned to use were removed from consideration during this study. In an effort to prove or disprove the hypothesis that the error was directly related to the amount the natural frequencies were modified, the author (at the time of this writing)

returned to the lab and reset-up all the test equipment as shown in Fig 10. Two new masses of significantly larger size than the others were used in one test run each. The first, a .259 Kg rectangular hexahedron, was placed in location 1, denoted configuration 10, as shown in Fig 5. The second, a .592 Kg solid cylinder, was placed in location 3, denoted configuration 11. Each was tested in the same manner as that outlined in Chapter III under "Test Method 3". Then, all the necessary computations were performed on the computer to yield the predicted natural frequencies and the gathered data was reduced to yield the actual values. The results of these, along with the per cent error incurred are included in Tables XIII and XIV.
In order to determine whether or not this additional testing accomplished what it was hoped, these new results were compared to those found using the smaller masses in the same locations. The results from configuration 10 were compared to those from configurations 1, 4, and 7 (all masses in location 1) and the results from configuration 11 were compared to those from configurations 3, 6, and 9 (all masses in location 3). Unfortunately even the heavier masses used did not modify the natural frequencies as much as it was hoped. As a result, this new information was not sufficient to enable any concrete, indisputable conclusions to be drawn. However, some valuable information was gleened from it. Comparing the configurations in the manner stated above, it was seen that for both of these two new cases, the error margins are generally higher than any of the three other respective cases for each. Accordingly, most of the natural frequencies were altered somewhat more than before. This indicated that the accuracy of the algorithm diminishes hand in hand with increasing magnitude of the mass load with respect to panel mass. This performance degradation is not a desirable property, as it means that the algorithm could only be used in cases where

Table XIII DATA RESULTS - CONFIGURATION 10

MODE	ACTUAL FREQUENCY	PREDICTED FREQUENCY	PERCENT ERROR
1	( )	167.59	( )
2	173.13	177.72	2.65
3	183.17	189.83	3.64
4	201.09	205.62	2.25
5	239.25	235.45	- 1.59
6	256.05	240.50	- 6.07
7	280.42	270.96	- 3.37
8	293.71	291.91	- 0.61
9	332.18	362.07	9.00

Table XIV DATA RESULTS - CONFIGURATION 11

MODE	ACTUAL FREQUENCY	PREDICTED FREQUENCY	PERCENT ERROR
1	( )	162.03	( )
2	170.25	167.20	- 1.79
3	180.18	190.86	5.92
4	208.42	200.81	- 3.65
5	239.42	229.67	- 4.07
6	252.90	241.59	- 4.47
7	280.23	273.83	- 2.28
8	293.11	236.81	-19.21
9	311.41	295.48	- 5.12

the mass loads are relatively small, such that they cause little change in the natural frequencies. This area needs to be examined in relation to the forced response, to discover how much error will result in calculating the predicted forced response for a given amount of error in the prediction of the natural frequencies. Such an examination would yield a yardstick for determining how much error in the natural frequencies is acceptable. This is discussed briefly in the section that follows.

Forced Response

This section develops a method of calculating the Power Spectrum of the forced response for a hypothetical case where the forcing function is a white noise process. Then, since comparing two power spectra to determine any error incurred would require plotting in 4 - dimensions, the RMS (Root Mean Square) value of the forced response is calculated, giving a good indicator of the overall difference between two forced responses. A "best case" and "worst case" error model is then examined for a constant error in all predicted natural frequencies. It should be noted here that no comparison of the actual versus predicted forced response could be done during the course of this study due to the manner in which the experimental testing was conducted. The force input excitation finally used after encountering the problems outlined in Chapter III of this study was fifteen impulse excitations of random strength and location. Since these inputs were not one of the parameters measured (response at two points, reference and one data point, were measured) there was no known way to calculate the actual system transfer function or to compute statistical information (such as the Power Spectrum) of the input. Without this information, the experimental forced response could not be computed and therefore could not be compared to any predicted forced response.

$$S_w(x,y,\omega) = \sum_{j=1}^{n} \left\{ \frac{M_o N_o \phi_j(x_o,y_o)\phi_j(x,y)}{(\omega^2{}_j - \omega^2)^2 + (.1\omega\omega_j)^2} \right\} \qquad (26c)$$

d. Integrate over all frequencies to yield the RMS value of the responses (also called average power):

$$E\{x(t)Y(t)\} = R_{xy}(o)$$

$$R_{xy}(o) = \int_{-\infty}^{\infty} \left[\sum_{j=1}^{n} \left\{ \frac{M_o N_o \phi_j(x_o,y_o)\phi_j(x,y)}{(\omega_j{}^2 - \omega^2) + (.1\omega\omega_j)^2} \right\} \right] d\omega$$

$$= \sum_{j=1}^{n} \phi_j(x_o,y_o)\,\phi_j(x,y) M_o N_o \int_{-\infty}^{\infty} \frac{d\omega}{(\omega_j{}^2 - \omega^2)^2 + (.1\omega\omega_j)^2}$$

$$= \sum_{j=1}^{n} M_o N_o \phi_j(x_o,y_o)\phi_j(x,y) \left\{ \frac{\pi}{4(.1)\omega_j{}^2} \right\}$$

$$= \frac{\pi M_o N_o}{.4} \sum_{j=1}^{n} \frac{\phi_j(x_o,y_o)\,\phi_j(x,y)}{\omega_j{}^2}$$

$$R_{xy}(o) = (1.5\pi M_o N_o) \sum_{j=1}^{n} \frac{\phi_j(x_o,y_o)\,\phi_j(x,y)}{\omega_j{}^2} \qquad (27)$$

Error Model

a. Worst case. The worst error was in configuration 11, and it was -19.21%. So, if it is assumed that all predicted frequencies are 20% low:

let n=9 as in this study

$$R_{xy}(o) = 1.5\pi\, M_o N_o \sum_{j=1}^{9} \frac{\phi_j(x_o,y_o)\,\phi_j(x,y)}{(.8\,\omega_j)^2}$$

$$= 1.5\pi\, M_o N_o \sum_{j=1}^{9} \frac{\phi_j(x_o,y_o)\phi_j(x,y)}{64\omega_j{}^2}$$

Development. From Bogdanoff (Ref 1) we have:

$$S_w(x,y,\omega) = \sum_{j=1}^{n} \{[\int_{oo}^{ba} P(x,y)\phi_j(x,y)dxdy\ S_i(\omega)\phi_j(x,y)]|H(\omega)|^2\} \qquad (25)$$

where: $P(x,y)$ = panel loading as a function of x and y

$\phi_j(x,y)$ = unloaded mode shapes

$S_i(\omega)$ = Power Spectrum the Forced Input

$H(\omega)$ = System Transfer Function

n = number of modes being considered

$S_w(x,y,\omega)$ = Power Spectrum of the response as a function of x, y, and frequency

a. Substituting in expression for the System Transfer Function:

$$H(\omega) = \frac{1}{\omega_j^2 - \omega^2 + 2j\zeta\omega\omega_j}$$

where ω_j = panel natural frequencies

ζ = damping factor chosen = .05

$$S_w(x,y,\omega) = \sum_{j=1}^{n} \{\frac{\int_{oo}^{ba} P(x,y)\phi_j(x,y)dxdy S_i(\omega)\phi_j(x,y)}{(\omega^2_j - \omega^2)^2 + (2(.05)\omega\omega_j)^2}\} \qquad (26a)$$

b. Substitute in expression for Panel Loading and Integrate:

for point mass loading:

$$P(x,y) = M_o\delta(x_o,y_o)$$

where M_o = magnitude of mass load

δ = dirac delta function

$$Sw(x,y,\omega) = \sum_{j=1}^{n} \{\frac{(M_o\phi_j(x_o,y_o))(S_i(\omega)\phi_j(x,y)}{(\omega_j^2-\omega^2)^2 + (0.1\ \omega\omega_j)^2}\} \qquad (26b)$$

c. Modelling random noise input as a white noise process:

$S_i(\omega) = N_o$

$$= \frac{1}{.64} \{1.5M_o N_o \sum_{j=1}^{9} \frac{\phi_j(x_o,y_o)\phi_j(x,y)}{\omega_j^2}$$

$$= \frac{1}{.64} R_{xy}(o)_{correct}$$

$$= 1.563\ R_{xy}(o)_{correct}$$

Therefore, if the natural frequencies were all predicted 20% below their true values, the predicted RMS value of the response is 56.3% higher than the true value (note that this discounts any error that is a result of mode shape warping due to the mass load which will result because unloaded mode shapes are used in this prediction). This amount of error is obviously unacceptable.

b. Best case. Again, looking at configuration 11, the smallest error incurred was -1.79%. Therefore, assuming that the predictions are all only 2% low:

$$R_{xy}(o) = 1.5\pi\ M_o N_o \sum_{j=1}^{9} \frac{\phi_j(x_o,y_o)\phi_j(x,y)}{(.98\omega_j)^2}$$

$$= 1.5\pi\ M_o N_o \sum_{j=1}^{9} \frac{\phi_j(x_o,y_o)\phi_j(x,y)}{.96\omega_j^2}$$

$$= \frac{1}{.96} \{1.5\pi\ M_o N_o \sum_{j=1}^{9} \frac{\phi_j(x_o,y_o)\phi_j(x,y)}{\omega_j^2}\}$$

$$= \frac{1}{.96} R_{xy}(o)_{correct}$$

$$= 1.042\ R_{xy}(o)_{correct}$$

This time only a 4.2% error results which for most applications would be an acceptable value.

c. General Result

$$E = \{[\frac{1}{(1+\varepsilon)^2} - 1] \times 100\} \% \qquad (28)$$

E = overall error in the prediction of RMS value of response

ε = % error of natural frequency predictions expressed as a decimal

Note that this hold only if all predictions are in error by the same amount and all are either high or low. If any of these conditions do not hold, then Eq (24) must be solved implicitly to determine the exact error (requires a computer program, as the calculation involves operations on 3-dimensional mode shapes). It is also important to notice that in the most of the 11 configurations finally tested, some of the errors are positive, and some are negative. In cases like that, some large errors may be acceptable as they will have a cancelling effect if the signs are opposite from one another.

Using this "yardstick" to examine the error in the output forced response of the nine original configurations, the two worst cases would be 6 (all errors negative - i.e., all predictions low) and 8 (all errors positive).

i. Configuration 6. The highest errors were -7.21, and -6.11, but these occurred on the two highest order modes where the magnitude of the natural frequencies lessens their importance in the summation (24). Therefore, consider the average error = -2.88% (simply an algebraic average of all the errors in configuration 6).

$$E = \left[\frac{1}{(1-.0288)^2} - 1\right] \times (100)$$

$$= 6.011\ \%$$

which is an acceptable error.

ii. Configuration 8. Here the largest error = 9.17% and is on the first or most important term so to yield an indication of what to expect a weighted average is computed by doubling this worst error. Now average error = +4.17%

$$E = \left[\frac{1}{(1 + .0417)^2} - 1\right] \times (100)$$

$$= -7.846\%$$

which is also acceptable.

One must remember that these are only good indications of what the actual error would be. Since all the errors are differenct, Eq (27) must be solved implicitly to find exact error. However, these figures provide a reliable figure upon which some conclusions can be made. These are discussed in the section that follows. It is also important not to forget that these calculations determine only the error resulting from the inexact predictions of the natural frequencies, and do not consider those due to mode shape warping. This error can only be found by comparing the predicted forced response, and the experimentally determined one. As was discussed earlier, this was not possible during the course of this study, and must be left to future research. Also, from an examination of Eq (27) it must be noted that since the first mode is divided by the lowest number (lowest frequency) its suppression is likely to have significant effect

on the forced response which will cause a large error in the prediction as the algorithm does not predict its disappearance. Exactly how large this error is, must also be left to future studies.

VII Conclusions & Recommendations

Conclusions

The following conclusions can be stated regarding the use of the algorithm as a means of predicting mass loaded natural frequencies of complex structures:

1) The algorithm is both effective and accurate for predicting the mass loaded natural frequencies when the lumped masses are of the same relative magnitudes as those used during the course of this study (up to 20% of total panel mass).

2) On the basis of the forced response error model calculations the algorithm also yields acceptably small errors in estimating the forced response.

3) Some mass loading configurations cause the suppression of the first mode which will have a significant effect both on the forced response of the structure and on the error of the prediction.

4) Results indicate that as the relative magnitudes of the mass loads increase so do the errors in predicting the natural frequencies and therefore the forced response. So, the applications of the algorithm are limited to comparatively small loads.

5) The rate at which these errors increase seems to depend not only upon the magnitude of the added mass, but also on its location on the panel surface and radii of gyration. This is borne out by the fact that in the case of the rectangular .259 Kg mass errors increased in almost exactly direct proportion to the increase in mass, but for the cylindrical .592 Kg mass, the average error increased at only slightly greater than half the rate of increasing mass.

Recommendations

It is recommended that further studies be conducted to determine the following:

1) An exact measure of the accuracy of this method as a means of predicting the forced response of complex structures, and the effect of suppressed modes. To accomplish this, a different test method than the one finally employed here should be used. There are two recommended test procedures outlined in Appendix F. Both are capable of supplying all information necessary to compute the experimental force response. Briefly, these methods are:

a. Use exactly the same test procedure as was outlined earlier under Test Method 1, but with a new data processing method (called "Overlap Processing") that was not available at the time of this study.

b. A classic approach using an impulse hammer with a force gauge to measure the input force, and an accelerometer to measure output response. The Fourier analyzer does all data processing.

Once the experimental response has been computed, the predicted force response can be calculated using the development given in the previous Chapter, and then the two can be compared. In these future tests, it is also suggested the grid layout of accelerometer locations be extended to the edges of the test specimen. This will eliminate the error incurred by excluding the edges of the panel from the bi-cubic spline continuous mode shape calculations, as discussed in the previous chapter.

2) The limitations, in terms of the relative magnitudes of the mass loads on the capability of the algorithm to predict the natural frequencies to within acceptable errors. In other words, since indications are that

the accuracy of the algorithm decreases as the size of the mass loads is increased, there is a limit to the algorithm's effectiveness. Beyond this limit, a different method will have to be used.

Bibliography

1. Bogdanoff, J.L. and Goldberg, J.E., "On the Bernoulli - Euler Beam Theory with Random Excitation", Journal of the Aero/Space Sciencies, May 1969, pp. 371-376.

2. Eringen, A.C., "Response of Beams and Plates to Random Loads", Journal of Applied Mechanics, March 1957, pp. 46-51.

3. Henderson, D.A., Whaley, P.W., and Brown, D.L., "Test Report on Modal Survey of a Massloaded, Cantilevered Flat Plate", AFFDL/FBG/78-3, April 1978.

4. Hewlett Packard, "HP5451 B Fourier Analyzer", Operating and Service Manuals, Vol. 1-8, Hewlett Packard Co., January 1974.

5. Lee, J. and Whaley, P.W., "Prediction of the Angular Vibration of Aircraft Structures", Journal of Sound and Vibration, Vol. 49(4), 1976, pp. 541-549.

6. Pomazal, R.J., and Snyder, V.W., "Local Modifications of Damped Linear Systems", AIAA Journal, Vol. 9, No. 11, November 1971, pp. 2216-2221.

7. Private conversation, Prof. D. Brown, Head Mechanical Eng. Dept., University of Cincinnati, 14 July 1979.

8. Private conversation, Mr. R. Talmadge, Test Engineer, AFFDL, 16 August 1979.

9. Richardson, M., "Modal Analysis Using Digital Test Systems", Seminar on Understanding Digital Control and Analysis in Vibration Test Systems, Published by the Shock & Vibration Information Center, 1976.

10. Thomson, W.T., Vibration Theory and Applications, Englewood Cliffs, New Jersey, 1965.

11. Timoshenko, S., Yound, D.H., and Weaver, Jr., W., Vibration Problems in Engineering, 4th Edition, New York, 1974.

12. Weissenburger, J.T., "Effect of Local Modifications on the Vibration Characteristics of Linear Systems", Journal of Applied Mechanics, Vol. 35, June 1968, pp. 327-332.

13. Whaley, P.W., "Calculation of Natural Frequencies and Mode Shapes of Mass Loaded Aircraft Structures", Shock and Vibration Bulletin, No. 48, Pt. 3, 1978, pp. 13-20.

14. Whaley, P.W., "Prediction of the Change in Natural Frequency of a Cantilevered Flat Plate with added Lumped Mass", Not Yet Published.

15. , "Overlap Processing", Spectral Dynamics Corporation, DSP-022, June 1978.

Appendix A

Plots of Power Spectral Densities for Unloaded Case

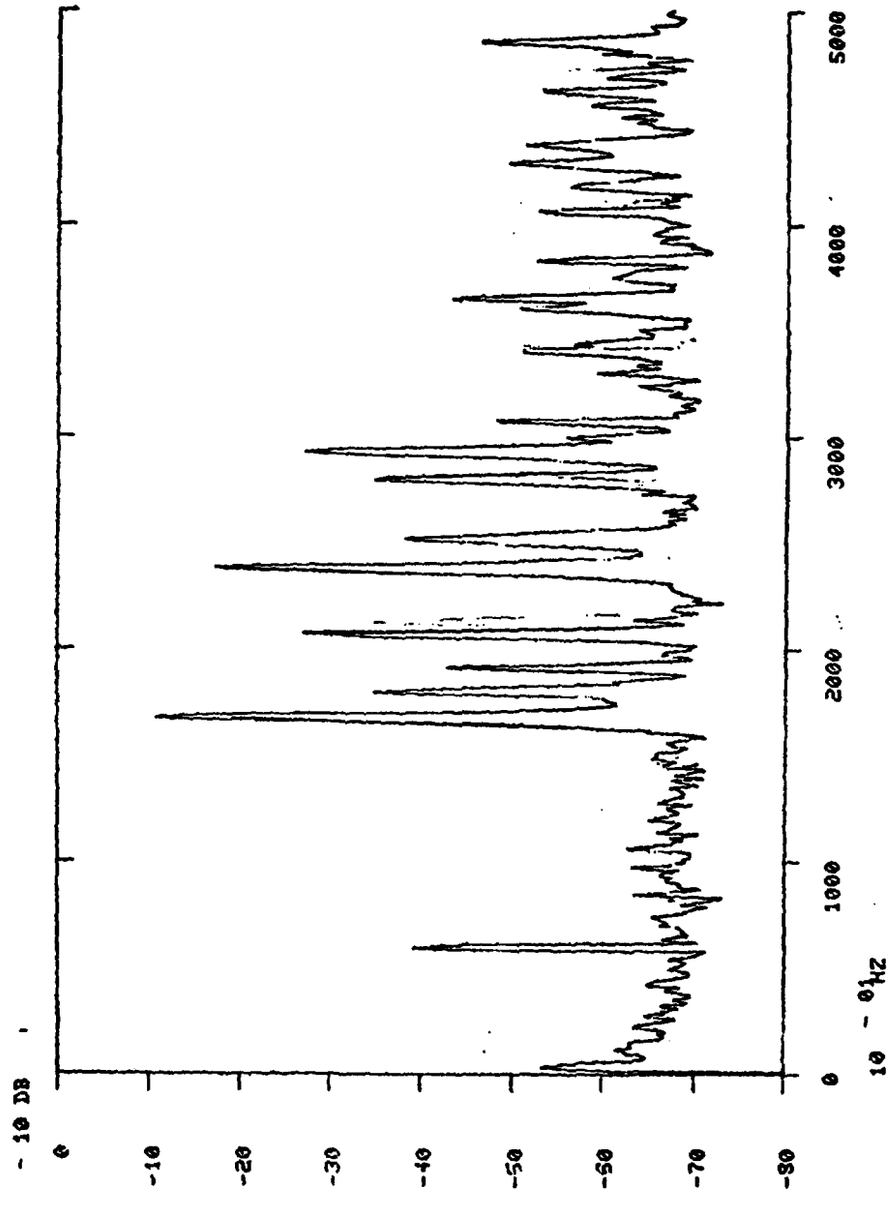

Fig. A-1 PSD Plot - Point (1,1)

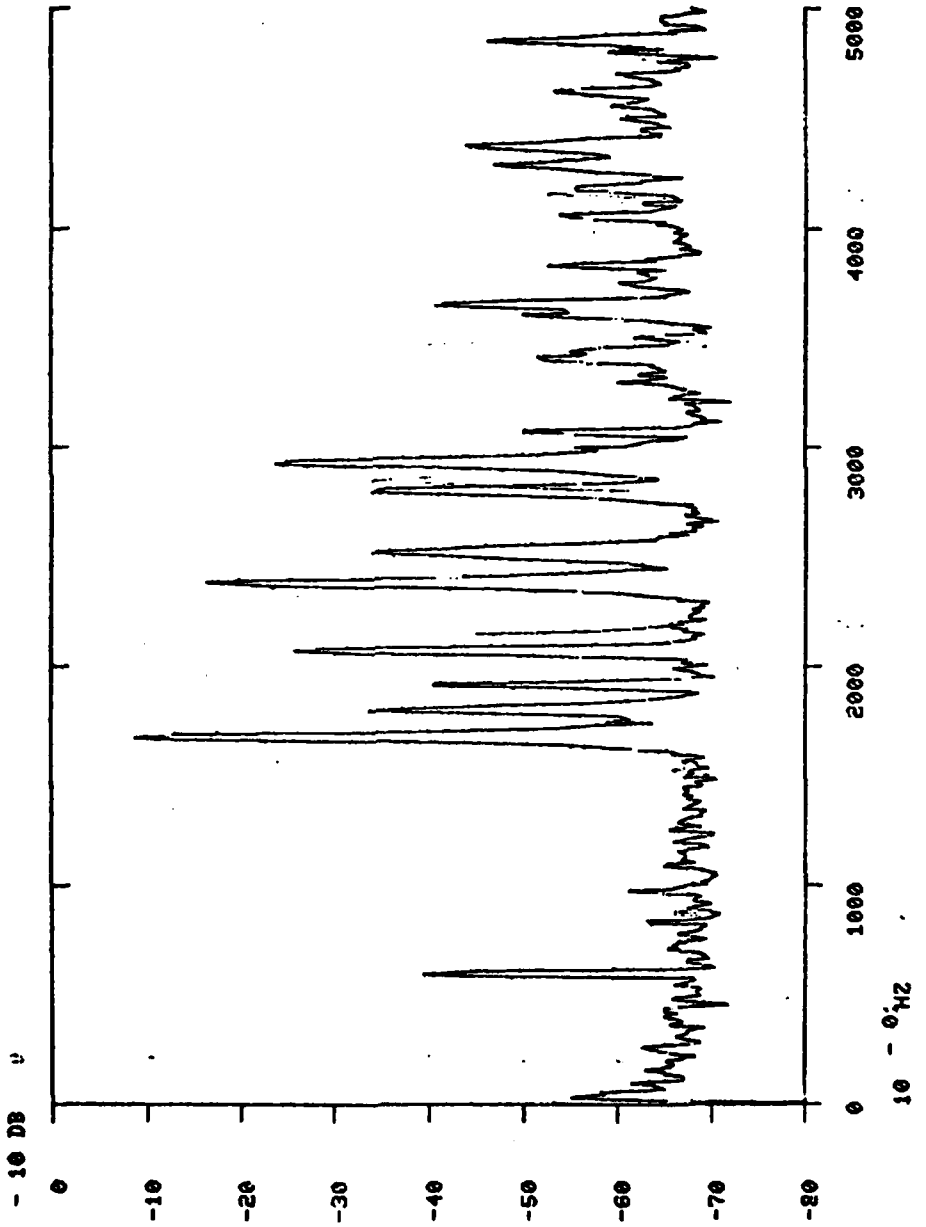

Fig. A-2 PSD Plot - Point (1,2)

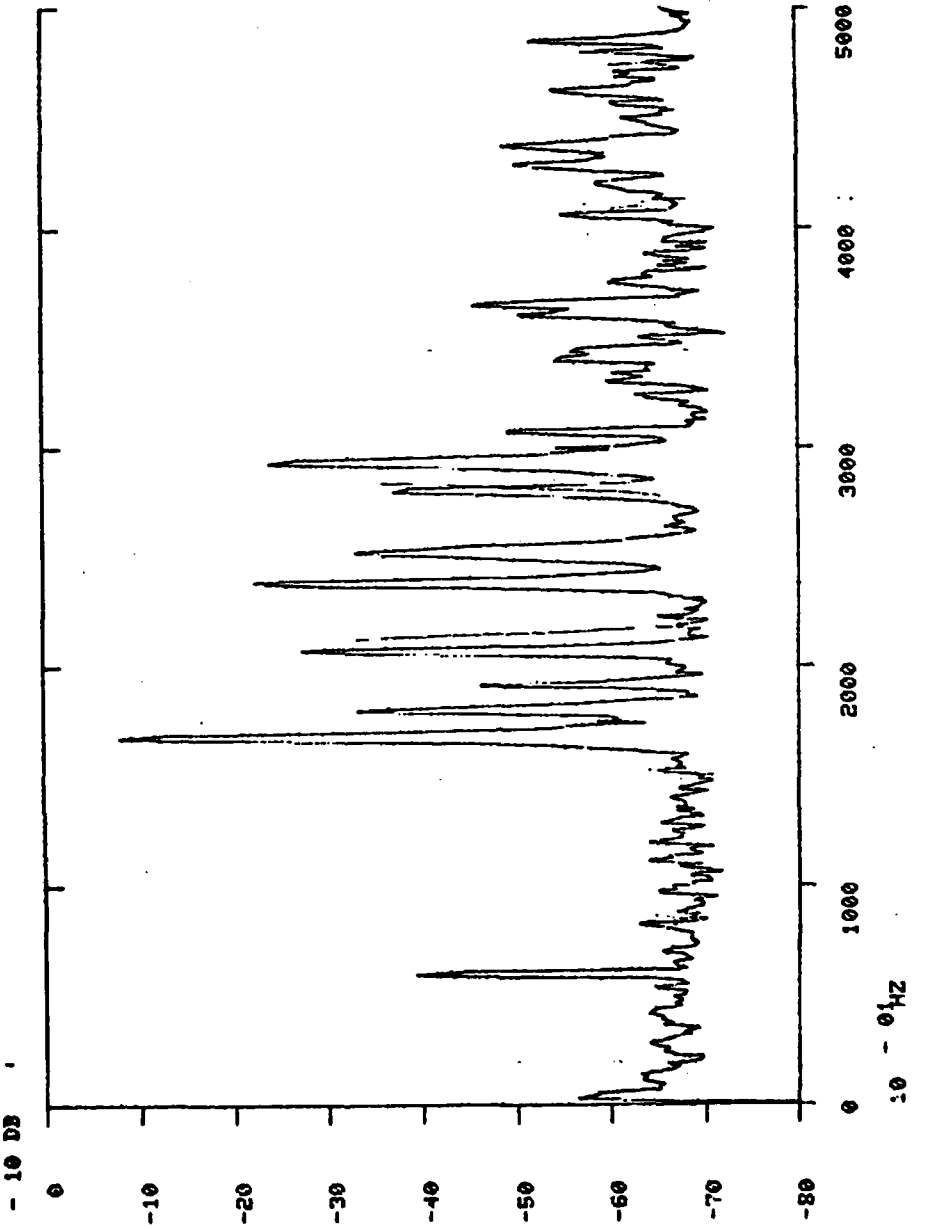

Fig. A-3 PSD Plot - Point (1,3)

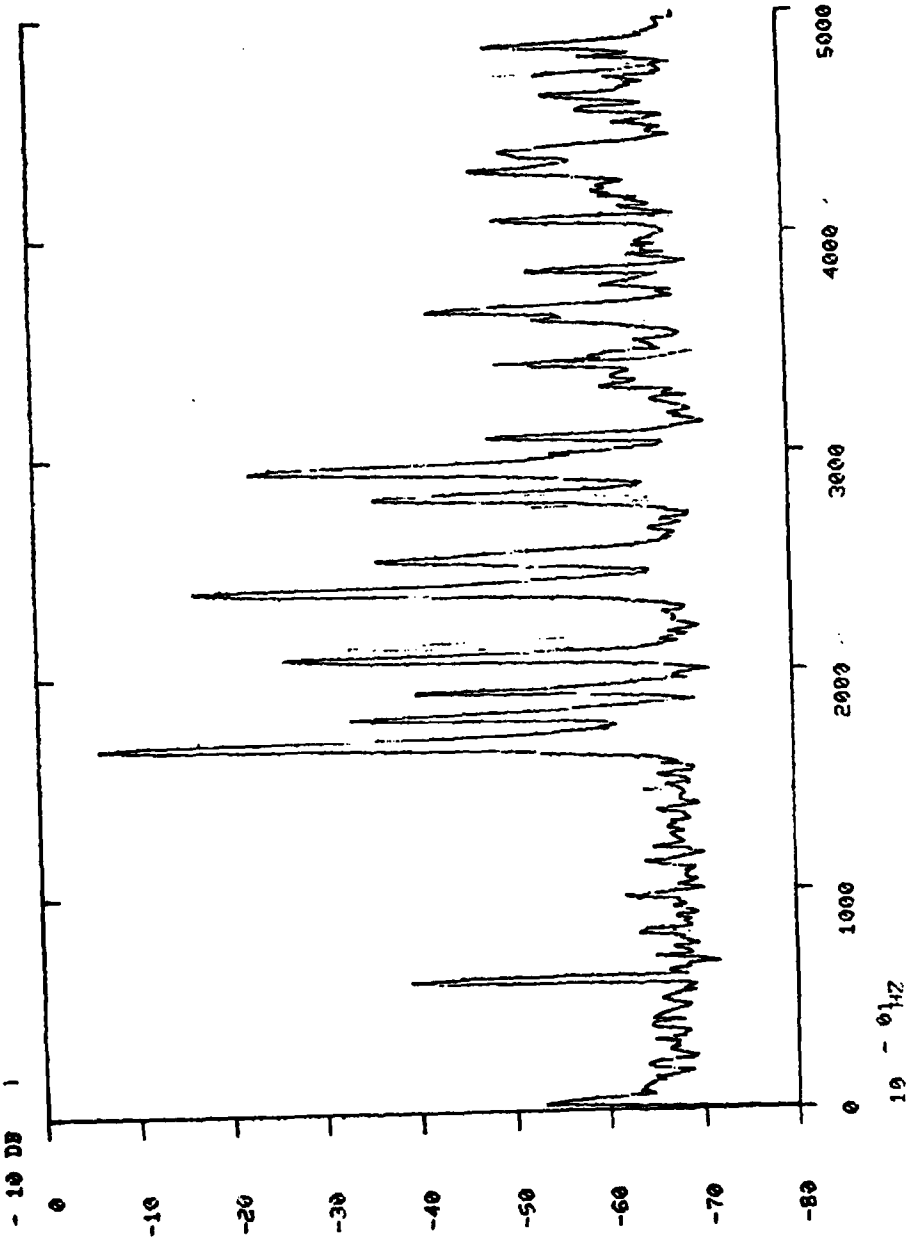

Fig. A-4 PSD Plot - Point (1,4)

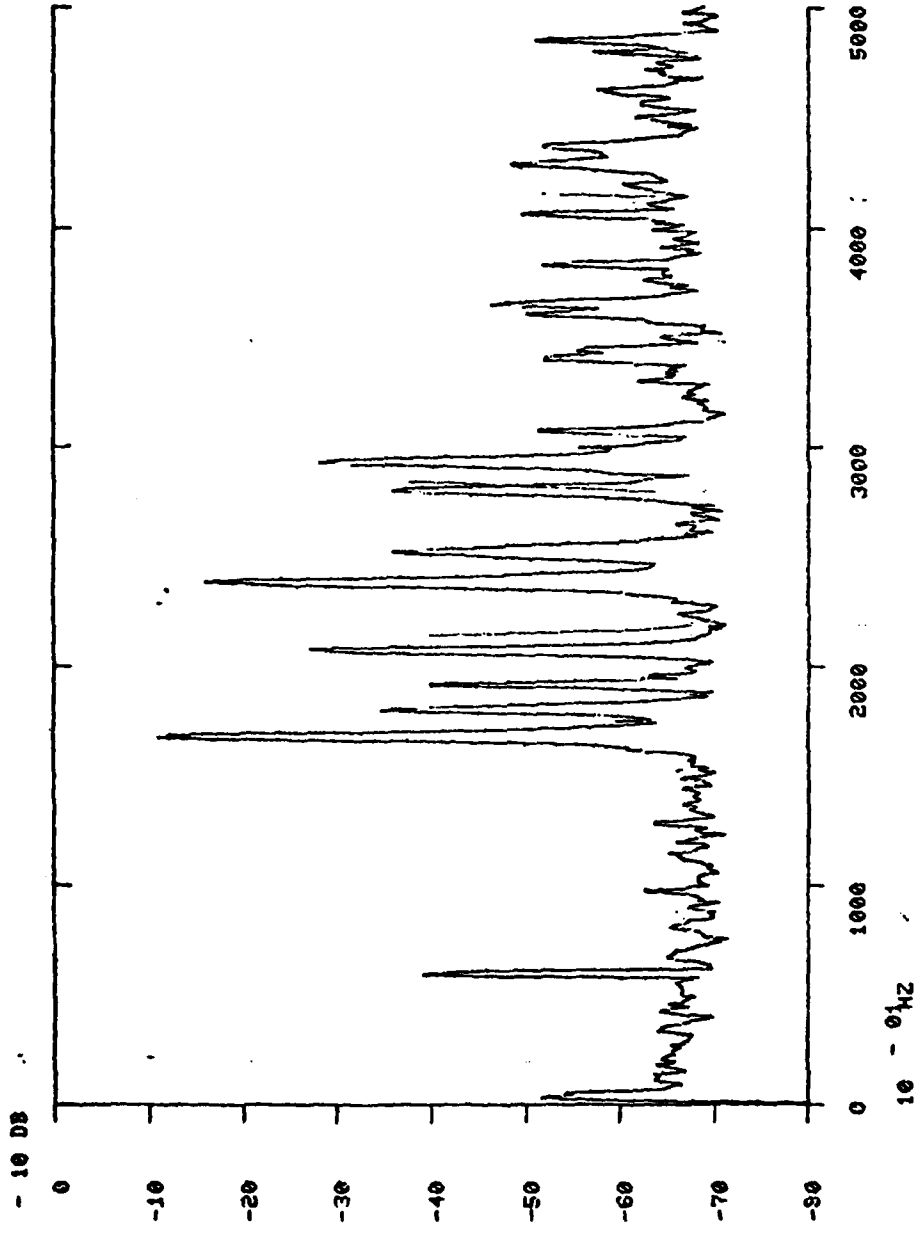

Fig. A-5 PSD Plot - Point (1,5)

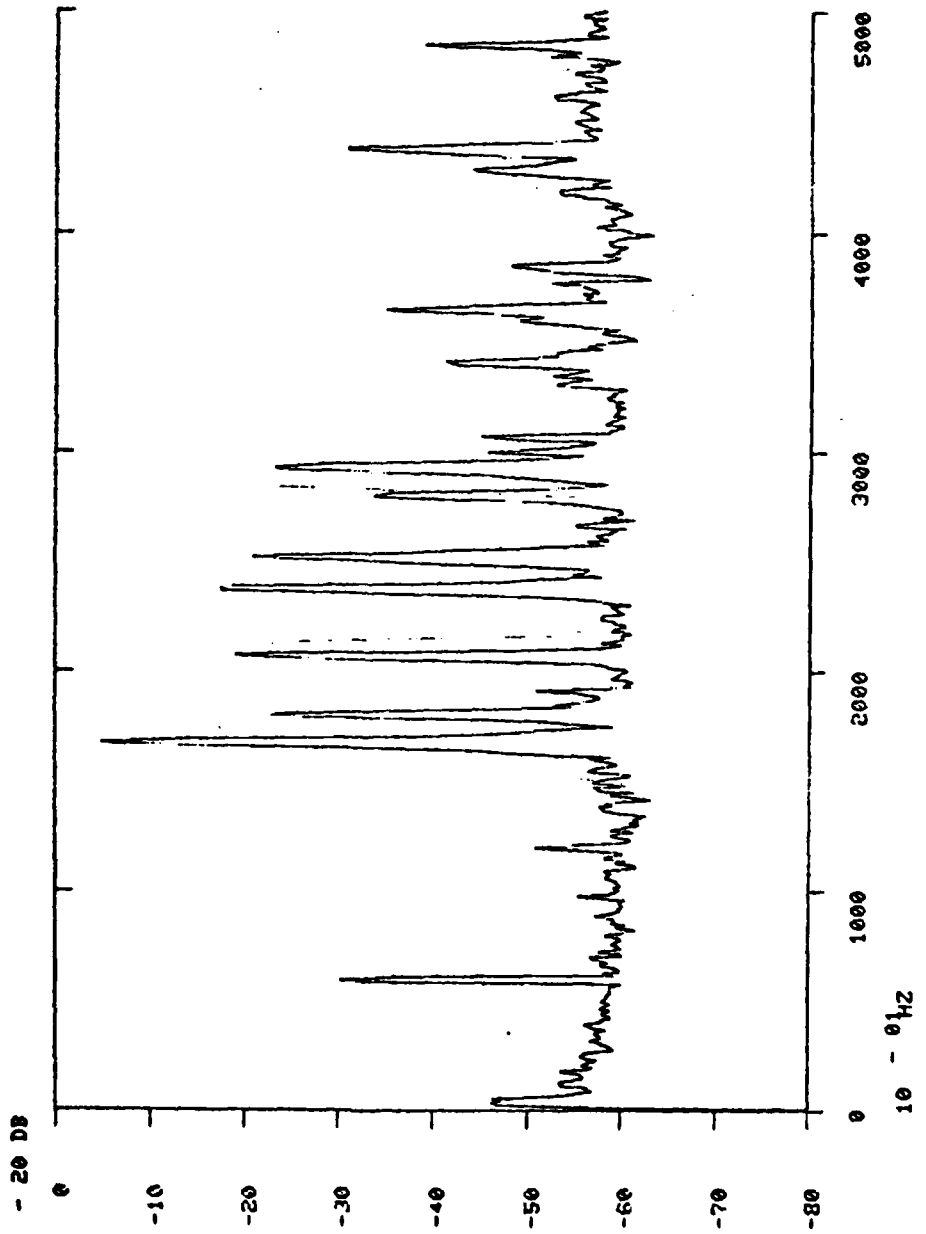

Fig. A-6 PSD Plot - Point (2,1)

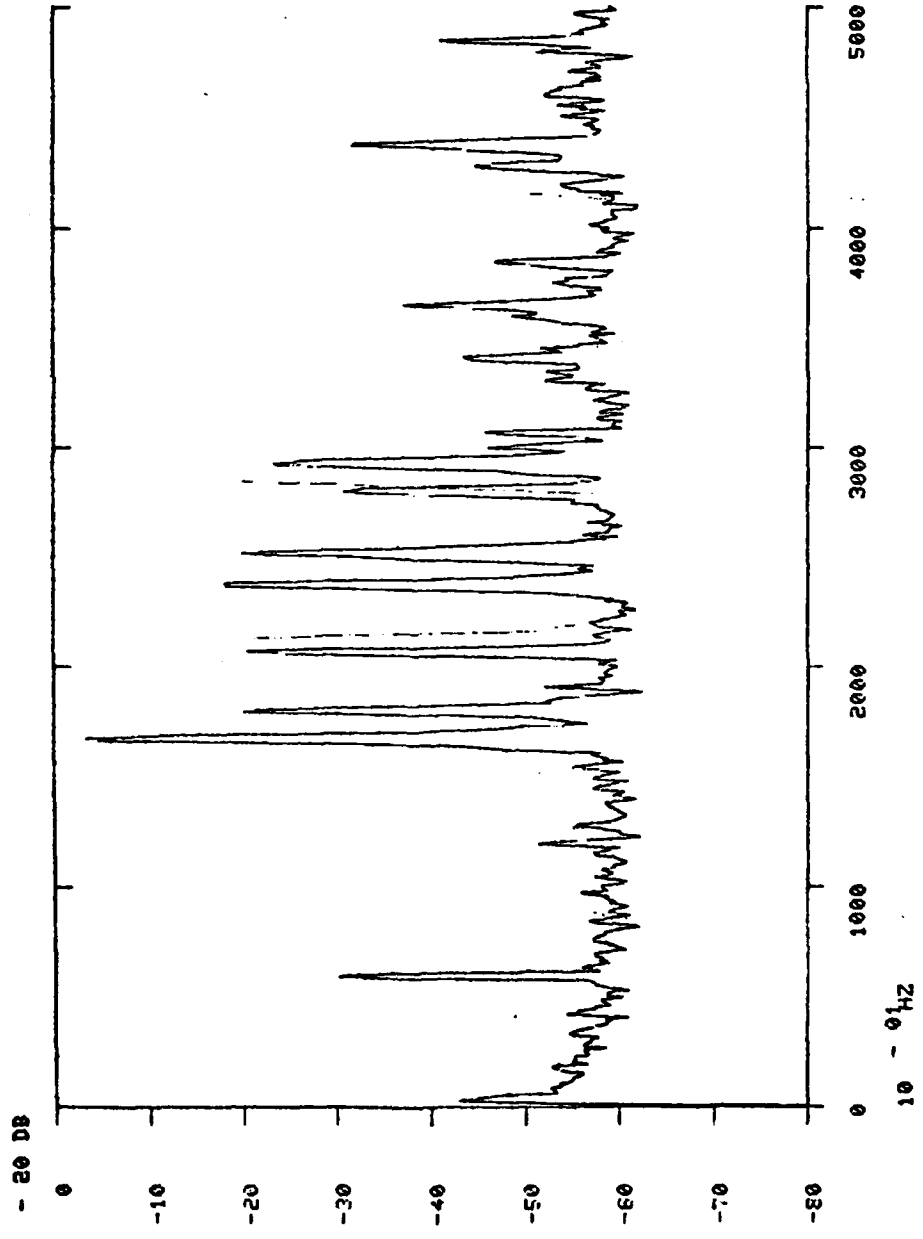

Fig. A-7 PSD Plot - Point (2,2)

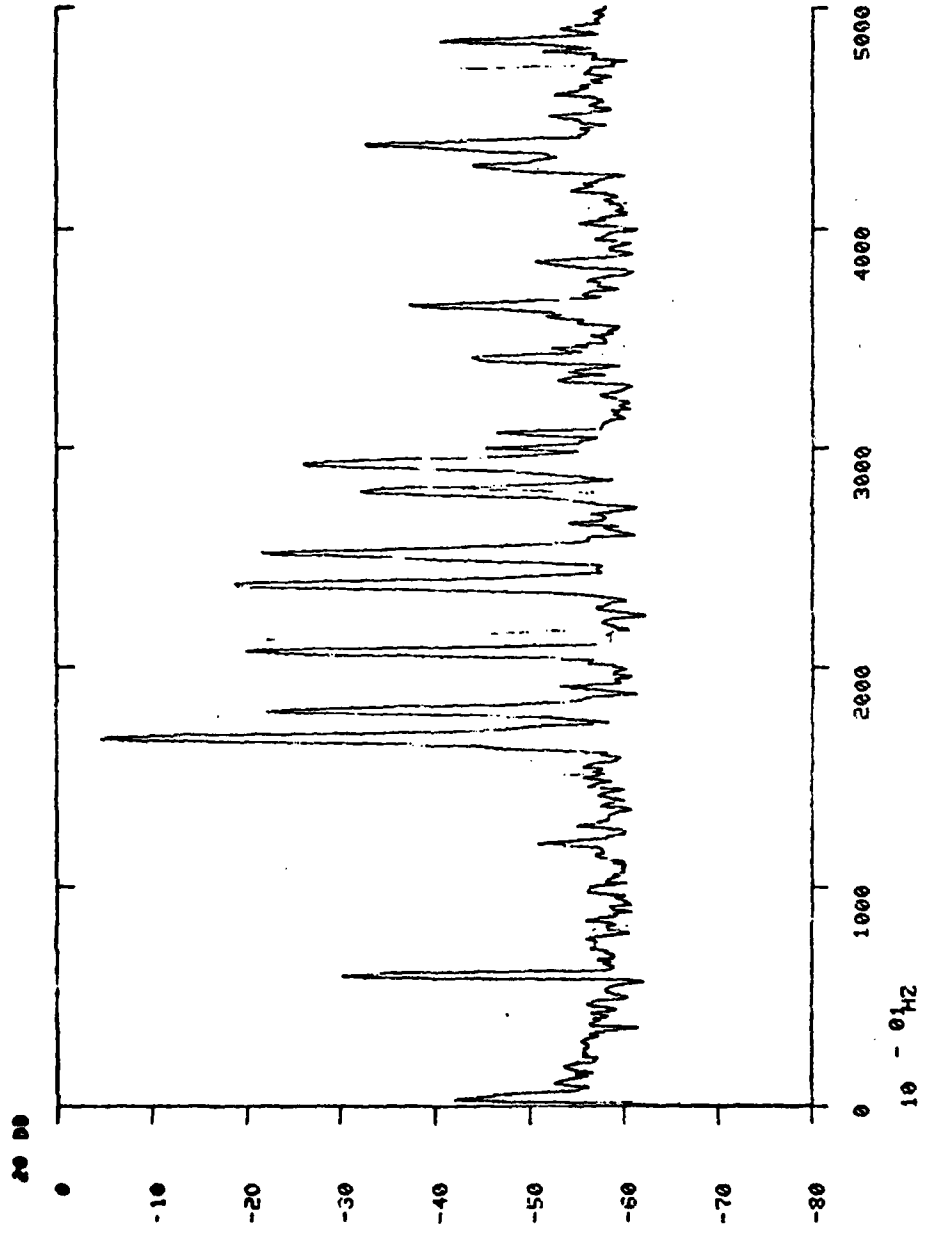

Fig. A-8 PSD Plot - Point (2,3)

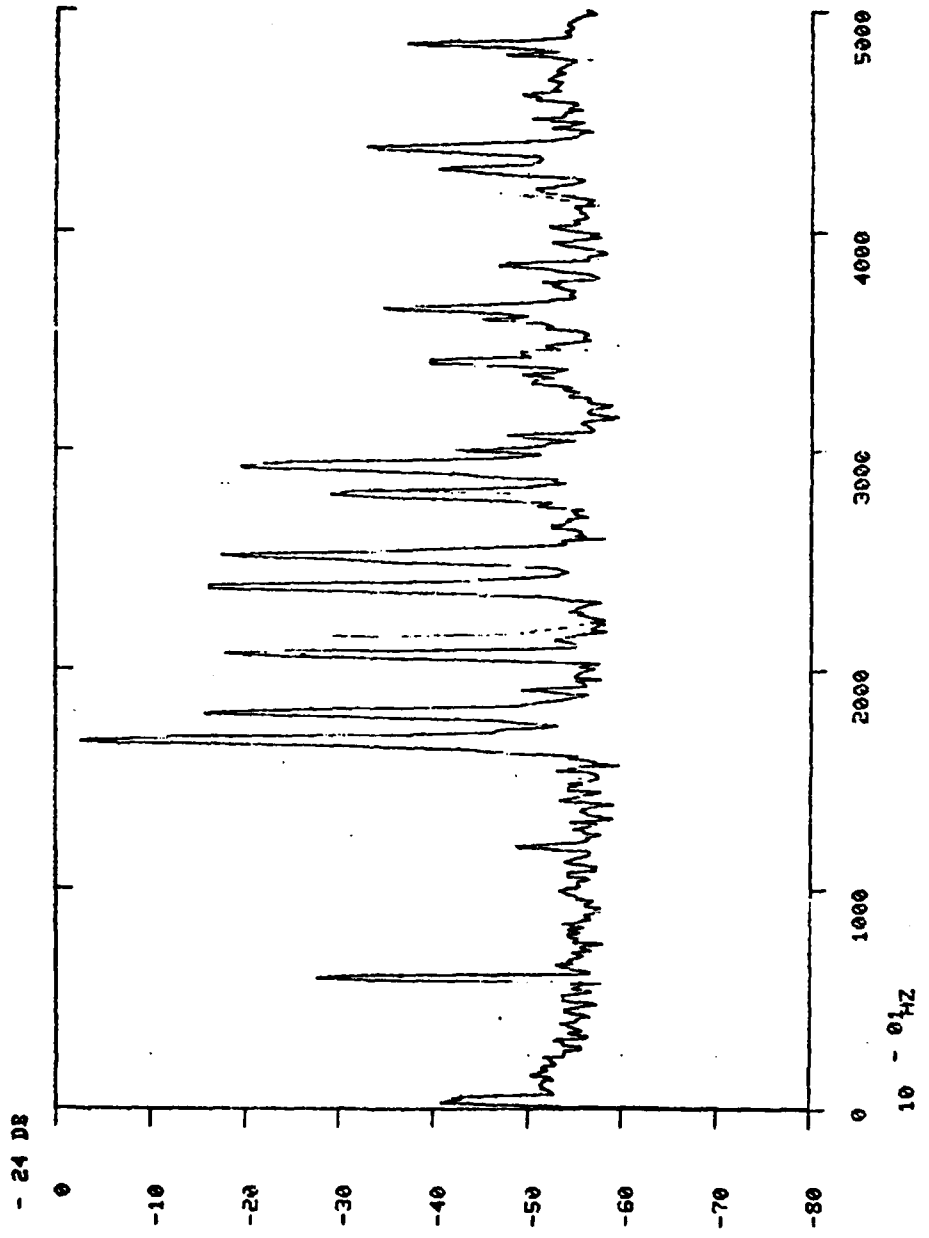

Fig. A-9 PSD Plot - Point (2,4)

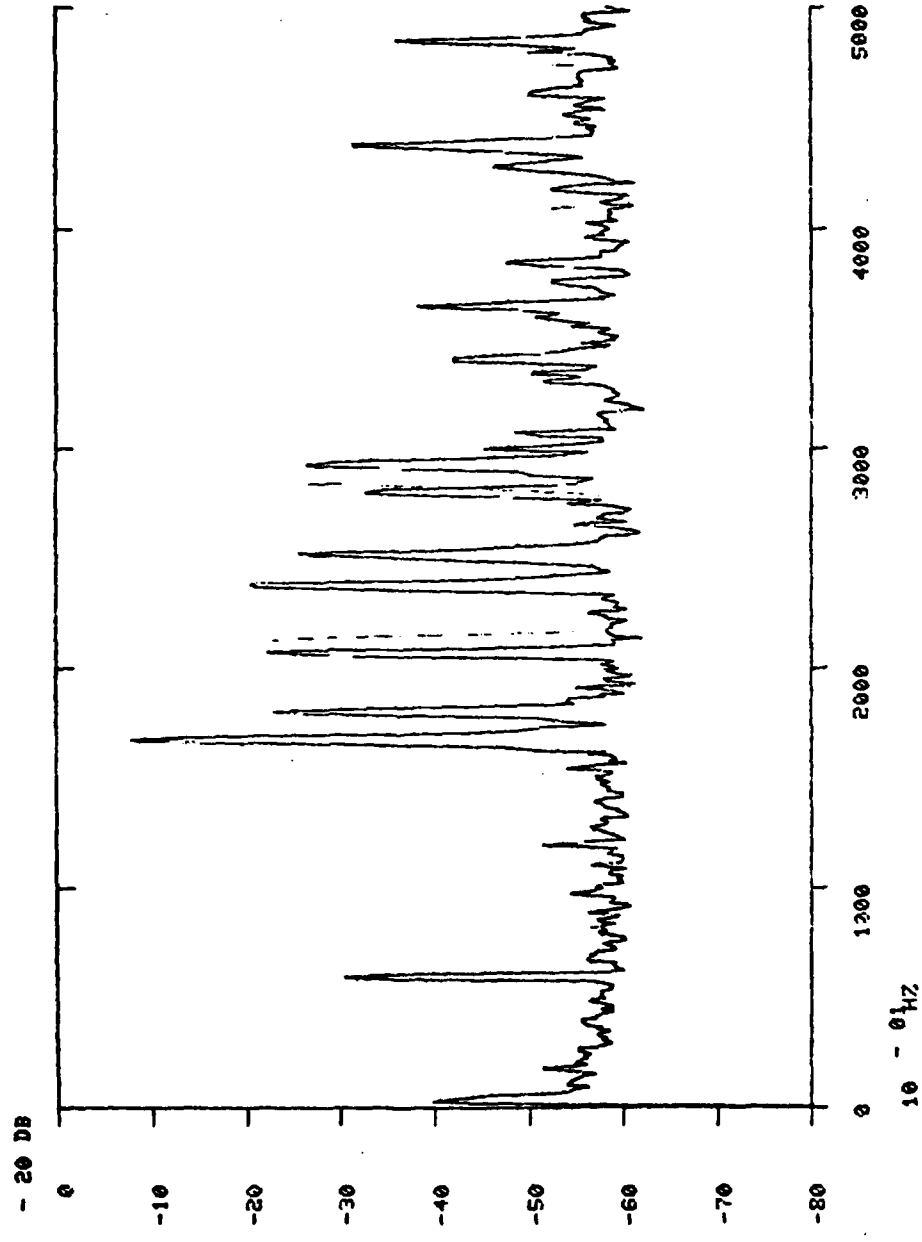

Fig. A-10 PSD Plot - Point (2,5)

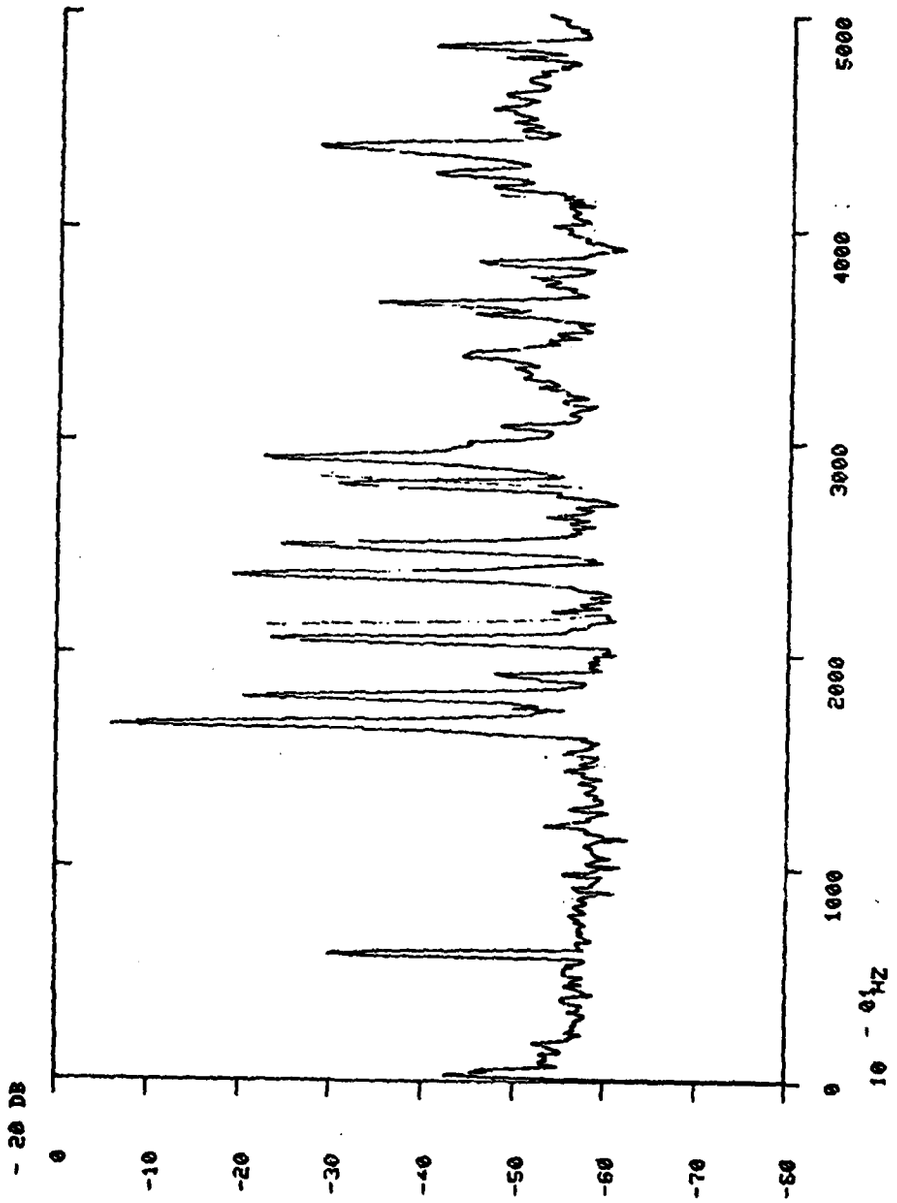

Fig. A-11 PSD Plot - Point (3,1)

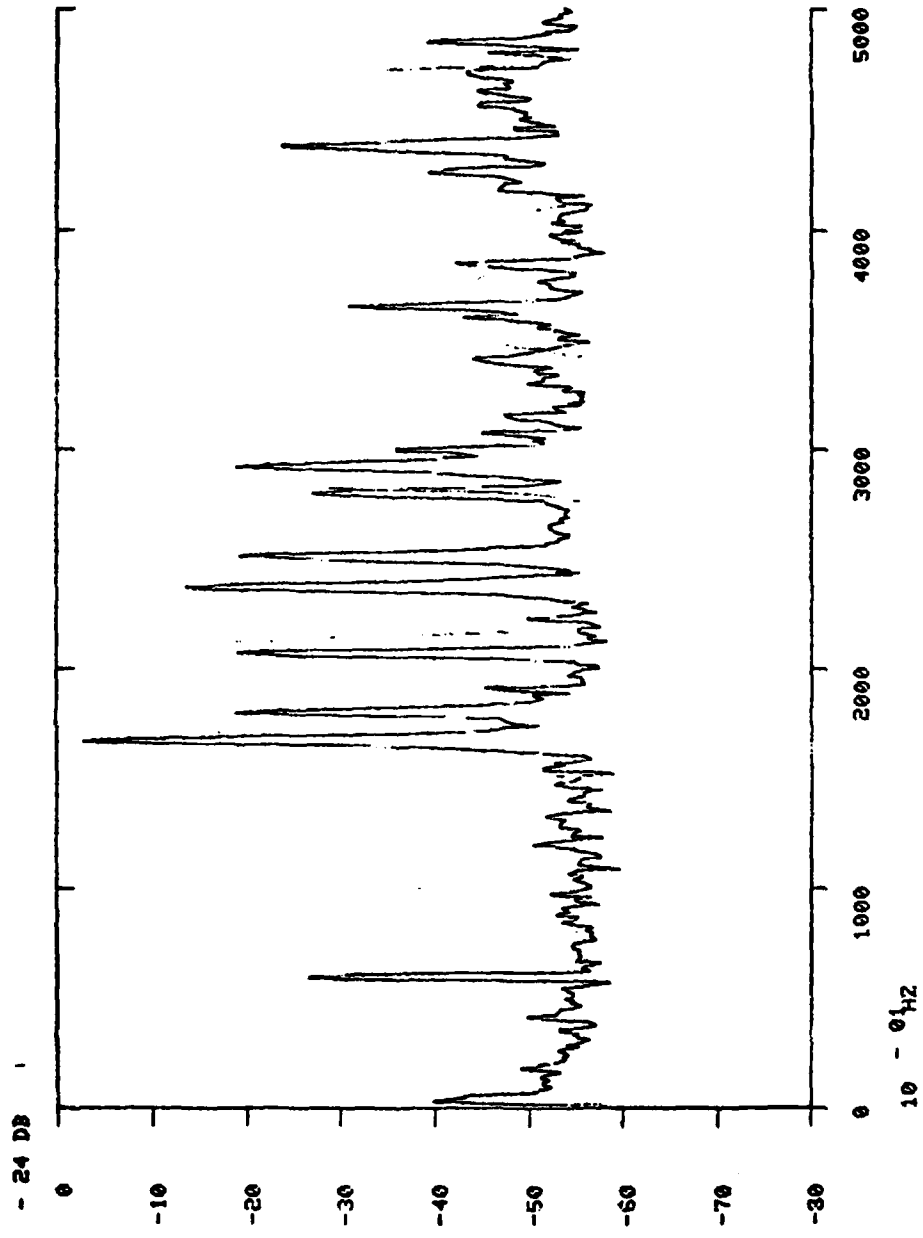

Fig. A-12 PSD Plot - Point (3,2)

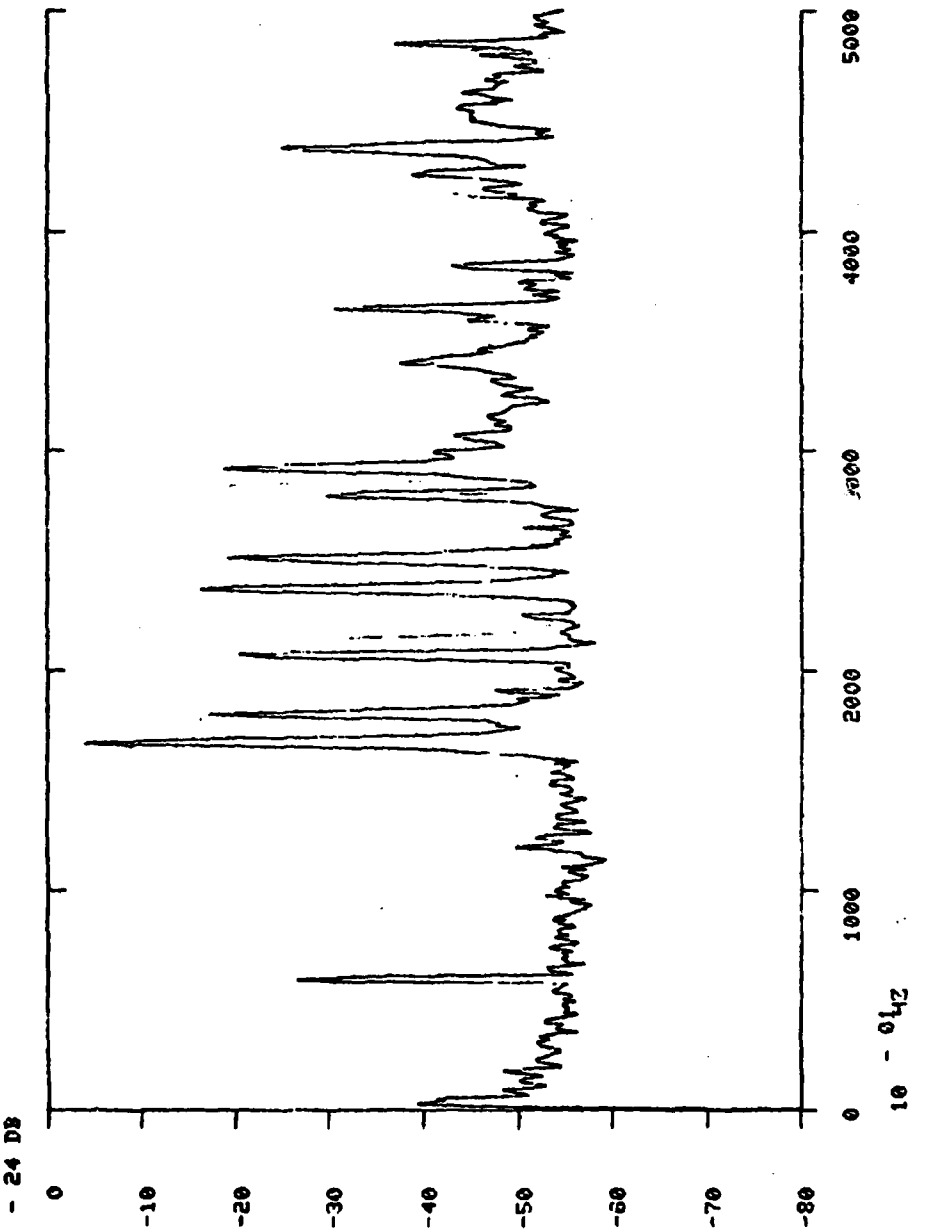

Fig. A-13 PSD Plot - Point (3,3)

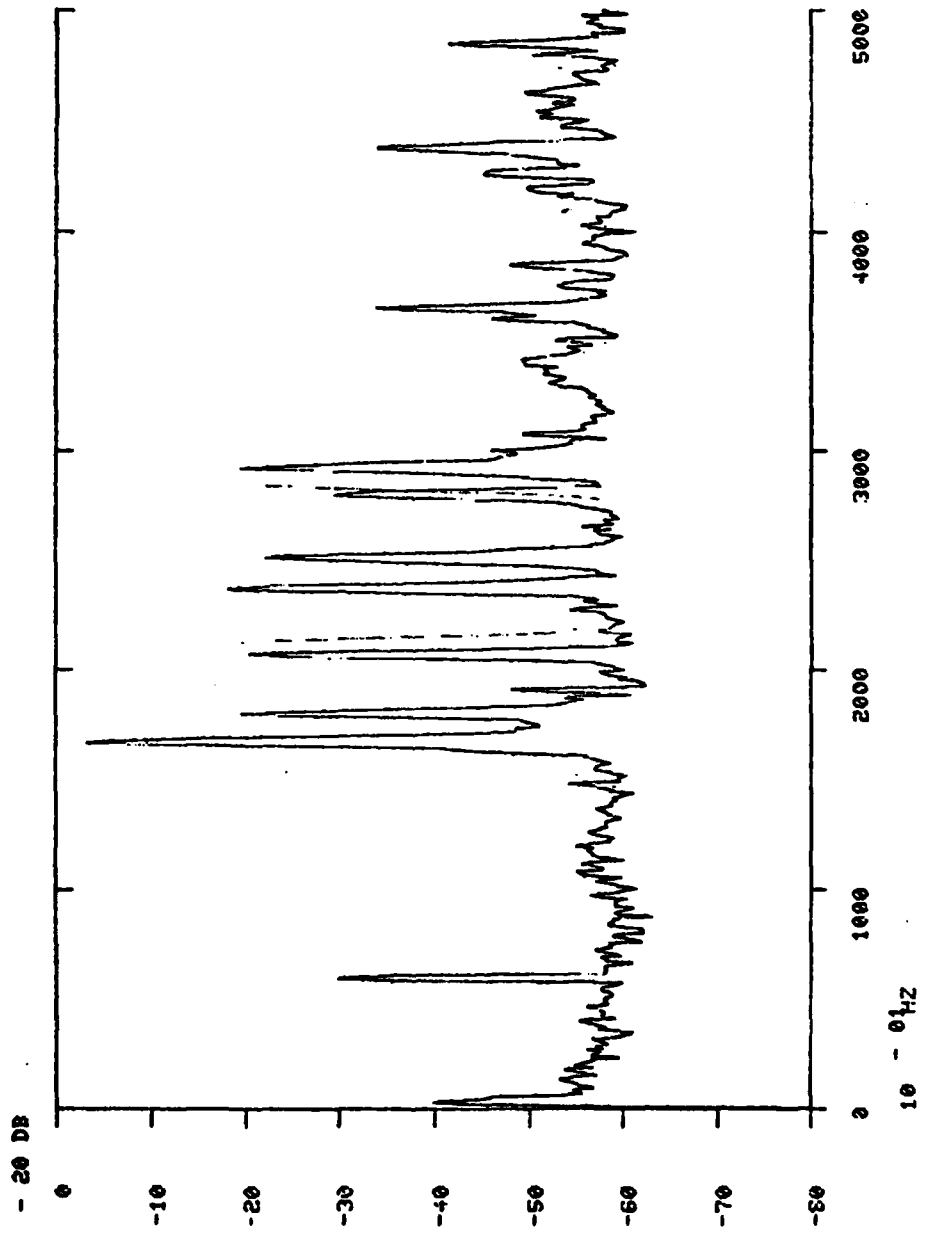

Fig. A-14 PSD Plot - Point (3,4)

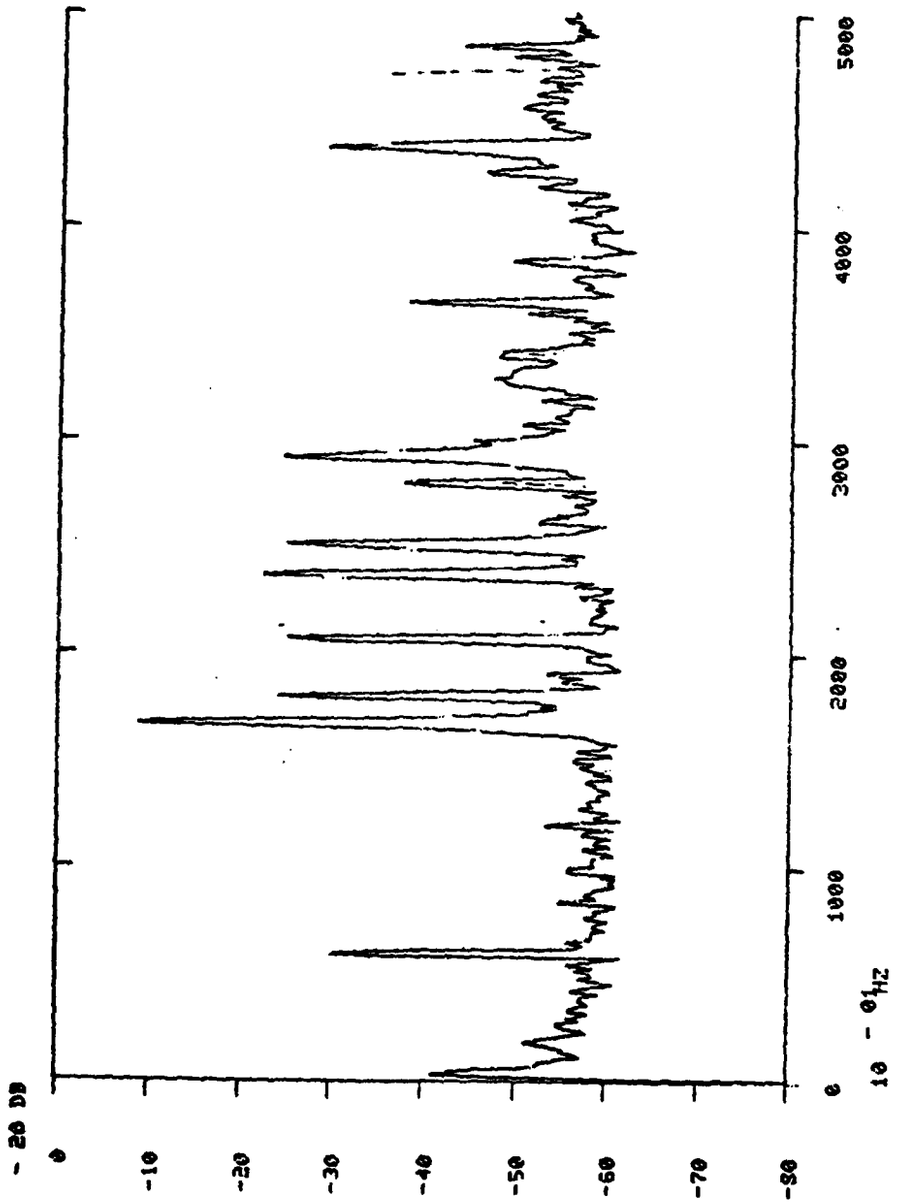

Fig. A-15 PSD Plot - Point (3,5)

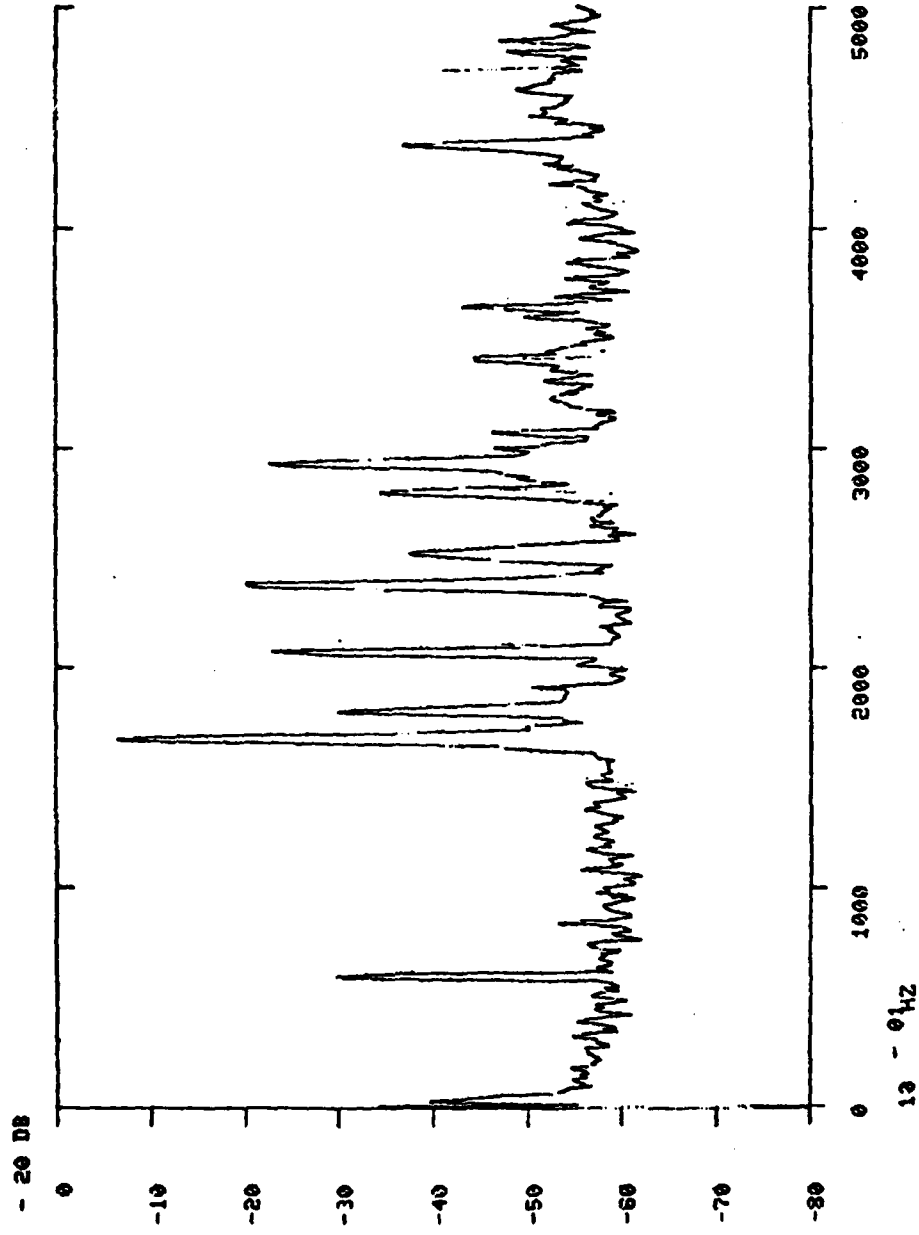

Fig. A-16 PSD Plot - Point (4,1)

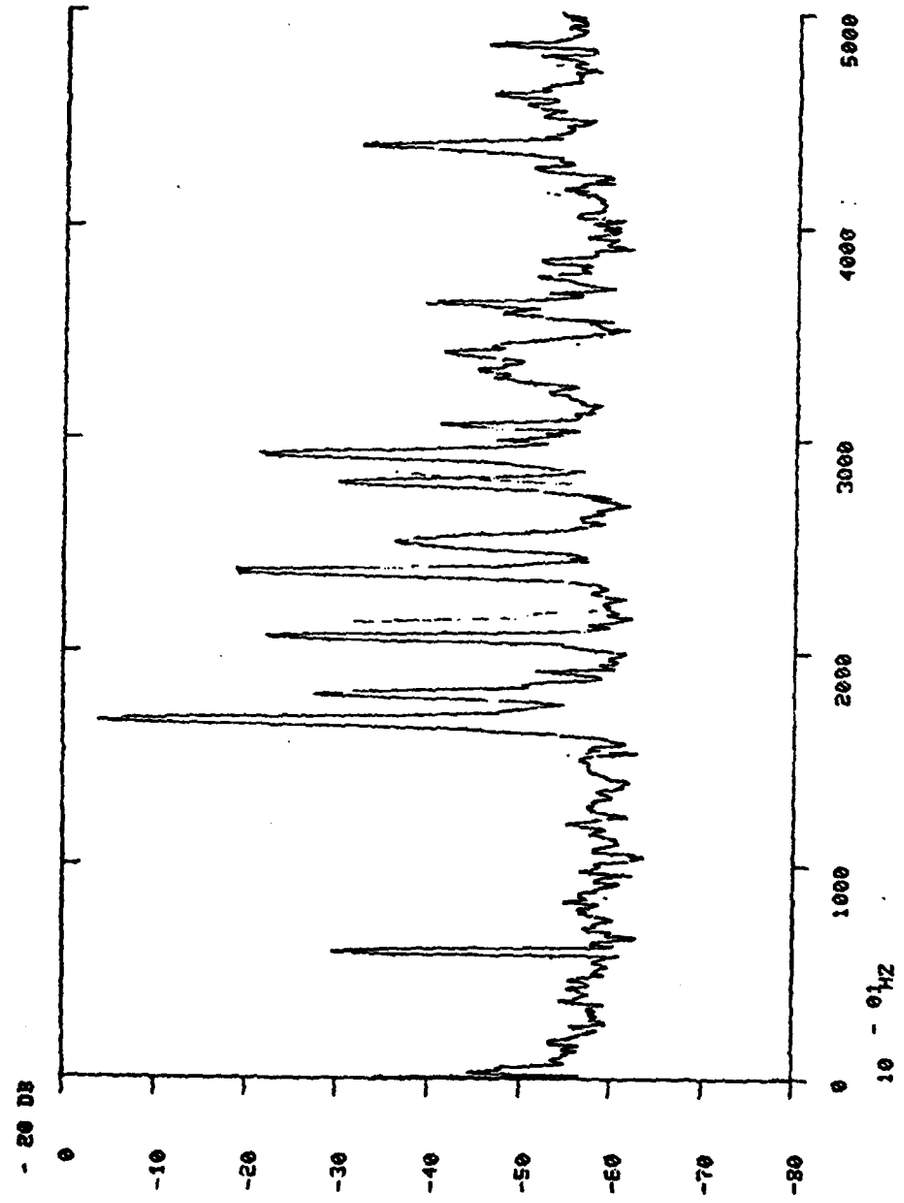

Fig. A-17 PSD Plot - Point (4,2)

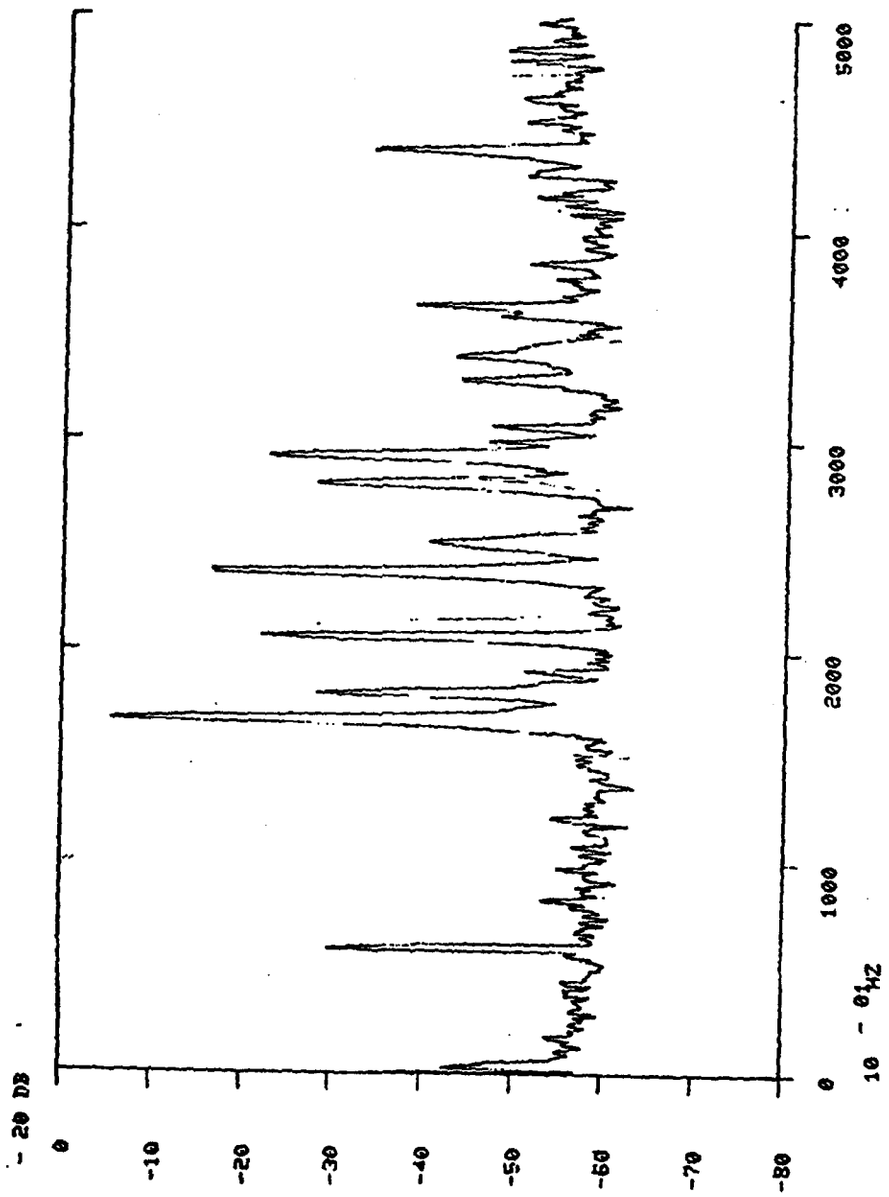

Fig. A-18 PSD Plot - Point (4,3)

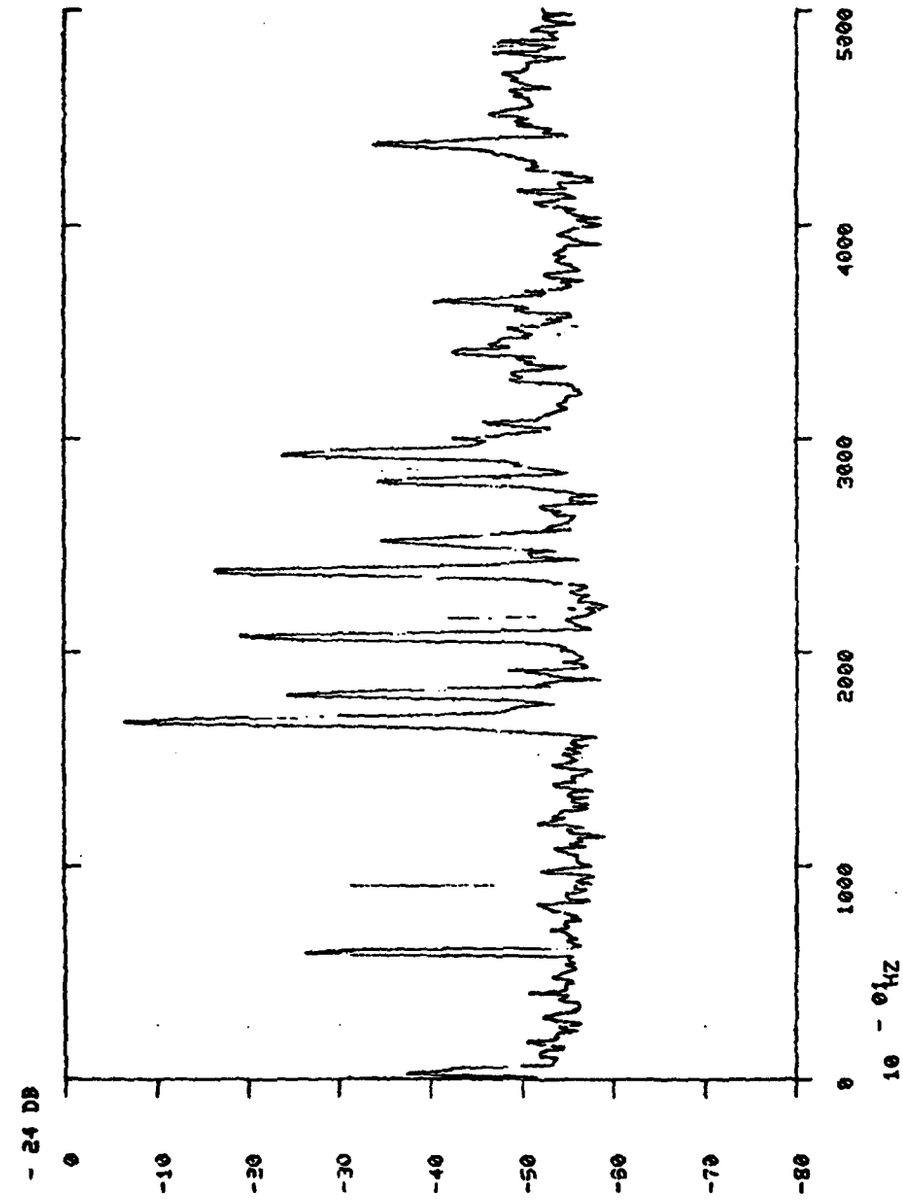

Fig. A-19 PSD Plot - Point (4,4)

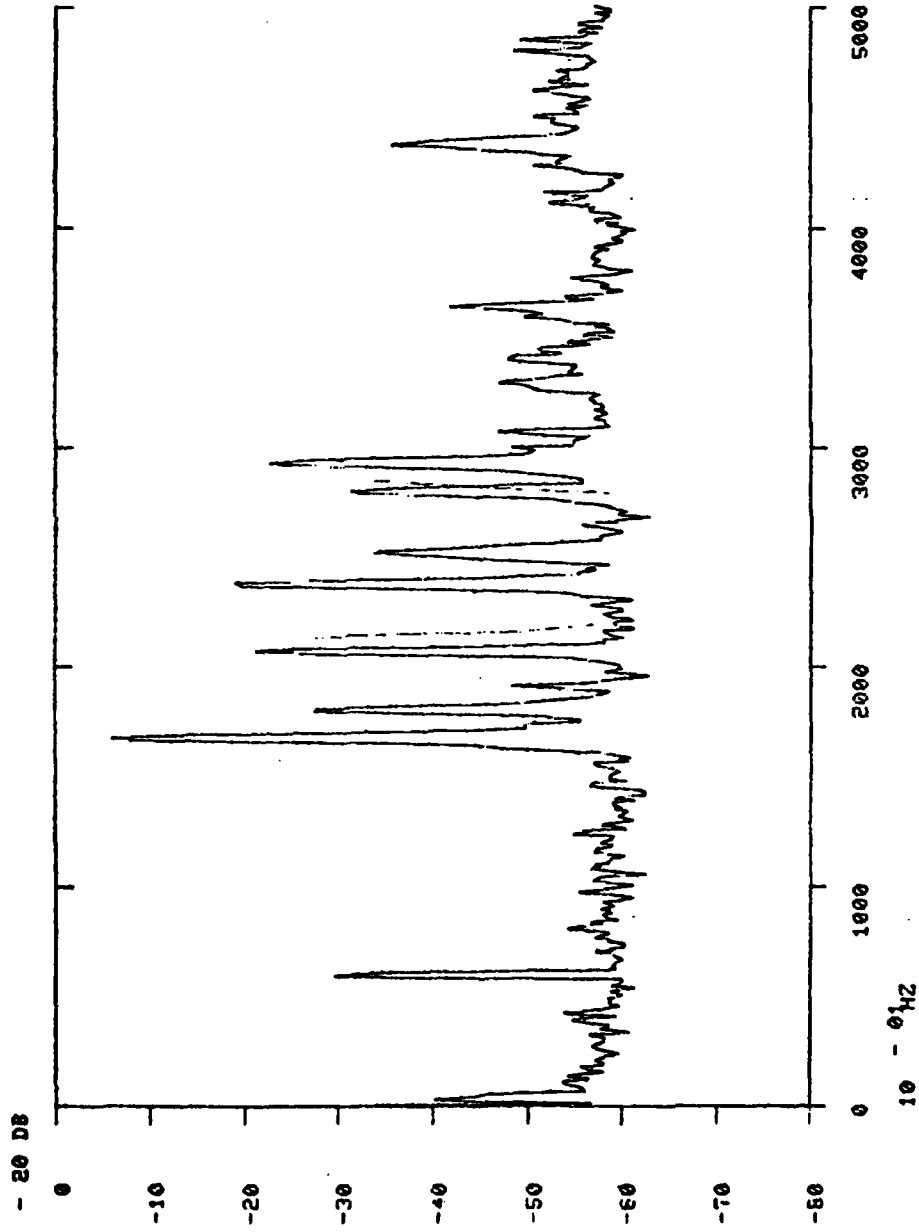

Fig. A-20 PSD Plot - Point (4,5)

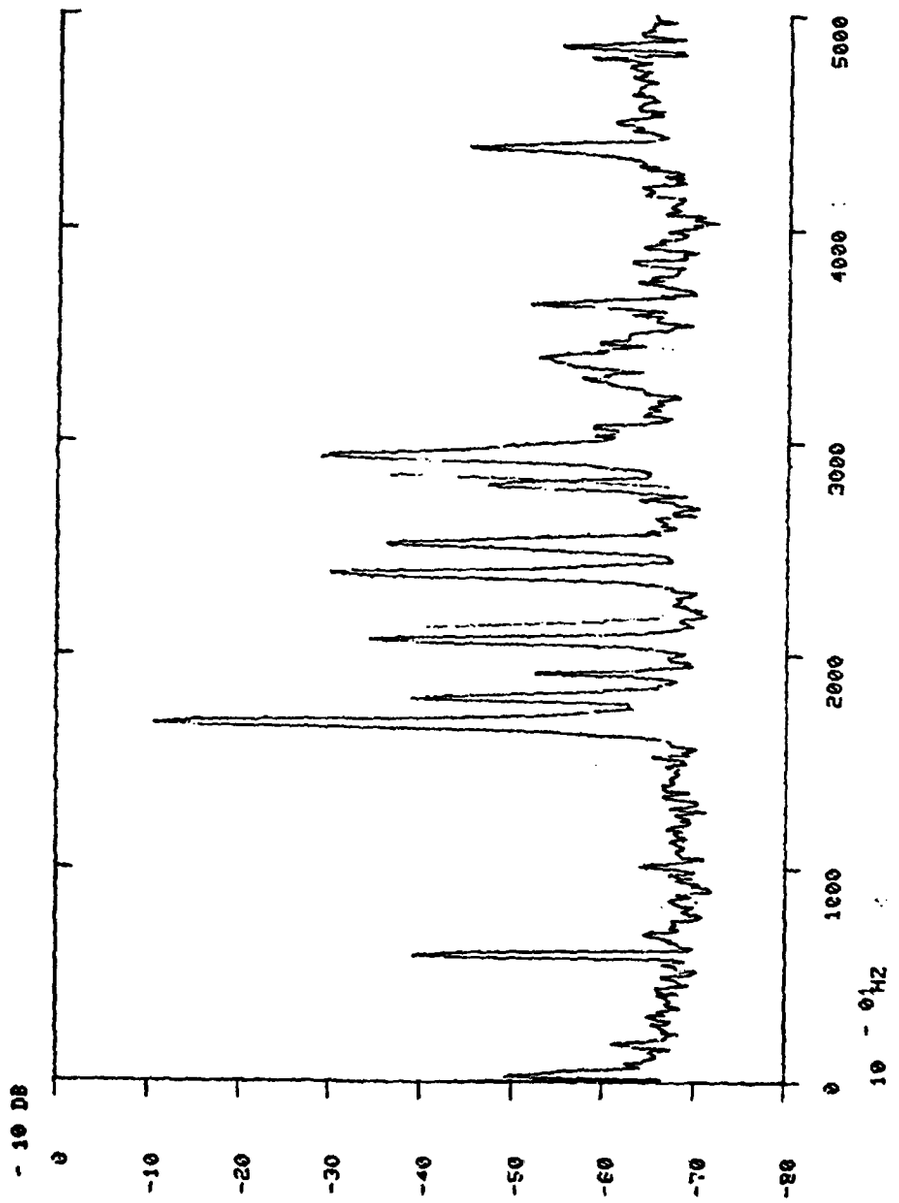

Fig. A-21 PSD Plot - Point (5,1)

AD-A079 856 AIR FORCE INST OF TECH WRIGHT-PATTERSON AFB OH SCHOO--ETC F/G 20/4
THE PREDICTION OF MASS LOADED NATURAL FREQUENCIES AND FORCED RE--ETC(U)
DEC 79 L B GLENESK

UNCLASSIFIED AFIT/GAE/AA/79D-5 NL

2 OF 2
AD A079856

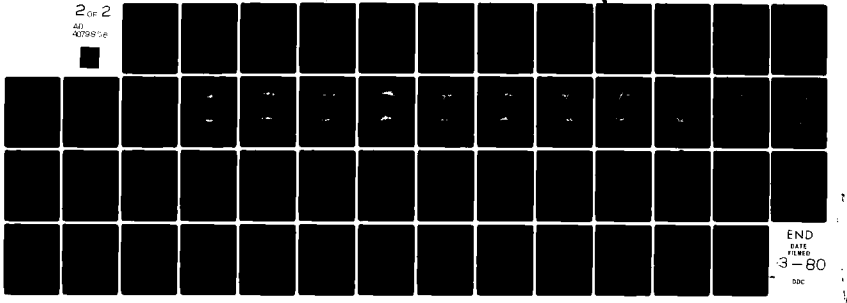

END
DATE FILMED
3-80
DDC

Fig. A-22 PSD Plot - Point (5,2)

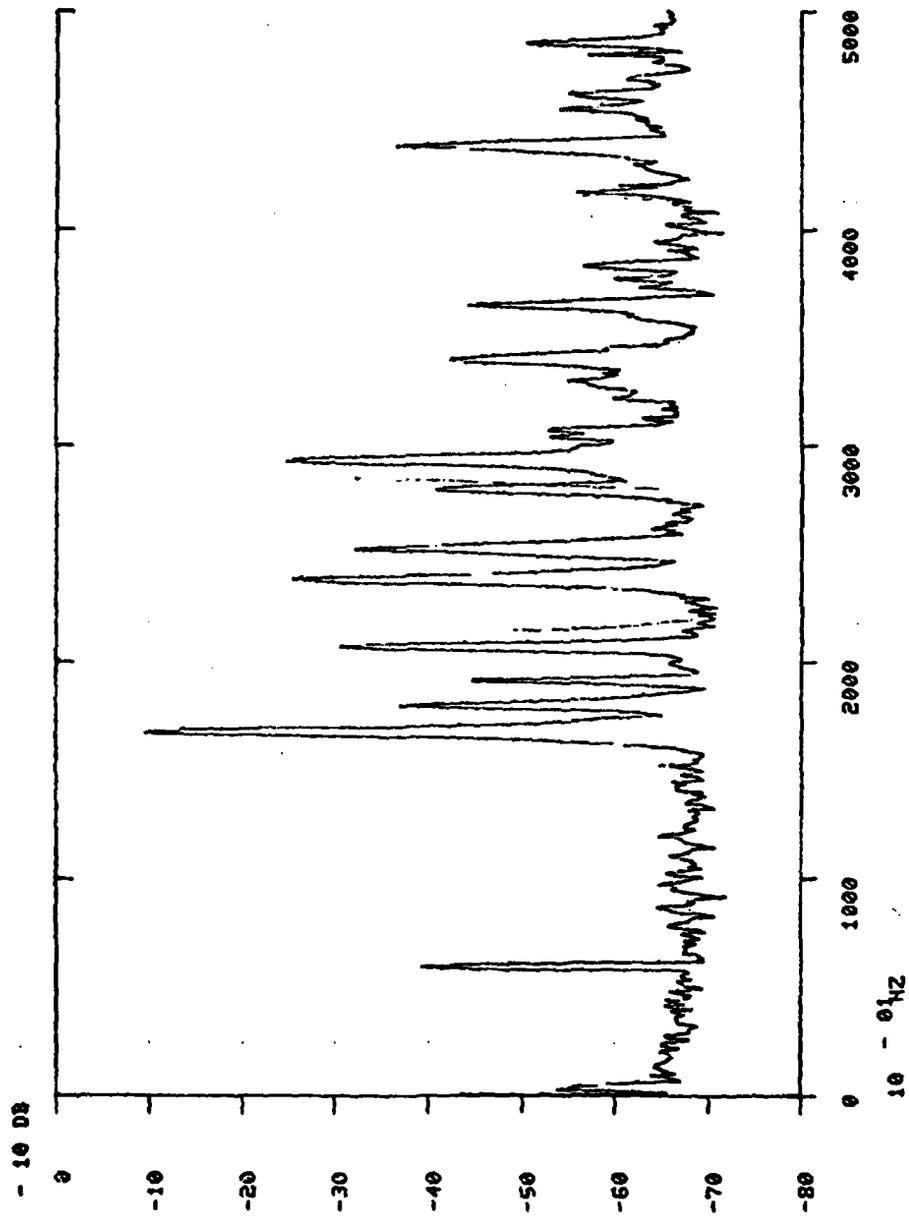

Fig. A-23 PSD Plot - Point (5,3)

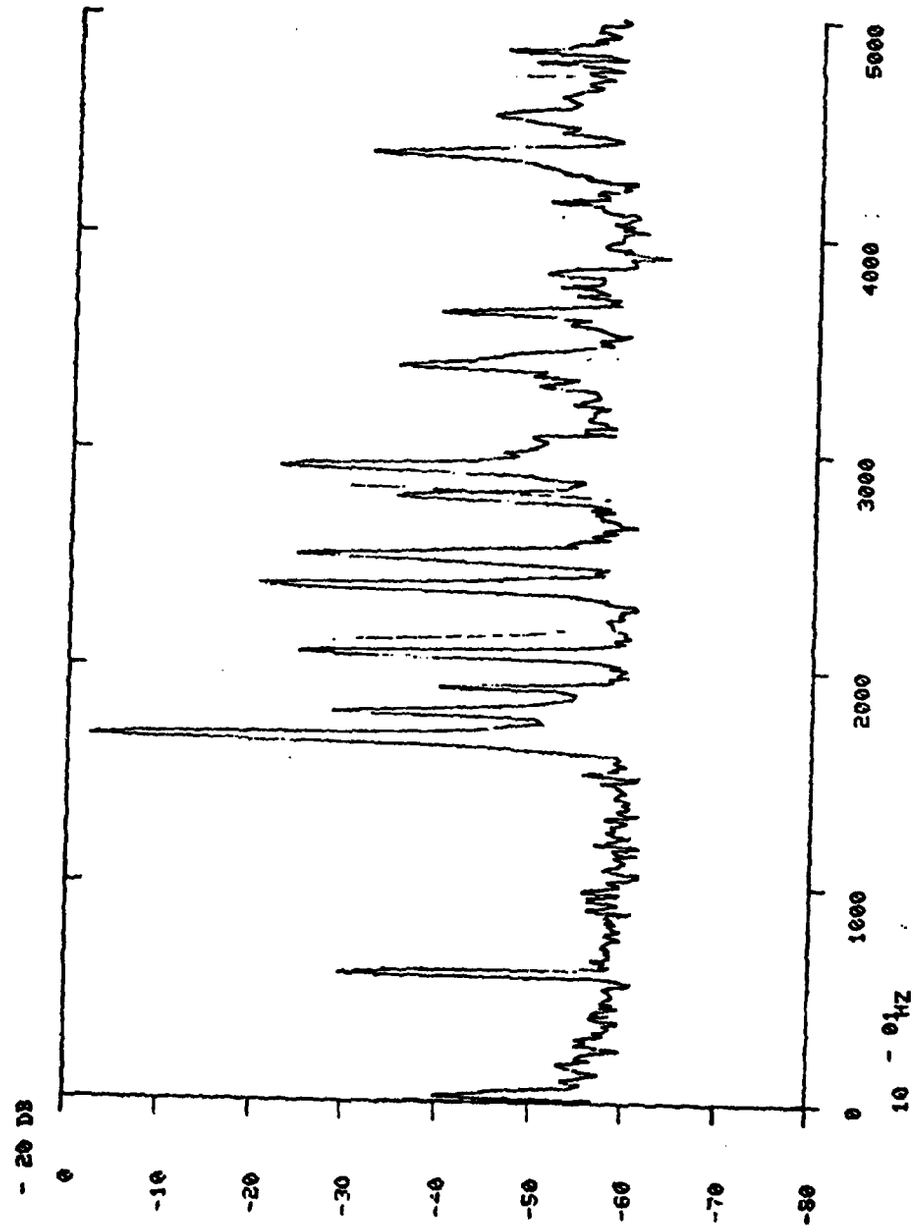

Fig. A-24 PSD Plot - Point (5,4)

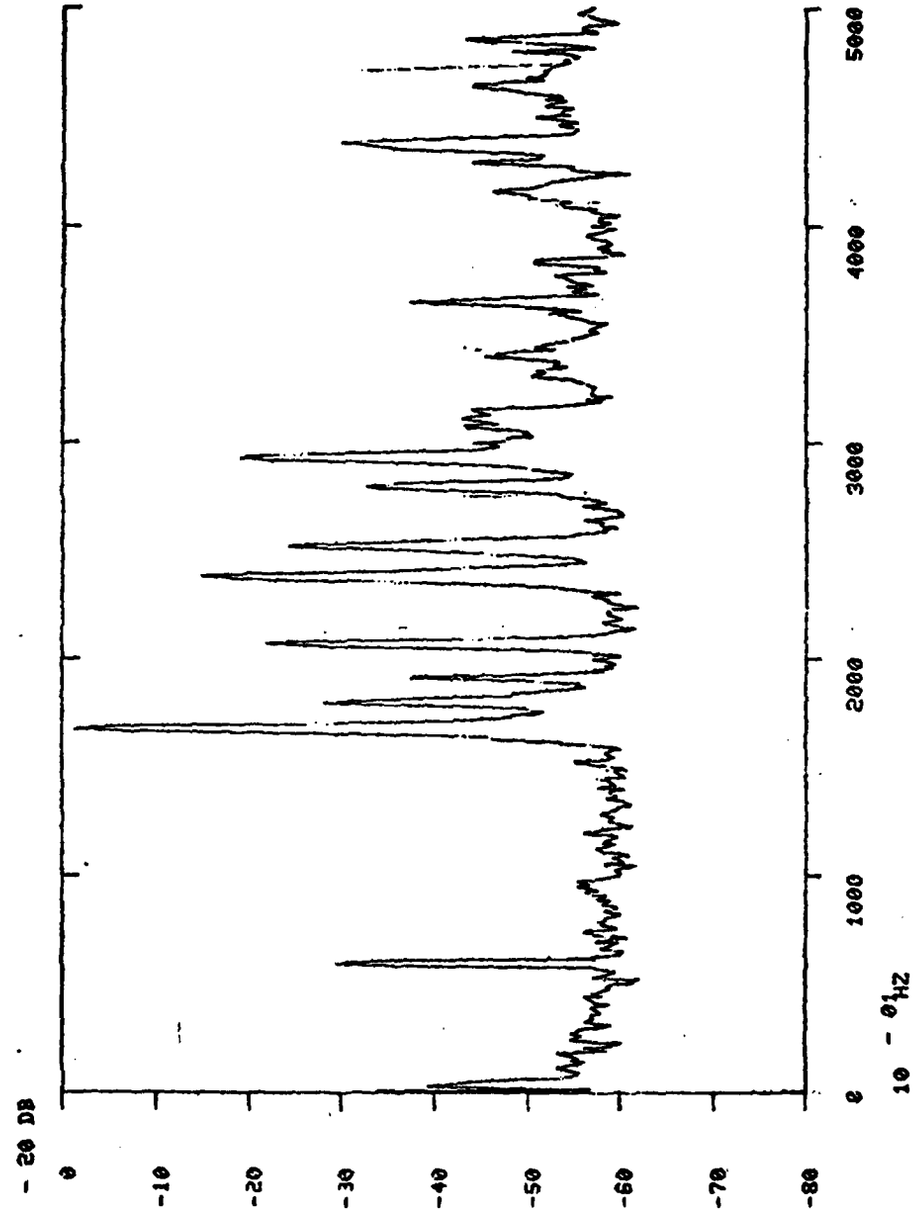

Fig. A-25 PSD Plot - Point (5,5)

Appendix B

Discrete Mode Shape Plots - Unloaded Case

CONFIGURATION # 0 MODE # 1 FREQUENCY 167.8

VECTORS:

1	1.000	6	.046	11	.035	16	.049	21	-.699
2	-1.650	7	-.009	12	-.006	17	-.016	22	-.093
3	.089	8	.038	13	.036	18	.011	23	.051
4	-.582	9	-.015	14	-.011	19	-.016	24	.224
5	.259	10	-.038	15	-.027	20	-.033	25	.221

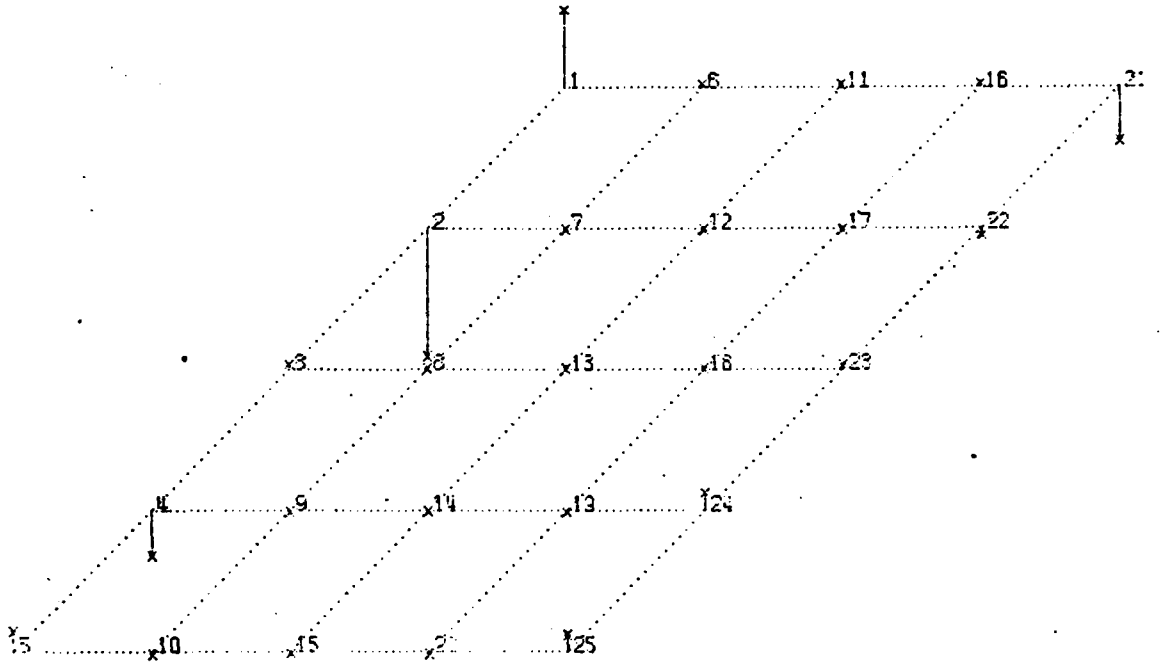

Fig. B-1 Discrete Mode Shape - Mode 1

CONFIGURATION # 0 MODE # 2 FREQUENCY 180.6

VECTORS:

1	.573	6	-.117	11	-.035	16	-.126	21	.453
2	.163	7	.091	12	.078	17	.066	22	.154
3	.145	8	.077	13	.054	18	.071	23	.132
4	.205	9	.203	14	.255	19	.195	24	.197
5	1.000	10	-.121	15	-.091	20	-.132	25	.709

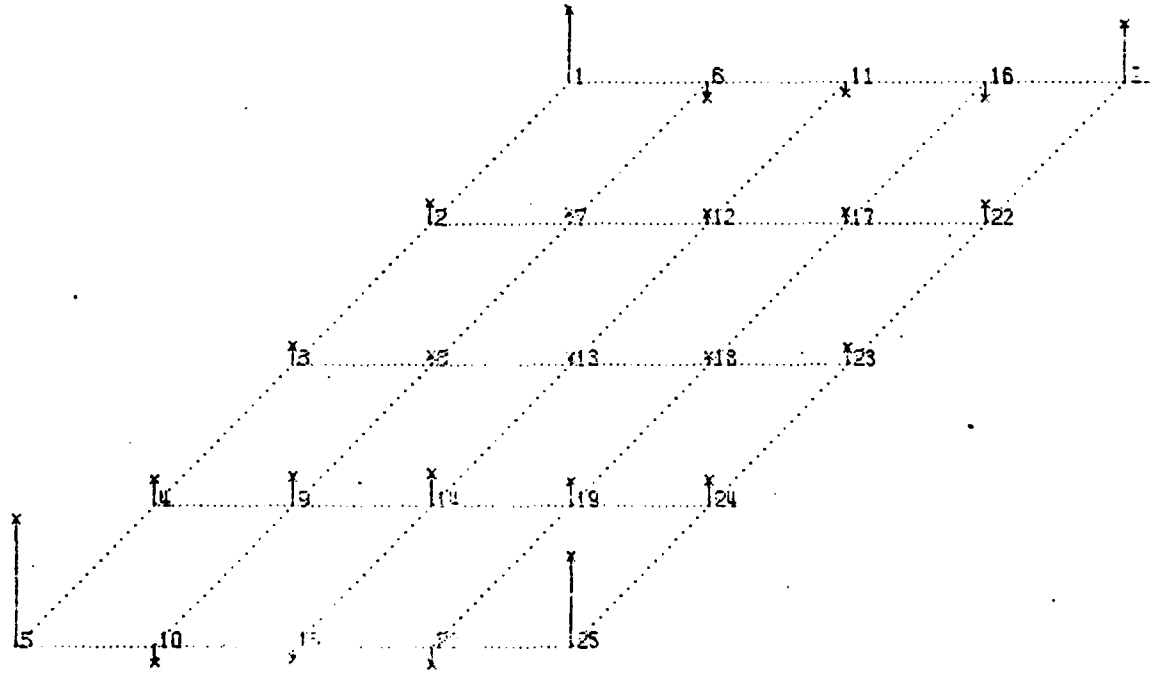

Fig. B-2 Discrete Mode Shape - Mode 2

CONFIGURATION # 0 MODE # 3 FREQUENCY 191.2

VECTORS:

1	.759	6	-.008	11	.025	16	-.025	21	.464
2	.561	7	.008	12	-.008	17	.008	22	.211
3	-1.000	8	.000	13	-.000	18	.013	23	.312
4	-.127	9	-.004	14	.004	19	-.004	24	.127
5	-.548	10	.021	15	-.038	20	.108	25	-.253

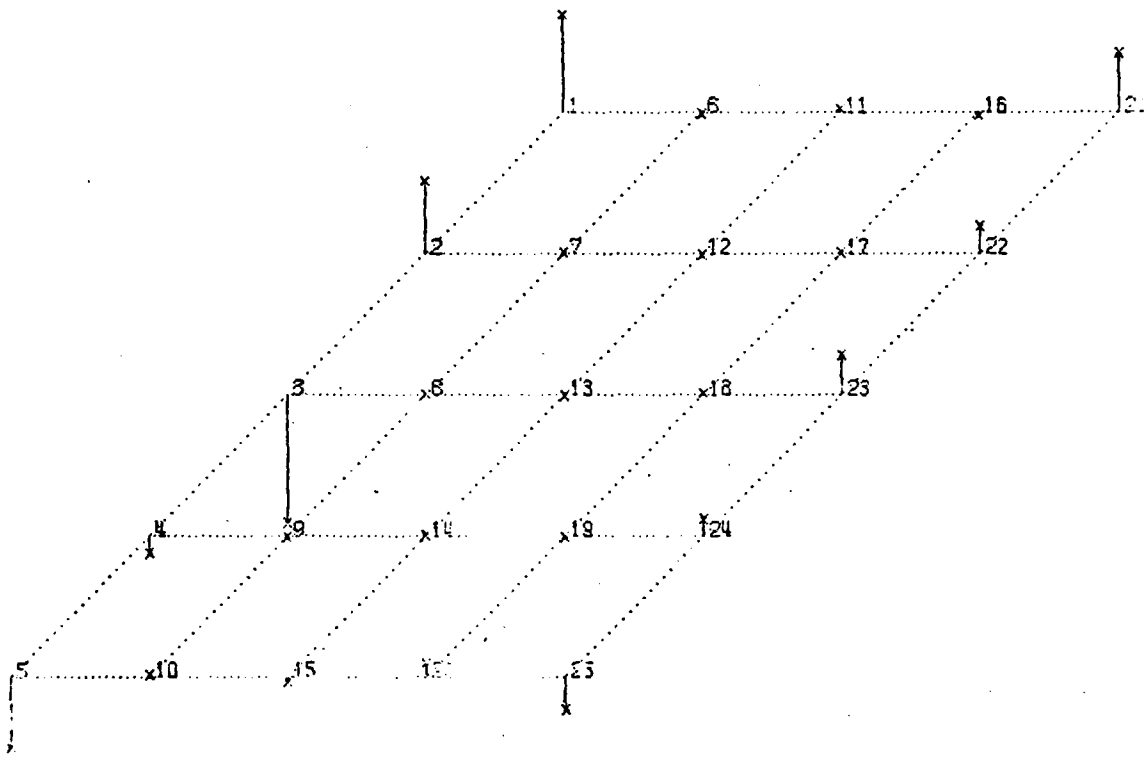

Fig. B-3 Discrete Mode Shape - Mode 3

CONFIGURATIO. # D MODE # 4 FREQUENCY 207.3

VECTORS:

1	-.342	6	-.192	11	-.161	16	-.220	21	-.330
2	-.601	7	-.125	12	-.095	17	-.122	22	-.484
3	1.000	8	.156	13	.093	18	.128	23	.530
4	.379	9	.110	14	.085	19	.105	24	.317
5	.440	10	-.288	15	-.179	20	-.339	25	.354

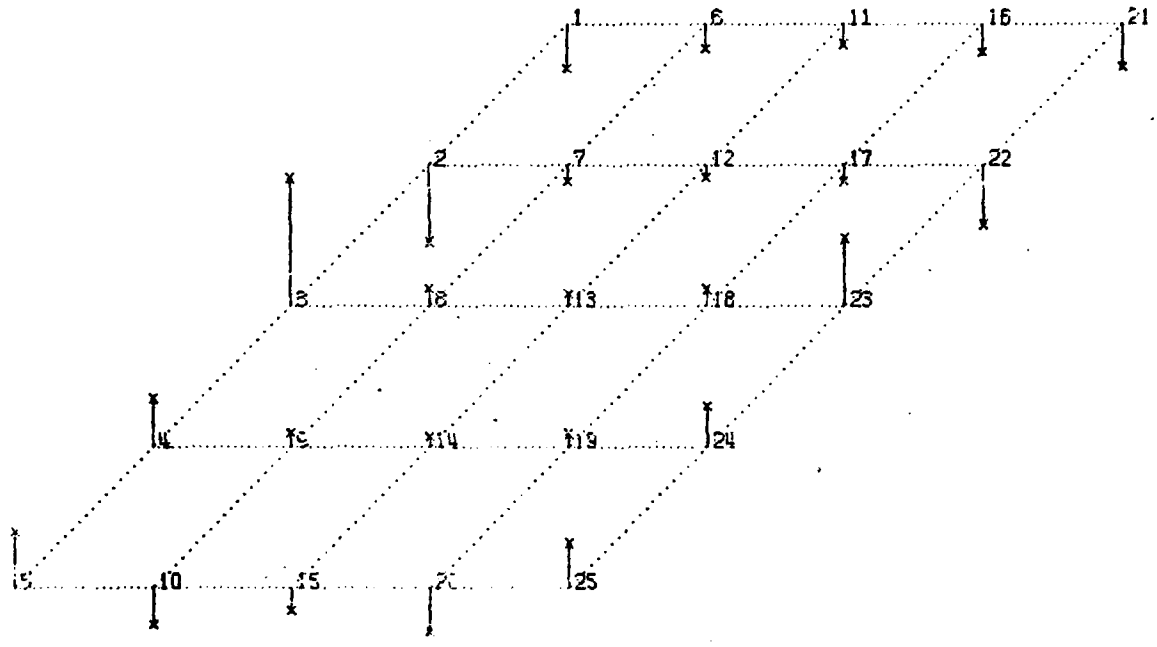

Fig. B-4 Discrete Mode Shape - Mode 4

CONFIGURATION # 0 MODE # 5 FREQUENCY 237.7

VECTORS:

1	.389	6	-.235	11	-.154	16	-.274	21	.317
2	.389	7	.126	12	.093	17	.131	22	.069
3	-.803	8	-.064	13	-.049	18	-.038	23	-.458
4	1.000	9	.033	14	.021	19	.029	24	.000
5	-.155	10	-.065	15	-.054	20	-.045	25	-.172

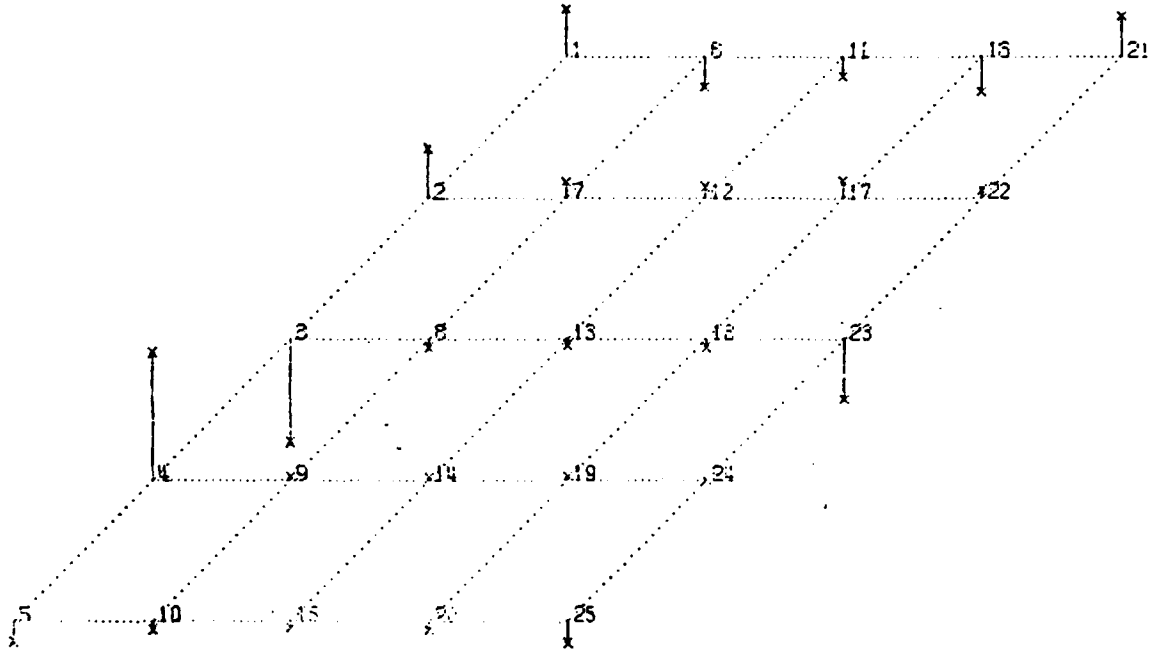

Fig. B-5 Discrete Mode Shape - Mode 5

CONFIGURATION # 0 MODE # 6 FREQUENCY 252.1

VECTORS:

1	-.129	6	-.179	11	-.195	16	-.090	21	-.137
2	-1.000	7	.080	12	.022	17	.031	22	-.288
3	-.852	8	-.050	13	-.036	18	-.051	23	-.229
4	.253	9	-.125	14	-.076	19	-.125	24	.318
5	.158	10	-.525	15	-.254	20	-.333	25	.132

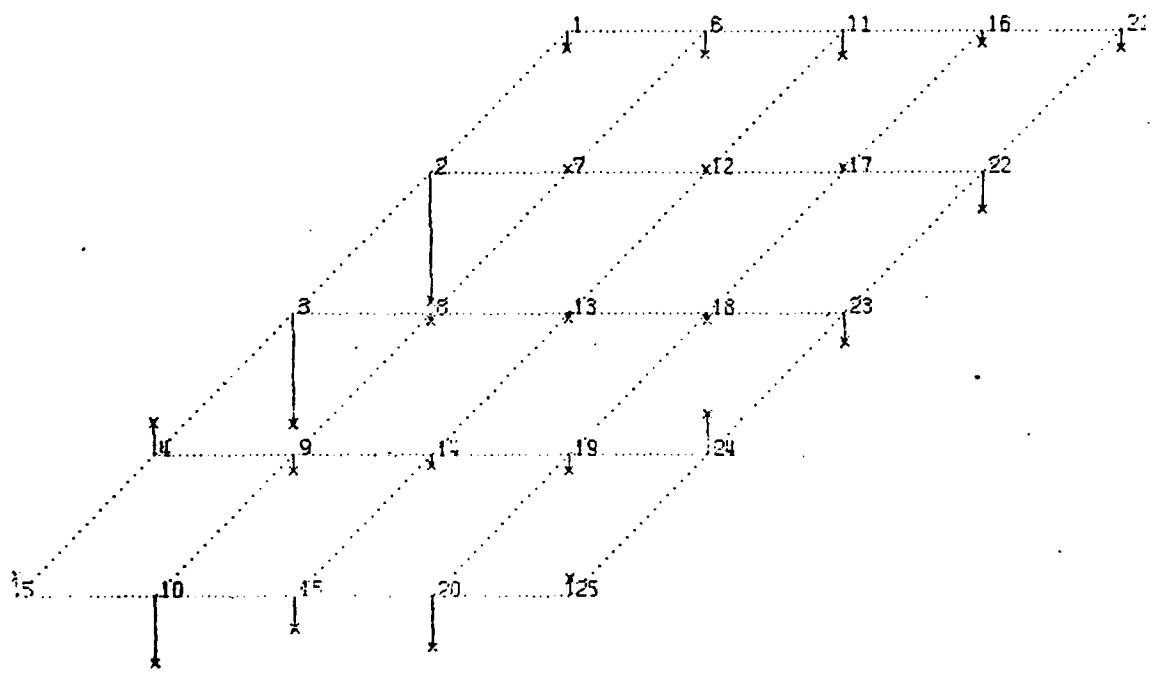

Fig. B-6 Discrete Mode Shape - Mode 6

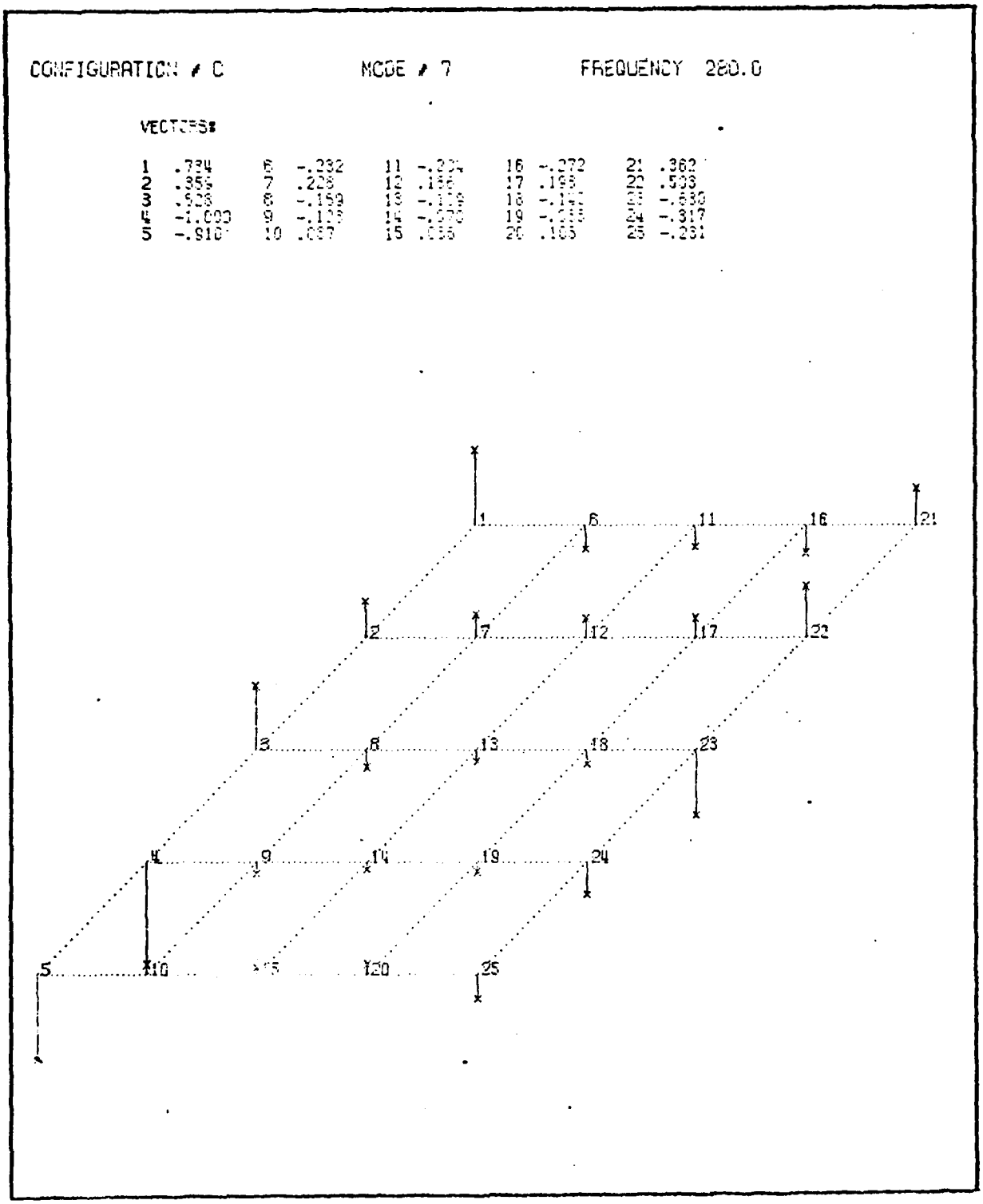

Fig. B-7 Discrete Mode Shape - Mode 7

CONFIGURATION # 0 MODE # 8 FREQUENCY 292.8

VECTORS:

1	.255	6	.125	11	.105	16	.125	21	.269
2	.217	7	-.109	12	-.080	17	-.095	22	.144
3	-.492	8	-.040	13	-.092	18	-.041	23	.572
4	-.527	9	-.124	14	-.084	19	-.134	24	1.000
5	.783	10	.174	15	.133	20	.169	25	.651

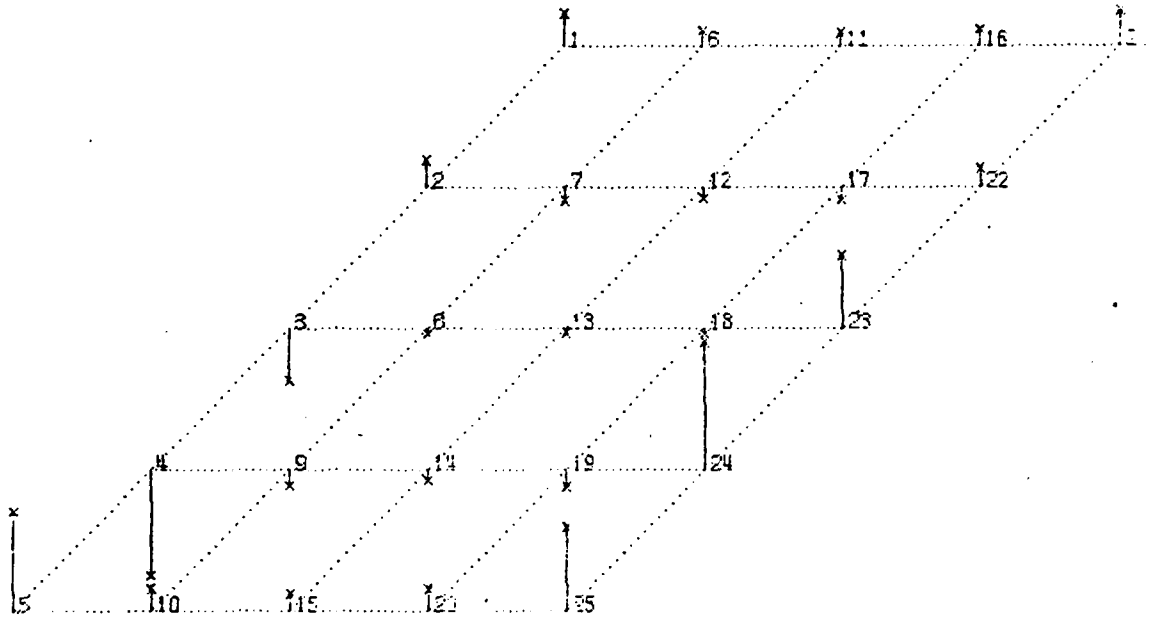

Fig. B-8 Discrete Mode Shape - Mode 8

CONFIGURATION # 0 MODE # 9 FREQUENCY 365.0

VECTORS:

1	-.547	6	-.109	11	-.125	16	-.230	21	.292
2	.208	7	.198	12	-.068	17	-.045	22	-.292
3	.202	8	-.425	13	-.217	18	-.134	23	-.205
4	-.687	9	-.048	14	.258	19	.035	24	-1.000
5	-.398	10	.128	15	.123	20	.257	25	-.406

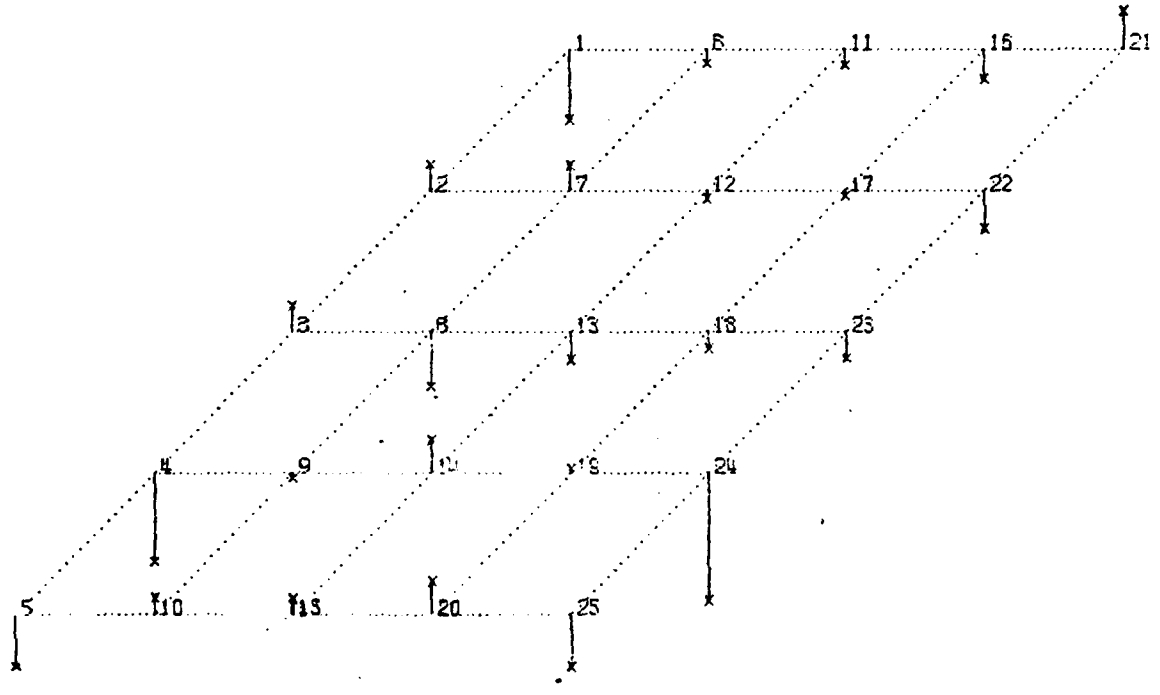

Fig. B-9. Discrete Mode Shape - Mode 9

Appendix C

Continuous Mode Shape Plots

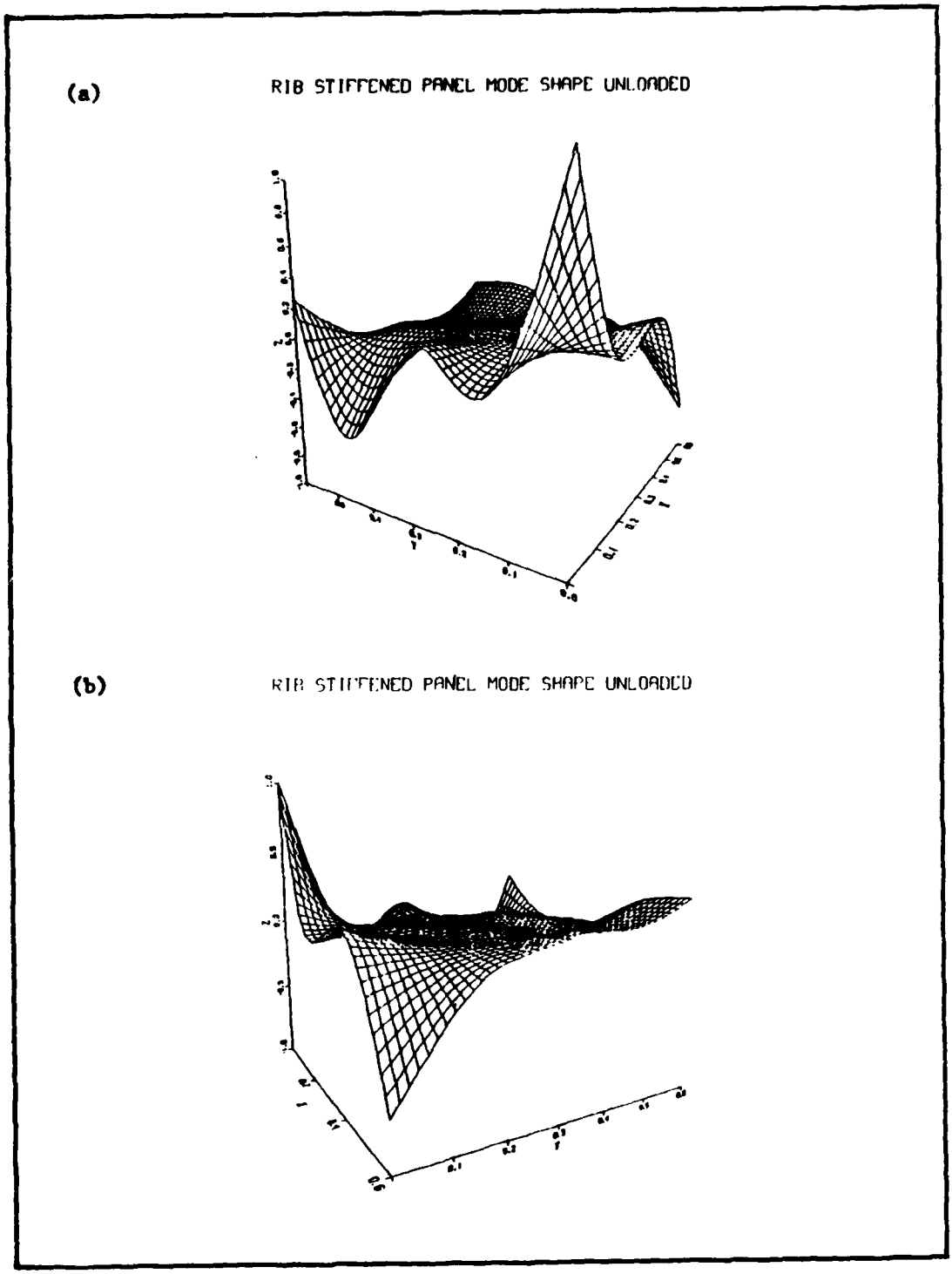

Fig. C-1 (a) View 1 - Mode 1; (b) View 2 - Mode 1 (167.93 Hz)

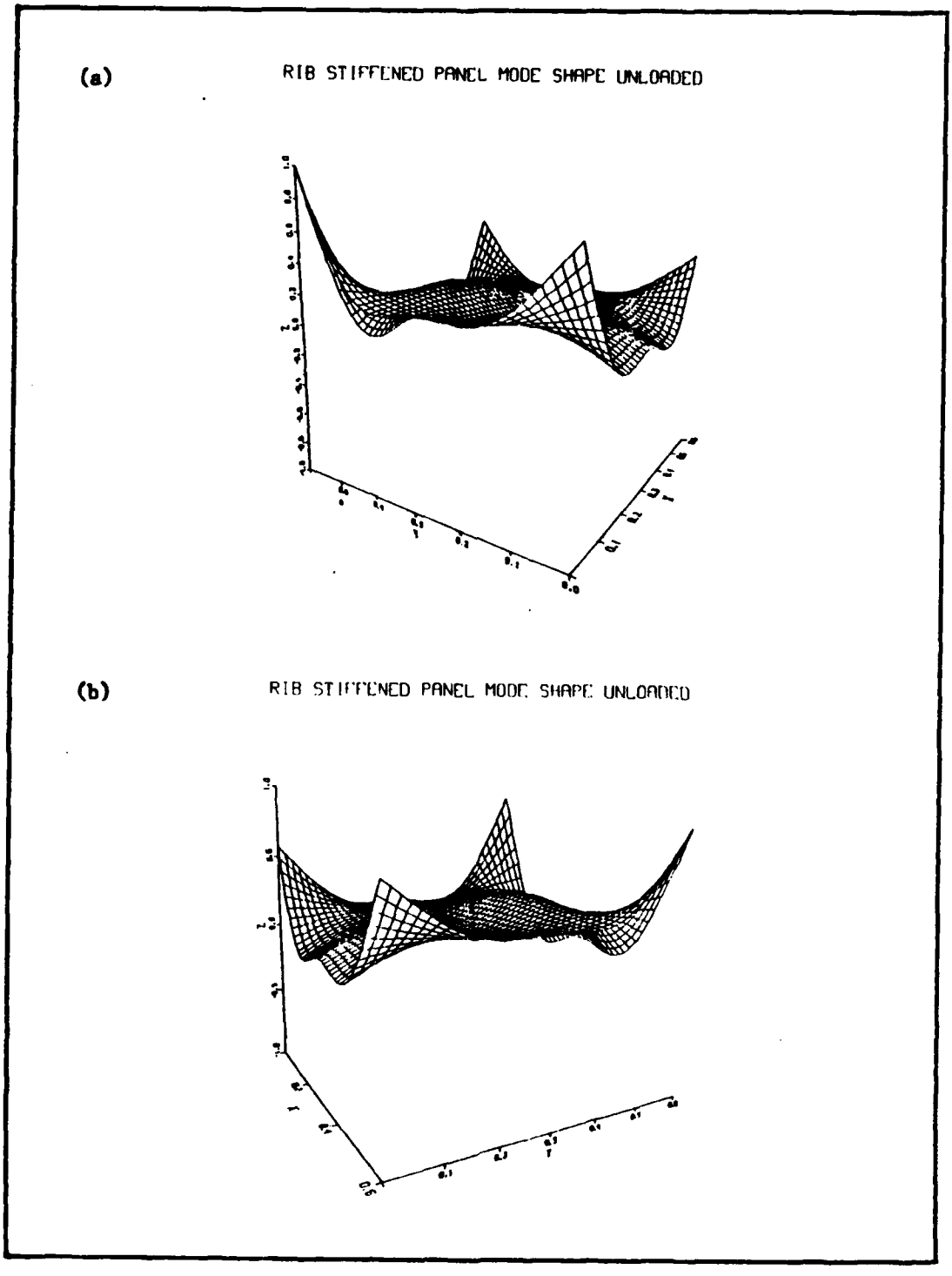

Fig. C-2 (a) View 1 - Mode 2; (b) View 2 - Mode 2 (180.50 Hz)

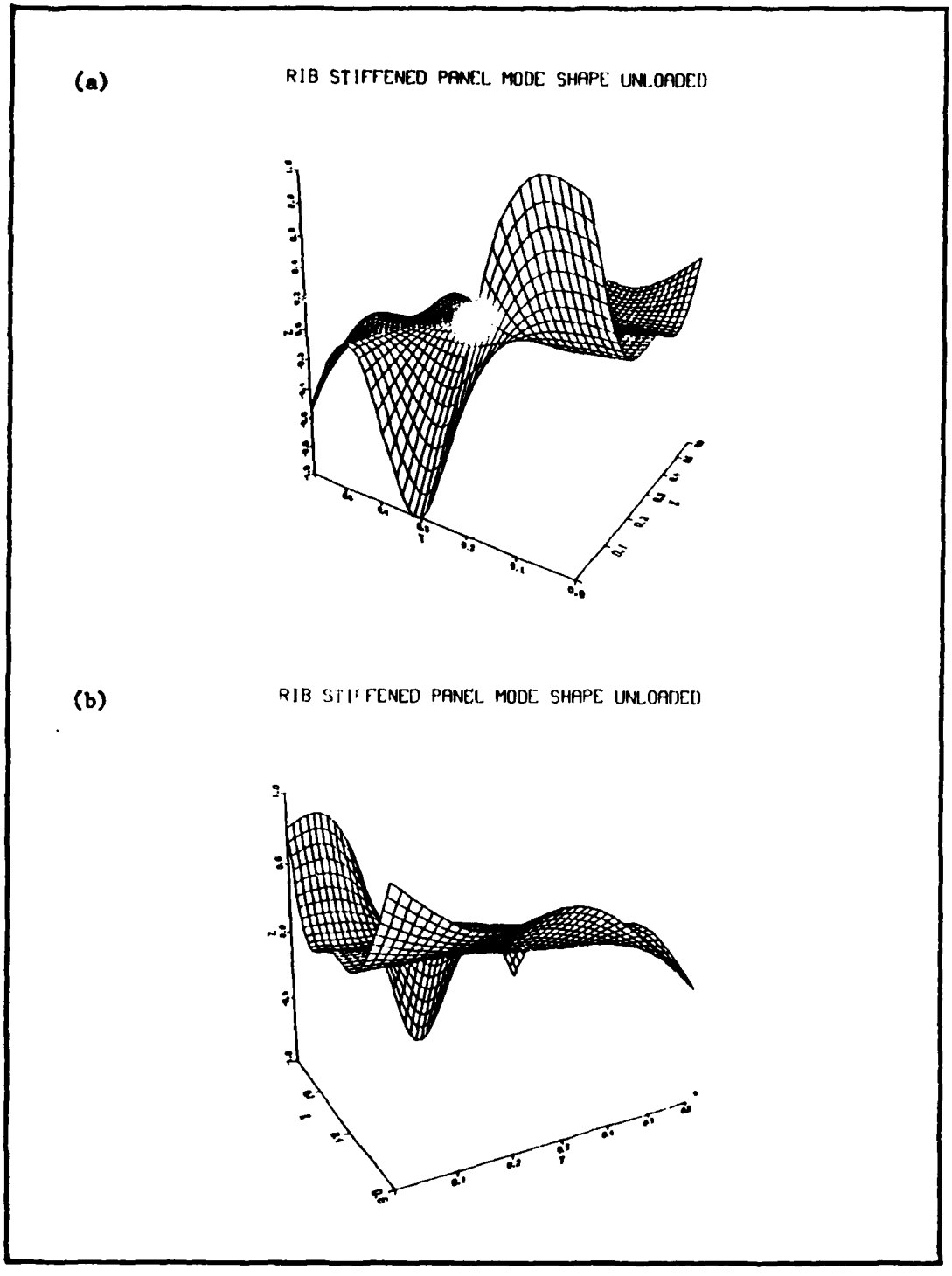

Fig. C-3 (a) View 1 - Mode 3; (b) View 2 - Mode 3 (191.22 Hz)

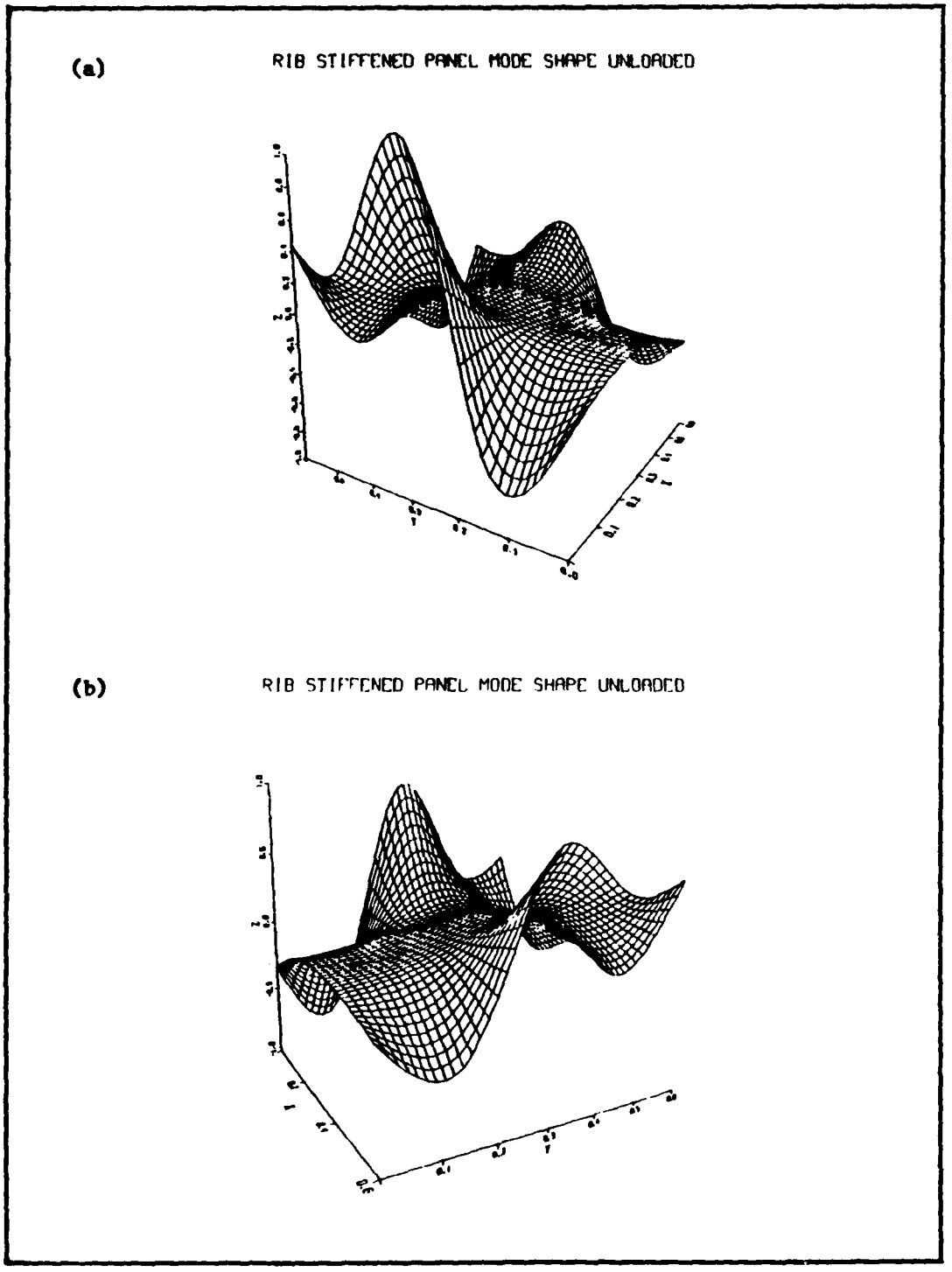

Fig. C-4 (a) View 1 - Mode 4; (b) View 2 - Mode 4 (207.31 Hz)

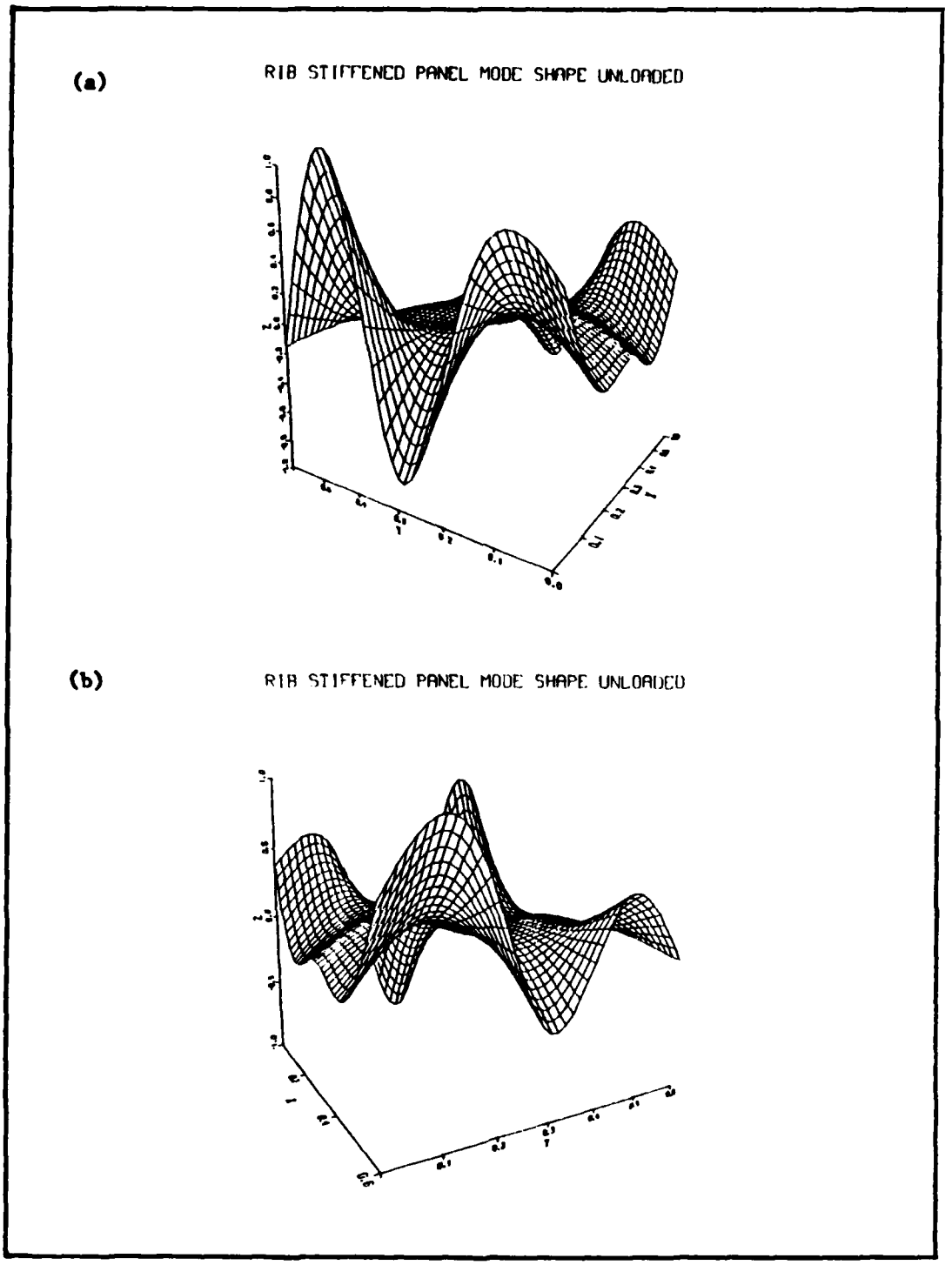

Fig. C-5 (a) View 1 - Mode 5; (b) View 2 - Mode 5 (237.74 Hz)

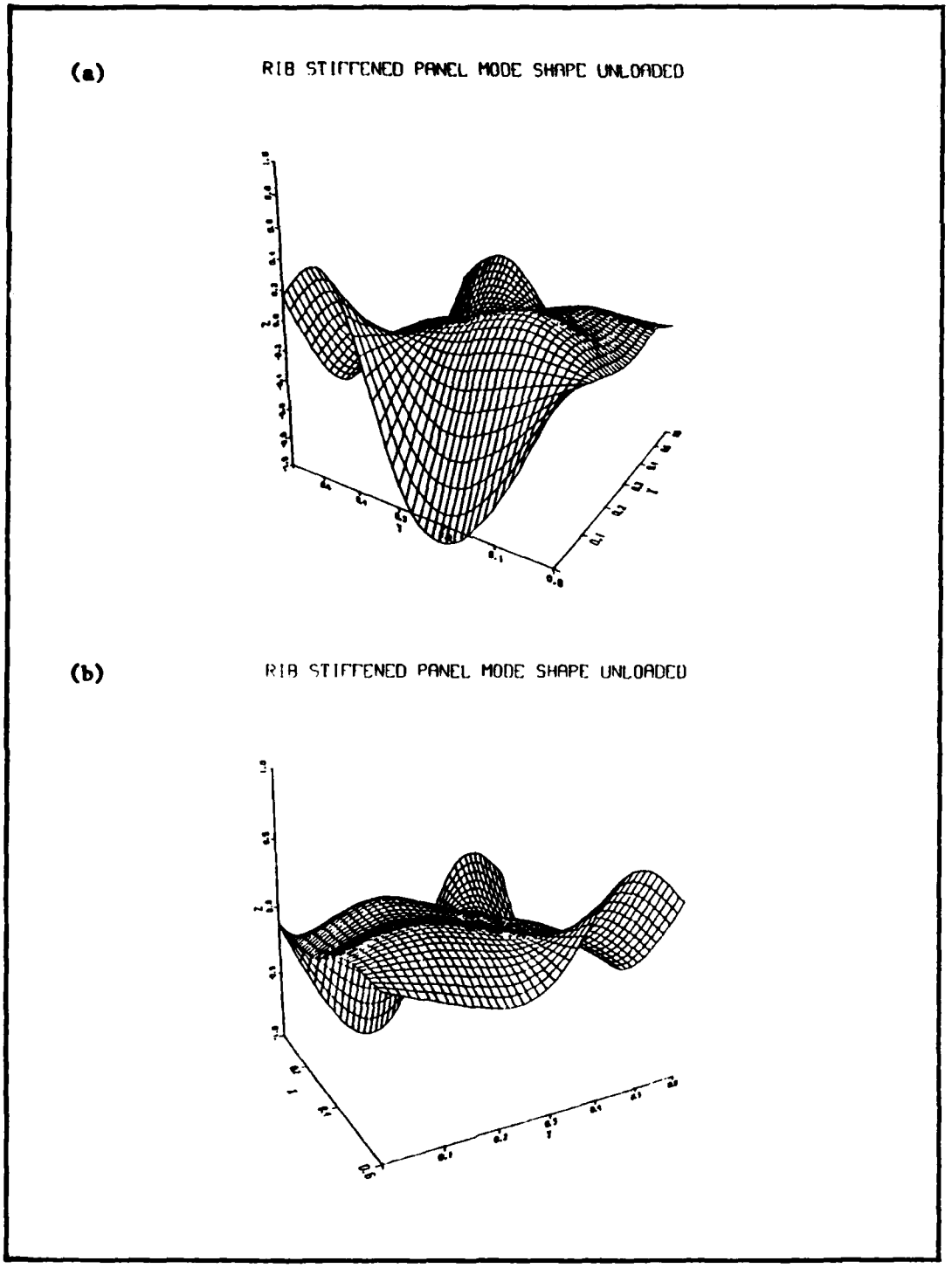

Fig. C-6 (a) View 1 - Mode 6; (b) View 2 - Mode 6 (252.12 Hz)

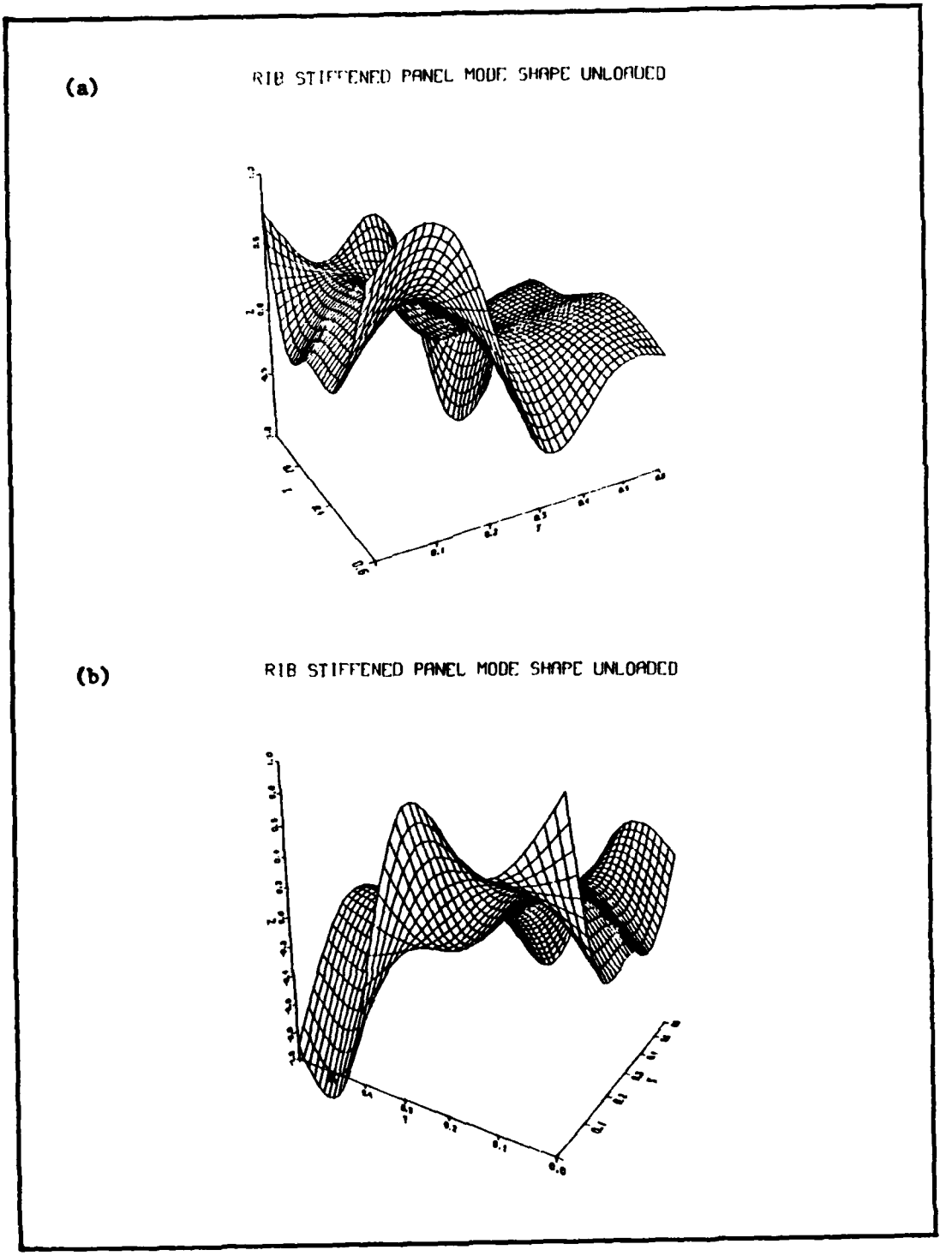

Fig. C-7 (a) View 1 - Mode 7; (b) View 2 - Mode 7 (280.02 Hz)

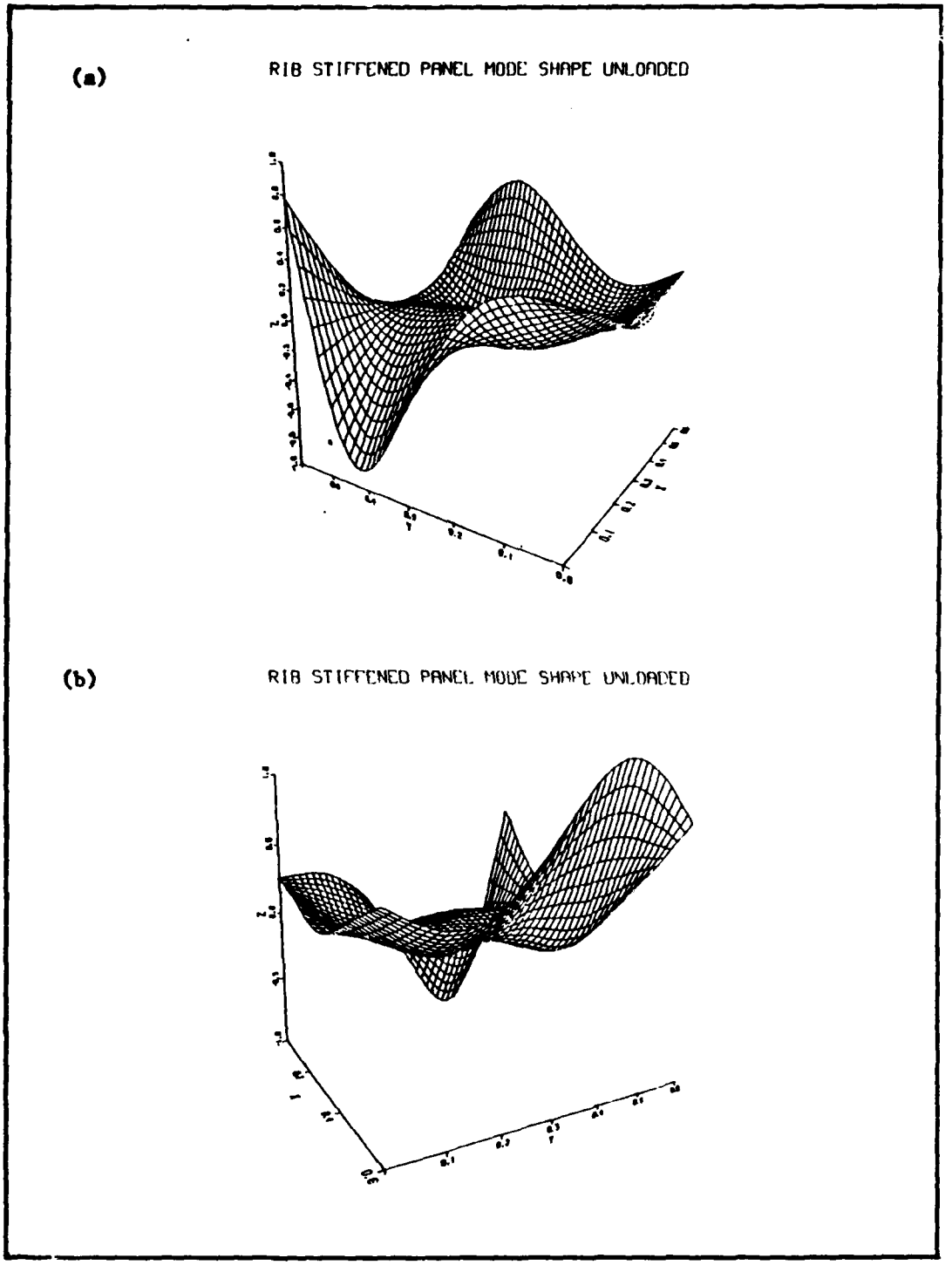

Fig. C-8 (a) View 1 - Mode 8; (b) View 1 - Mode 8 (292.77 Hz)

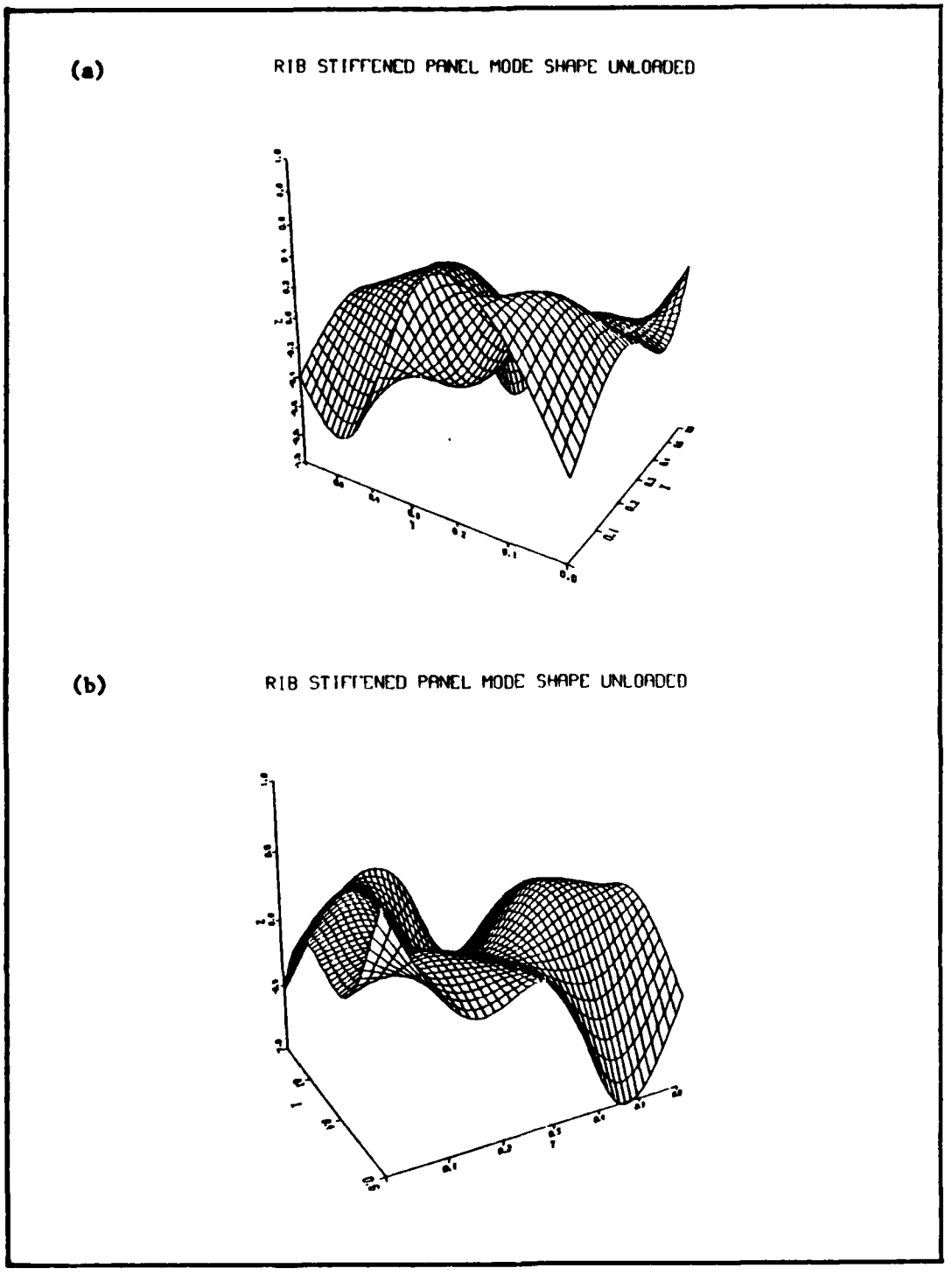

Fig. C-9 (a) View 1 - Mode 9; (b) View 2 - Mode 9 (365.00 Hz)

(a)

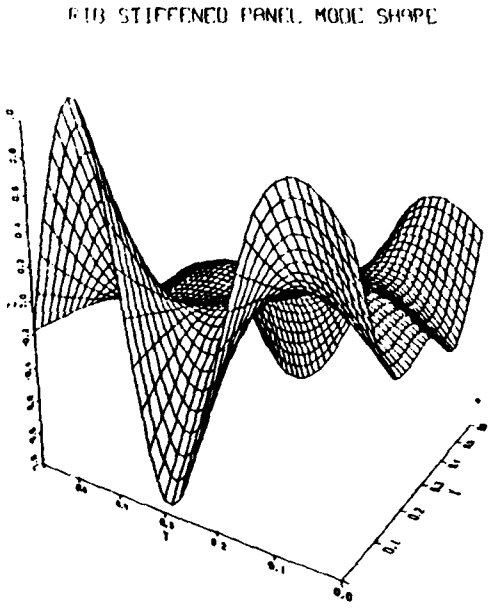

(b)

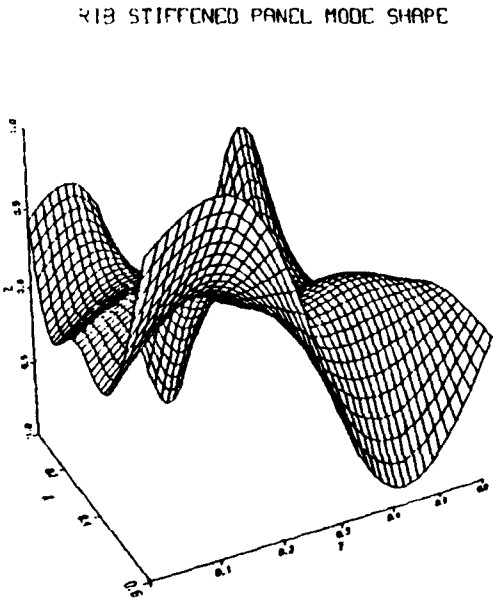

Fig. C-10 (a) View 1 - Mode at 238.22 Hz - Configuration 6

(b) View 2 - Mode at 238.22 Hz - Configuration 6

(a)

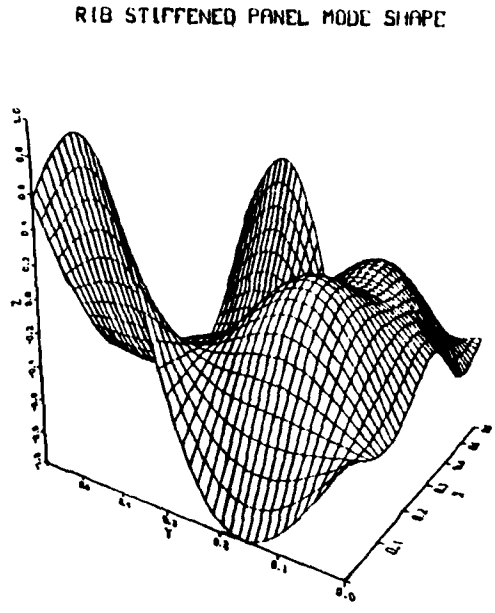

(b)

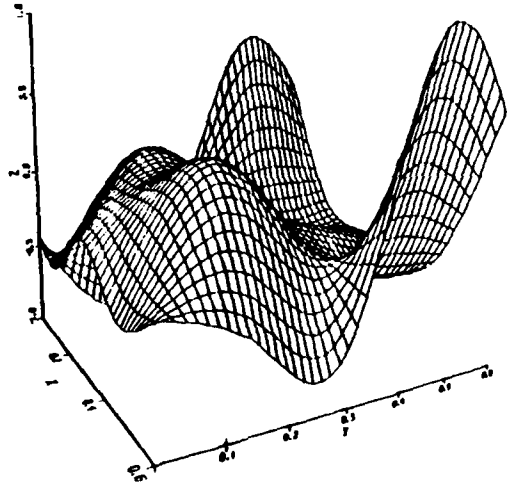

Fig. C-11 (a) View 1 - Mode at 257.2 Hz - Configuration 7

(b) View 2 - Mode at 257.2 Hz - Configuration 7

Appendix D

Computer Program Listings

```
      C    THIS PROGRAM CALCULATES THE GENERALIZED MASS(GM) AND GENERALIZED
      C    STIFFNESS(GS) OF EACH MODE FOR AS MANY CONFIGURATIONS AS THE USER
      C    INPUTS DATA.
           PROGRAM SLOAD(INPUT,OUTPUT,TAPE5=INPUT,TAPE6=OUTPUT,PLFILE=0)
           DIMENSION GM(9),GS(9),GSP(9)
      C    NO=NO THE NUMBER OF NATURAL FREQUENCIES BEING EXAMINED.
           DIMENSION COSP(9,25),X(5),Y(5),C(4,4),CSPLIN(5,4,4)
      C    COSP(NO,I)IN=THE NUMBER OF GRID POINTS AT WHICH DATA WAS TAKEN.
      C    X(NX),Y(NY)(NX,NY=# GRID POINTS IN X AND Y DIRECTIONS RESPECTIVELY.
           DIMENSION GX(41),GY(41),PHISQ(41,41),WOK(2260)
      C    GX(IX),GY(IY)(IX,IY=#OF POINTS IN X AND Y DIRECTIONS AT WHICH VALUES
      C    OF THE BICUBIC SPLINE ARE DESIRED.
      C    WOK=WORK VECTOR OF LENGTH(NY+5)*NX+NY-1+MAX(5 NX-4,5*NY-2),FOR
      C    SUBROUTINE DBCQDU.
           DIMENSION WK(250),F(5,5),POS(6)
      C    WK=WORK VECTOR OF LENGTH(MAX(4,NY)+MAX((NX-1)*3,(NY-1)*3+NY),FOR
      C    SUBROUTINE IBCICU.
      C    F=NX BY NY MATRIX OF FUNCTION VALUES.
           DIMENSION WORK(250)
      C    WORK=WORK VECTOR OF LENGTH(MAX((NX-1)*3,(NY-1)*3+NY),FOR SUBROUTINE
      C    IBCIEU(CALLED BY IBCICU-IS A BICUBIC SPLINE INTERPOLATOR).
           DIMENSION FCN2D(41,41)  ,PSQR(41,41)
           COMMON/PARAM/AA,RX,RY,FA,AB
      C    AA,AB(PANEL DIMENSIONS IN X AND Y DIRECTIONS RESPECTIVELY(METERS)
           COMMON/PARM/E,T,XNU,RHO
      C    E=MODULUS OF ELASTICITY,T=PANEL THICKNESS,XNU=YOUNG'S MODULUS,RHO=
      C    PANEL DENSITY.
           COMMON/MODES/COSP,X,Y,CSPLIN
           NAMELIST/DATA/AM,RX,RY,COREX,COREY,COREM,LLX,LLY
      C    COREX=X LOCATION OF ADDED MASS,COREY=Y LOCATION OF ADDED MASS,COREM=
      C    VALUE OF ADDED MASS,LLX=INTERVAL ON GRID IN X DIRECTION OF LOCATION
      C    OF ADDED MASS,LLY=INTERVAL IN Y DIRECTION OF LOCATION OF ADDED MASS.
           DATA PI,IX,IY,NO,N/3.141592,41,41,9,9/
      C    INPUT VALUES OF UNLOADED NATURAL FREQUENCIES.
           DATA (GS(M),M=1,9)/167.0,190.6,211.1,207.2,237.6,252.1,263.1,292.7
          1,365.0/
           NCON=1
       120 READ(5,DATA)
           IF(EOF(5))195,105
       105 PRINT DATA
           WRITE(6,113) NCON
           NCON=NCON+1
           IFD=0
           NX=5
           NY=5
           DX=AA/40.
           DY=AB/40.
           WRITE(6,133)
           DO 520 M=1,9
           M1=M
           GSP(M1)=GS(M1)
           DO 940 II=1,NX
           DO 940 JJ=1,NY
       940 F(II,JJ)=COSP(M1,NY*(II-1)+JJ)
           GX0=GY0=0.
           LU=LY=0
           DO 910 I=1,IX
```

```
PROGRAM SLOAD      /H/74   OPT=1                    FTN 4.1+H/74      1.11:79  12.27.32

                   DO 1001 II=2,NX
                   IF(X(II)-GX0)1003,1001,1002
69          1002   LX=II-1
                   GX1=1.
                   GO TO 921
                1003  CONTINUE
                921   DO 920 J=1,IY
71                 DO 1111 JJ=2,NY
                   IF(Y(JJ)-GY0)1110,1100,1102
                1102  LY=JJ-1
                   GO TO 922
                1110  CONTINUE
79              922   CONTINUE
                   IF(LU.EQ.LX.AND..V.EQ.LY)GO TO 71
                   LU=LX
                   LV=LY
                C     CALCULATE 2-D BICUBIC SPLINE COEFFICIENTS.
73                 CALL IBCICU(F,IFD,X,NX,Y,NY,LX,LY,C,MK,IER)
                C     CALCULATE MIXED PARTIAL DERIVATIVES OF BICUBIC SPLINE FOR LUMPED
                C     MASS AND PANEL.
                   CALL DBCEVU(X,NX,Y,NY,LLX,LLY,C,COREX,COREY,POS,IER)
                C     COREX  MATRIX CONTAINING SPLINE COEFFICIENTS.
88              C     POS IS A VECTOR OF LENGTH 6 CONTAINING THE EVALUATED BICUBIC SPLINE
                C     S(U,V) AND ITS MIXED PARTIAL DERIVATIVES(POS(1)=S(XL,YL),POS(2)=
                C     DS/DY,POS(3)=DS/DX,POS(4)=D(DS/DX)/DY,POS(5)=D(DS/DX)/DX,POS(6)=
                C     D(DS/DY)/DY.
                   CORE=COREX*POS(1)**2
83                 CALL DBCEVU(X,NX,Y,NY,IX,LX,C,GX1,GY1,POS,IER)
                   PHI2A(I,JJ)=POS(1)**2
                   PCH2P(I,JJ)=POS(1)
                   GY(J)=GY1
                920   GY1=FY1+DY
91                 GX(I)=GX1
                910   GX1=GX1+DX
                   ILX=COREX/DX+1
                   ILY=COREY/DY+1
                    PSUM(ILX,ILY)=CORE/(DX*DY)
93              C     CALCULATE BICUBIC SPLINE QUADRATURE-COMPUTE DOUBLE INTEGRAL USING
                C     NATURAL BICUBIC SPLINE INTERPOLANTOVER RECTANGLE (X(I),X(NX))BY(Y(I),Y(NY)
                C     -ONCE FOR THE PANEL ,ONCE FOR THE LUMPED MASS.EACH RESULTS IN EVALUATION
                C     AT A SINGLE POINT(COREY,COREY).
                   CALL DBCDQU(PSUM,IX,GX,IX,GY,IY,GY(I),GX(LX),GY(I),GY(IY),CORR,MJK
1.1               *,IER)
                   CALL DBCDQU(PSUM,IX,GX,IX,GY,IY,GX(II),GX(IX),GY(I),GY(IY),QM,MQK,
                  *IER)
                C     COMPUTE GENERALIZED MASS.
                   EM(MI)=RHO*I*QM      *CORR
1.5             C     COMPUTE GENERALIZED STIFFNESS.
                   GSF(I)=OMIM1)**(2.*PI*FSP(MI))**2.
                   WRITE(6,1000)GSF(MI),FSP(MI)
                939   CONTINUE
                   GO TO 1?0
110             100   FORMAT(2X,3E22.8)
                  135  FORMAT(1HX,"****THIS IS CONFIGURATION NUMBER",I2,1X,"****")
                  124  FORMAT(/,9X,"GENERALIZED MASS",6X, GENERALIZED STIFFNESS")
                  145  FORMAT(2(8X,E1..))
                  151  FORMAT(2X,"X=",E12.8)


111             172   FORMAT(2X,"Y=",E12.8)
                  195 STOP
                      END
```

```
      BLOCK DATA
      COMMON/MODES/COSP,X,Y,CSPLIN
      DIMENSION COSP(9,25),X(5),Y(5),CSPLIN(3,5,4)
      COMMON/PARAM/IM,DY,ZY,FA,AP
      COMMON/PARM/E,T,XNU,RHO
      DATA AA,BB/.538,.561/
      DATA E,T,XNU,RHO/.3E11,2.036E-3,.33,3.3253/
      DATA (X(I),I=1,5)/0.,.127,.254,.381,.508/
      DATA (Y(I),I=1,5)/0.,.135,.270,.405,.541/
      DATA (COSP(1,I),I=1,5)/1.00,-.165,.159,-.562,.259/
      DATA (COSP(1,I),I=6,10)/.046,-.303,.008,-.137,-.528/
      DATA (COSP(1,I),I=11,15)/.035,-.115,.006,-.111,-.027/
      DATA (COSP(1,I),I=16,20)/.069,-.103,.608,-.119,-.039/
      DATA (COSP(1,I),I=21,25)/-.640,-.073,.051,.274,.221/
      DATA (COSP(2,I),I=1,5)/.577,.155,.161,.215,1.00/
      DATA (COSP(2,I),I=6,10)/-.117,.731,.177,.223,-.121/
      DATA (COSP(2,I),I=11,15)/-.003,.313,.056,.255,-.691/
      DATA (COSP(2,I),I=16,20)/-.126,.303,.071,.195,-.132/
      DATA (COSP(2,I),I=21,25)/.653,.154,.132,.197,.743/
      DATA (COSP(3,I),I=1,5)/.753,.551,-1.00,-.121,-.540/
      DATA (COSP(3,I),I=6,10)/-.400,.035,.001,-.104,.921/
      DATA (COSP(3,I),I=11,15)/.025,-.308,-.008,.110,-.038/
      DATA (COSP(3,I),I=16,20)/-.025,.109,.013,-.015,.105/
      DATA (COSP(3,I),I=21,25)/.464,.211,.312,.127,-.253/
      DATA (COSP(4,I),I=1,5)/-.342,-.511,1.00,.379,.446/
      DATA (COSP(4,I),I=6,10)/-.192,-.123,.135,.110,-.200/
      DATA (COSP(4,I),I=11,15)/-.111,-.095,.032,.003,-.179/
      DATA (COSP(4,I),I=16,20)/-.220,-.122,.128,.105,-.339/
      DATA (COSP(4,I),I=21,25)/-.130,-.164,.530,.317,.354/
      DATA (COSP(5,I),I=1,5)/.360,.349,-.103,1.00,-.155/
      DATA (COSP(5,I),I=6,10)/-.235,.126,-.004,.020,-.165/
      DATA (COSP(5,I),I=11,15)/-.159,.398,-.049,.021,-.654/
      DATA (COSP(5,I),I=16,20)/-.274,.131,-.063,.029,-.066/
      DATA (COSP(5,I),I=21,25)/.317,.612,-.466,.219,-.172/
      DATA (COSP(6,I),I=1,5)/-.129,-1.00,-.062,.253,.130/
      DATA (COSP(6,I),I=6,10)/-.179,.730,-.050,-.125,-.525/
      DATA (COSP(6,I),I=11,15)/-.193,.122,-.036,-.076,-.254/
      DATA (COSP(6,I),I=16,20)/-.094,.131,-.051,-.125,-.390/
      DATA (COSP(6,I),I=21,25)/-.137,-.273,1.223,.311,.132/
      DATA (COSP(7,I),I=1,5)/.734,.327,.623,-1.00,-.714/
      DATA (COSP(7,I),I=6,10)/-.232,.220,-.169,-.110,.107/
      DATA (COSP(7,I),I=11,15)/-.204,.105,-.109,-.073,.006/
      DATA (COSP(7,I),I=16,20)/-.272,.179,-.114,-.108,.153/
      DATA (COSP(7,I),I=21,25)/.362,.553,-.630,-.317,-.231/
      DATA (COSP(8,I),I=1,5)/.255,.217,-.112,-.527,.163/
      DATA (COSP(8,I),I=6,10)/.125,-.117,-.009,-.121,.174/
      DATA (COSP(8,I),I=11,15)/-.132,-.072,-.315,.37[illegible],.181/
      DATA (COSP(8,I),I=16,20)/.123,-.195,-.042,-.135,.169/
      DATA (COSP(8,I),I=21,25)/.263,.114,.572,1.00,-.151/
      DATA (COSP(9,I),I=1,5)/-.547,.235,.262,-.387,-.396/
      DATA (COSP(9,I),I=6,10)/-.109,.135,-.425,-.143,.120/
      DATA (COSP(9,I),I=11,15)/-.125,-.063,-.211,.25[illegible],.125/
      DATA (COSP(9,I),I=16,20)/-.237,-.1[illegible],-.135,.03[illegible],.257/
      DATA (COSP(9,I),I=21,25)/.232,-.292,-.128,-1.0[illegible],-.006/
      END
```

```
$DATA
AM     = .11E+00,
RX     = .129E-01,
RY     = .129E-01,
COREX  = .96E-01,
COREY  = .134E+00,
COREM  = .11E+00,
LLX    = 1,
LLY    = 2,
$END
```

***THIS IS CONFIGURATION NUMBER 1 ***

GENERALIZED MASS	GENERALIZED STIFFNESS
.27627E-01	.30710E+05
.59932E-01	.74723E+03
.58364E-01	.84321E+05
.11935E+00	.18702E+06
.79427E-01	.17702E+06
.91440E-01	.22444E+05
.12382E+00	.38352E+06
.13238E+00	.44774E+06
.14782E+00	.77321E+05

```
$DATA
AM     = .11E+00,
RX     = .129E-01,
RY     = .129E-01,
COREX  = .1E+00,
COREY  = .271E+00,
COREM  = .11E+00,
LLX    = 3,
LLY    = 3,
$END
```

***THIS IS CONFIGURATION NUMBER 2 ***

GENERALIZED MASS	GENERALIZED STIFFNESS
.55509E-01	.72813E+05
.37783E-01	.12137E+06
.38961E-01	.14297E+06
.15073E+00	.25547E+05
.11709E+00	.26273E+06
.12963E+00	.32325E+06
.16444E+00	.50931E+05
.13238E+00	.44773E+06
.15496E+00	.81380E+06

```
$DATA
AM     = .11E+00,
RX     = .129E-01,
RY     = .129E-01,
COREX  = .432E+00,
COREY  = .444E+00,
COREM  = .11E+00,
LLX    = 4,
LLY    = 4,
$END
```

***THIS IS CONFIGURATION NUMBER 3 ***

GENERALIZED MASS	GENERALIZED STIFFNESS
.74364E-01	.82395E+04
.18291E+00	.13299E+06
.10105E+00	.15137E+06
.19737E+00	.26372E+06
.12706E+00	.28318E+06
.19771E+00	.34352E+06
.17145E+00	.53103E+05
.18495E+00	.92412E+05
.17429E+00	.91367E+06

```
$DATA
AM      = .189E+00,
RX      = .142E-01,
RY      = .142E-01,
COREX   = .948E-01,
COREY   = .106E+00,
COREM   = .189E+00,
LLX     = 1,
LLY     = 2,
$END
```

***THIS IS CONFIGURATION NUMBER 4 ***

GENERALIZED MASS	GENERALIZED STIFFNESS
.55962E-01	.63313E+05
.31782E-01	.11009E+06
.95642E-01	.12373E+06
.13073E+00	.23383E+06
.19061E+00	.24263E+05
.12202E+00	.30214E+05
.19764E+00	.47273E+06
.19802E+00	.64403E+05
.29330E+00	.10697E+07

```
$DATA
AM      = .189E+00,
RX      = .142E-01,
RY      = .142E-01,
COREX   = .3E+00,
COREY   = .271E+00,
COREM   = .189E+00,
LLX     = 9,
LLY     = 9,
$END
```

***THIS IS CONFIGURATION NUMBER 5 ***

GENERALIZED MASS	GENERALIZED STIFFNESS
.51113E+00	.12509E+05
.16467E+00	.16323E+05
.14746E+00	.21304E+06
.28110E+00	.34490E+06
.15676E+00	.37166E+05
.17009E+00	.44504E+05
.21548E+00	.56433E+06
.18248E+00	.61720E+06
.29909E+00	.10397E+07

```
$DATA
AM      = .189E+00,
RX      = .142E-01,
RY      = .142E-01,
COREX   = .452E+00,
COREY   = .448E+00,
COREM   = .159E+00,
LLX     = 9,
LLY     = 6,
$END
```

***THIS IS CONFIGURATION NUMBER 6 ***

GENERALIZED MASS	GENERALIZED STIFFNESS
.12909E+00	.12219E+05
.16805E+00	.18137E+06
.15160E+00	.20463E+06
.19325E+00	.32759E+05
.18310E+00	.36367E+05
.17264E+00	.43313E+05
.28719E+00	.64179E+05
.20195E+00	.60304E+05
.22297E+00	.11787E+07

```
$DATA
AN     = .52E-01,
RX     = .123E-01,
RY     = .188E-01,
COREX  = .98E-01,
COREY  = .138E+00,
COREN  = .52E-01,
LLX    = 1,
LLY    = 2,
$END
 ***THIS IS CONFIGURATION NUMBER 7 ***

      GENERALIZED MASS      GENERALIZED STIFFNESS
         .72978E-01              .81121E+05
         .10920E+00              .12342E+06
         .10922E+00              .15282E+06
         .15066E+00              .26382E+06
         .12189E+00              .27835E+05
         .13786E+00              .34383E+05
         .16055E+00              .52315E+06
         .13568E+00              .52384E+06
         .17752E+00              .90730E+05

$DATA
AN     = .52E-01,
RX     = .189E-01,
RY     = .123E-01,
COREX  = .1E+00,
COREY  = .271E+00,
COREN  = .52E-01,
LLX    = 3,
LLY    = 3,
$END
 ***THIS IS CONFIGURATION NUMBER 8 ***

      GENERALIZED MASS      GENERALIZED STIFFNESS
         .77245E-01              .85967E+03
         .10132E+00              .13304E+05
         .11178E+00              .16009E+06
         .16111E+00              .27306E+05
         .12394E+00              .28358E+06
         .15147E+00              .35136E+05
         .17511E+00              .54239E+05
         .15381E+00              .68370E+06
         .16263E+00              .85938E+05

$DATA
AN     = .52E-01,
RX     = .188E-01,
RY     = .123E-01,
COREX  = .452E+00,
COREY  = .948E+00,
COREN  = .52E-01,
LLX    = 4,
LLY    = 4,
$END
 ***THIS IS CONFIGURATION NUMBER 9 ***

      GENERALIZED MASS      GENERALIZED STIFFNESS
         .58108E-01              .53356E+10
         .76364E-01              .95753E+09
         .91243E-01              .11753E+08
         .17182E+00              .22237E+09
         .10955E+00              .22497E+06
         .11207E+00              .28118E+05
         .16520E+00              .44374E+05
         .12847E+00              .40744E+03
         .13955E+00              .72372E+08
```

```
      C     THIS PROGRAM SOLVES FOR THE APPROXIMATED LOADED NATURAL FREQUENCIES.
            PROGRAM SLOAD(INPUT,OUTPUT,TAPE5=INPUT,TAPE6=OUTPUT)
             DIMENSION VAL(9),VEC(9,9),AMASS(9,9),WORK(9),FOST(9)
      C     WORK=WORK VECTOR OF LENGTH(MAX((NY-1)*3,(NY-1) 3+NY),FOR SUBROUTINE
      C     IBCIEU(CALLED BY IBCICU-IS A BICUBIC SPLINE INTERPOLATOR).
            DIMENSION FREQ(9)
            DIMENSION GM(9),GS(9)
      C     NO=9:THE NUMBER OF NATURAL FREQUENCIES BEING EXAMINED.
            DIMENSION COSP(9,25),X(5),Y(5),C(5,5),CSPLIN(9,5,5)
      C     C=CX MATRIX CONTAINING SPLINE COEFFICIENTS.
      C     COSP(NO,NXNY)=THE NUMBER OF GRID POINTS AT WHICH DATA WAS TAKEN.
      C     X(NX),Y(NY)(NX,NY=# GRID POINTS IN X AND Y DIRECTIONS RESPECTIVELY.
            DIMENSION WK(250),F(5,5)
      C     F=NX BY NY MATRIX OF FUNCTION VALUES.
      C     WK=WORK VECTOR OF LENGTH(MAX(5,NY)+MAX((NX-1)*3,(NY-1)*3+NY),FOR
      C     SUBROUTINE IBCICU.
            COMMON/PARAM/AM,RX,RY
      C     AM=VALUE OF ADDED MASS(KG),RX,RY=RADII OF GYRATION(METERS).
            COMMON/MODES/COSP,X,Y,CSPLIN,NX,NY
      C     INPUT THE FOLLOWING DATA FOR EACH MODE OF ALL CONFIGURATIONS TESTED:
      C     ADDED MASS VALUE(AM(KG)),RADII OF GYRATION(METERS),LOCATION POINT
      C     OF ADDED MASS (XP,YP)(METERS),GENERALIZED MASS (GM),GENERALIZED
      C     STIFFNESS (GS).
            NAMELIST/DATA/AM,RX,RY,XP,YP,GM,GS
            DATA PI,NO/3.141592,9/
            NCON=1
            DO 999 NUM=1,999
            READ(5,DATA)
            IF(EOF(5))998,997
      998   STOP
      997   CONTINUE
            PRINT DATA
            IFU=5
      C     IFU=ROW DIMENSION OF DATA MATRIX F.
            NX=5
            NY=5
            WRITE(6,143) NCON
            NCON=NCON+1
            WRITE(6,130)
            LU=LV=0
            DO 1200 III=2,NX
            IF(X(III)-XP)1200,1208,1202
      1202  LX=III-1
            GO TO 923
      1200  CONTINUE
      923   CONTINUE
            DO 1300 JJJ=2,NY
            IF(Y(JJJ)-YP)1300,1308,1302
      1302  LY=JJJ-1
            GO TO 924
      1300  CONTINUE
      924   CONTINUE
            IF(LU.EQ.LX.AND.LV.EQ.LY)GO TO 71
            LU=LX
            LV=LY
            DO 3  ML=1,NO
            DO 1  II=1,NX
```

```
PROGRAM SLOAD     74/74   OPT=1                      FTN 4.6+476        10/19/79  09.47.03

      DO 1  JJ=1,NY
    1 F(II,JJ)=COSP(NJ,NY*(II-1)+JJ)
C     CALCULATE 2-D BICUBIC SPLINE COEFFICIENTS.
      CALL IBCICU(F,IFD,X,NX,Y,NY,LX,LY,C,NK,IER)
      DO 35 II=1,4
      DO 35 JJ=1,4
   35 CSPLIN(NJ,II,JJ)=C(II,JJ)
   70 CONTINUE
      CALL GENCORD(GM,GS,XP,YP,AMASS,VAL,VEC,FORT,WORK,NO,LX,LY)
      DO 14 II=1,NO
   14 FREQ(II)=FORT(II)
      WRITE(6,100)(FREQ(JJ),JJ=1,NO)
  999 CONTINUE
  100 FORMAT(2X,3E20.8)
  105 FORMAT(10X,E20.8)
  150 FORMAT(/,10X,"LOADED PLATE FREQUENCIES")
  115 FORMAT(2X,"CONFIGURATION NUMBER =",I5)
      STOP
      END


SUBROUTINE GENCORD    74/74   OPT=1                      FTN 4.6+476        10/19/79  09.47.03

C     THIS SUBROUTINE COMPUTES VALUES OF THE MATRICES REQUIRED AND THEN
C     SOLVES THE EIGENVALUE PROBLEM FOR THE LOADED NATURAL FREQUENCIES.
      SUBROUTINE GENCORD(GM,GS,XO,YO,AMASS,VAL,VEC,FORT,WORK,NO,LX,LY)
      COMMON/PARAM/AM,RX,RY
      DIMENSION AMASS(NO,NO),VAL(NO),VEC(NO,NO),WORK(NO),FORT(NO)
      DIMENSION GM(NO),GS(NO)
      DO 20 K=1,NO
      CALL SHAPE(LX,LY,K,XO,YO,PHI,PHIDX,PHIDY)
      CNST=AM*PHI*PHI+AM*RX*RX*PHIDX*PHIDX+AM*RY*RY*PHIDY*
     1PHIDY
      AMASS(K,K)=(GS(K)+CNST)/(GM(K)+CNST)
      DO 20 KK=1,NO
      IF(K.EQ.KK)GO TO 20
      CALL SHAPE(LX,LY,KK,XO,YO,PHI1,PHIX1,PHIY1)
      AMASS(K,KK)=(AM*PHI*PHI1+AM*RX*RX*PHIDX*PHIX1+AM*RY*RY*PHI
     1DY*PHIY1)/(GM(K)+CNST)
   20 CONTINUE
      IND=1
      CALL RSEIG(NO,NO,AMASS,IND,VAL,VEC,WORK)
      DO 10 I=1,NO
      DO 10 J=1,NO
      IF(VEC(I,J).EQ.1.)FORT(I)=SQRT(VAL(J)*GM(I)/GS(I))
   10 CONTINUE
      RETURN
      END


SUBROUTINE SHAPE      74/74   OPT=1                      FTN 4.6+476        10/19/79  09.47.03

C     THIS SUBROUTINE SOLVES FOR THE PARTIAL DERIVATIVES OF THE MODE SHAPES
C     REQUIRED TO SET UP THE EIGENVALUE PROBLEM.
      SUBROUTINE SHAPE(LX,LY,KK,U,V,PHI,PHIDX,PHIDY)
      COMMON/MODES/COSP,X,Y,CSPLIN,NX,NY
      DIMENSION C(4,4),PDS(6)
      DIMENSION COSP(9,23),X(9),Y(5),CSPLIN(9,4,4)
      DO 10 I=1,4
      DO 10 J=1,4
   10 C(I,J)=CSPLIN(KK,I,J)
C     CALCULATE MIXED PARTIAL DERIVATIVES OF BICUBIC SPLINE  APPROXIMATED
C     MODE SHAPES.
      CALL DBCEVU(X,NX,Y,NY,C,LX,LY,U,V,PDS,IER)
C     PDS IS A VECTOR OF LENGTH 6 CONTAINING THE EVALUATED BICUBIC SPLINE
C     S(U,V) AND ITS MIXED PARTIAL DERIVATIVES(PDS(1)=S(XL,YL),PDS(2)=
C     DS/DX,PDS(3)=DS/DY,PDS(4)=D(DS/DX)/DY,PDS(5)=D(DS/DX)/DX,PDS(6)=
C     D(DS/DY)/DY.
      PHI=PDS(1)
      PHIDX=PDS(2)
      PHIDY=PDS(3)
   40 CONTINUE
      RETURN
      END
```

```
      BLOCK DATA
      COMMON/MODES/COSP,X,Y,CSPLIN,NX,NY
      DIMENSION COSP(9,25),X(5),Y(5),CSPLIN(9,25)
      DATA (X(I),I=1,5)/0.,.127,.254,.381,.508/
      DATA (Y(I),I=1,5)/0.,.135,.270,.405,.541/
      DATA (COSP(1,I),I=1,5)/1.17,-.155,.109,-.512,.259/
      DATA (COSP(1,I),I=6,10)/.046,-.019,.008,-.115,-.133/
      DATA (COSP(1,I),I=11,15)/.035,-.115,.006,-.011,-.027/
      DATA (COSP(1,I),I=16,20)/.049,-.007,.009,-.019,-.039/
      DATA (COSP(1,I),I=21,25)/-.590,-.133,.051,.224,.221/
      DATA (COSP(2,I),I=1,5)/.573,.167,.1.6,.205,1.00/
      DATA (COSP(2,I),I=6,10)/-.117,.031,.077,.223,-.121/
      DATA (COSP(2,I),I=11,15)/-.065,.178,.064,.255,-.091/
      DATA (COSP(2,I),I=16,20)/-.126,.185,.071,.155,-.132/
      DATA (COSP(2,I),I=21,25)/.493,.154,.132,.197,.03/
      DATA (COSP(3,I),I=1,5)/.759,.501,-1.00,-.127,-.548/
      DATA (COSP(3,I),I=6,10)/-.108,.012,.00,-.014,.421/
      DATA (COSP(3,I),I=11,15)/.025,-.208,-.002,.004,-.039/
      DATA (COSP(3,I),I=16,20)/-.025,.008,.013,-.006,.108/
      DATA (COSP(3,I),I=21,25)/.064,.211,.312,.127,-.253/
      DATA (COSP(4,I),I=1,5)/-.342,-.601,1.00,.319,.46/
      DATA (COSP(4,I),I=6,10)/-.192,-.123,.136,.119,-.206/
      DATA (COSP(4,I),I=11,15)/-.161,-.035,.030,.003,-.179/
      DATA (COSP(4,I),I=16,20)/-.220,-.122,.128,.105,-.339/
      DATA (COSP(4,I),I=21,25)/-.330,-.45,.530,.317,.350/
      DATA (COSP(5,I),I=1,5)/.309,.309,-.103,1.00,-.155/
      DATA (COSP(5,I),I=6,10)/-.235,.125,-.064,.028,-.165/
      DATA (COSP(5,I),I=11,15)/-.150,.100,-.049,.021,-.054/
      DATA (COSP(5,I),I=16,20)/-.214,.121,-.063,.029,-.060/
      DATA (COSP(5,I),I=21,25)/.317,.033,-.409,.219,-.172/
      DATA (COSP(6,I),I=1,5)/-.129,-1.00,-.062,.253,.158/
      DATA (COSP(6,I),I=6,10)/-.179,.130,-.030,-.125,-.025/
      DATA (COSP(6,I),I=11,15)/-.193,.122,-.035,-.076,-.254/
      DATA (COSP(6,I),I=16,20)/-.090,.131,-.051,-.125,-.398/
      DATA (COSP(6,I),I=21,25)/-.137,-.231,.229,.314,.132/
      DATA (COSP(7,I),I=1,5)/.734,.359,.628,1.00,-.311/
      DATA (COSP(7,I),I=6,10)/-.232,.228,-.169,-.100,.087/
      DATA (COSP(7,I),I=11,15)/-.204,.125,-.109,-.070,.056/
      DATA (COSP(7,I),I=16,20)/-.272,.153,-.116,-.008,.103/
      DATA (COSP(7,I),I=21,25)/.362,.337,-.033,-.317,-.231/
      DATA (COSP(8,I),I=1,5)/.255,.217,-.402,-.827,.783/
      DATA (COSP(8,I),I=6,10)/.129,-.160,-.044,-.124,.174/
      DATA (COSP(8,I),I=11,15)/.105,-.380,-.032,-.16 ,.133/
      DATA (COSP(8,I),I=16,20)/.123,-.195,-.042,-.134,.169/
      DATA (COSP(8,I),I=21,25)/.263,.144,.572,1.00,.51/
      DATA (COSP(9,I),I=1,5)/-.517,.205,.202,-.567,-.396/
      DATA (COSP(9,I),I=6,10)/-.109,.171,-.425,-.073,.120/
      DATA (COSP(9,I),I=11,15)/-.125,-.063,-.237,.25 ,.125/
      DATA (COSP(9,I),I=16,20)/-.230,-.0 ,-.124,.03 ,.257/
      DATA (COSP(9,I),I=21,25)/.292,-.237,-.275,-1.0 ,-.408/
      END
```

```
$DATA
AM      = .11E+00,
RX      = .129E-01,
RY      = .129E-01,
XP      = .35E-01,
YP      = .135E+00,
GM      = .27527E-01, .58732E-01, .58304E-01, .11635E+00, .73427E-01,       .91[illegible]E-01, .12382E+00, .13238E+00,
          .16782E+00,
GS      = .33?1E+05, .74725E+05, .8432E+05, .10782E+06, .17782E+06, .22[illegible]E+06, .33352E+06, .44774E+06, .17324E+06,
$END
 CONFIGURATION NUMBER =    1

        LOADED PLATE FREQUENCIES
       .39924133E+00       .59224609E+00       .99613978E+00
       .39953199E+00       .99783221E+00       .97934139E+06
       .93616618E+00       .99866834E+00       .99774477E+00

$DATA
AM      = .11E+00,
RX      = .129E-01,
RY      = .129E-01,
XP      = .32E+00,
YP      = .271E+00,
GM      = .51[illegible]E-01, .43482E-01, .38916E-01, .15073E+00, .11589E+00,       .12963E+00, .16[illegible]E+00, .13230E+00,
          .153[illegible]E+00,
GS      = .72[illegible]E+05, .12037E+06, .14237E+05, .25547E+06, .26[illegible]5E+06,       .32125E+05, .5[illegible]31E+06, .44773E+06,
          .815[illegible]E+00,
$END
 CONFIGURATION NUMBER =    2

        LOADED PLATE FREQUENCIES
       .99537622E+00       .99752919E+00       .99908975E+00
       .99527594E+00       .99901142E+00       .99903119E+00
       .99923[illegible]8E+00       .99742336E+00       .99386092E+00

$DATA
AM      = .11E+00,
RX      = .129E-01,
RY      = .129E-01,
XP      = .[illegible]2E+00,
YP      = .44E+00,
GM      = .74304E-01, .10291E+00, .10689E+00, .35737E+00, .12766E+00,       .13771E+00, .17145E+00, .15496E+00,
          .17529E+00,
GS      = .8259[illegible]E+05, .132E+06, .15437E+05, .26[illegible]72E+06, .28318E+06, .3[illegible]52E+06, .531[illegible]3E+06, .52[illegible]12E+06, .91669E+06,
$END
 CONFIGURATION NUMBER =    3

        LOADED PLATE FREQUENCIES
       .3924[illegible]914E+00       .9765344E+00       .99913742E+00
       .39453[illegible]8E+00       .99240461E+00       .99756220E+00
       .73[illegible]6[illegible]34E+00       .9435[illegible]272E+00       .9446577?E+00
```

```
$DATA
AR      = .1[illegible]E+00,
AI      = .11.2E-01,
BR      = .1.42E-01,
BP      = .31E-01,
YP      = .13[illegible]E+00,
GR      = .[illegible]E-01, .9178EE-01, .85642E-01, .13973E[illegible], .13[illegible]E+00,
          .12642E+01, .1526[illegible]E+00, .19642E+00,
          .2[illegible]E+00,
GS      = .[illegible]E+05, .11[illegible]E+06, .1237[illegible], .23683[illegible], .24[illegible]E+[illegible],
          .30215E+00, .[illegible]278E+06, .64[illegible]E+06,
          .1[illegible]97E+07,
$END
 CONFIGURATION NUMBER =   4

        LOADED PLATE FREQUENCIES
        .[illegible]E+00        .[illegible]E+00        .[illegible]E+00
        .[illegible]E+00        .[illegible]E+00        .[illegible]E+00
        .[illegible]E+00        .[illegible]E+00        .[illegible]E+00

$DATA
AR      = .1[illegible]E+00,
AI      = .1[illegible]E-01,
BR      = .1[illegible]E-01,
BP      = .3[illegible],
YP      = .12[illegible]E+00,
GR      = .11[illegible]E+00, .14[illegible]E+00, .16[illegible], .74[illegible]E+00, .13[illegible]E+00,
          .17[illegible]E+00, .21[illegible]E+00, .1[illegible]E+00,
          .2[illegible]E+00,
GS      = .12[illegible]E+05, .18[illegible]E+06, .2[illegible], .23683[illegible], .37[illegible]E+06,
          .4[illegible]E+05, .66[illegible]E+06, .6172E+06,
          .1[illegible]E+07,
$END
 CONFIGURATION NUMBER =   5

        LOADED PLATE FREQUENCIES
        .[illegible]E+00        .[illegible]E+00        .[illegible]E+00
        .[illegible]E+00        .[illegible]E+00        .[illegible]E+00
        .[illegible]E+00        .[illegible]E+00        .[illegible]E+00

$DATA
AR      = .1[illegible]E+00,
AI      = .1[illegible]E-01,
BR      = .1[illegible]E-01,
BP      = .1[illegible]E+00,
YP      = .[illegible]E+00,
GR      = .1[illegible]E+00, .[illegible]E+00, .[illegible]E+00, .[illegible]E+00, .[illegible]E+00,
          .1726[illegible]E+00, .2[illegible]E+00, .2b[illegible]E+00,
          .2[illegible]E+00,
GS      = .12[illegible]E+00, .[illegible]E+06, .[illegible]E+06, .[illegible]E+06, .[illegible]E+06,
          .41315[illegible]E+06, .6[illegible]E+06, .64[illegible]E+06,
          .1[illegible]E+07,
$END
 CONFIGURATION NUMBER =   6

        LOADED PLATE FREQUENCIES
        .[illegible]E+00        .[illegible]E+00        .[illegible]E+00
        .[illegible]E+00        .[illegible]E+00        .[illegible]E+00
        .[illegible]E+00        .[illegible]E+00        .[illegible]E+00
```

```
$DATA
AM      = .[illegible]2E-01,
AX      = .123E-01,
AY      = .199E-01,
XP      = .[illegible]3E-01,
YP      = .194E+00,
GM      = .72378E-01, .[illegible], .10922E+00, .1[illegible]56E+00, .12689E+00,        .13709E+01, .15959E+00, .15669E+00,
          .17272E+00,
GS      = .91192E+05, .12902E+06, .15232E+05, .26382E+06, .27835E+06,        .34349E+05, .57416E+06, .929[illegible]E+06,
          .9[illegible]E+06,
$END
 CONFIGURATION NUMBER =    7

        LOADED PLATE FREQUENCIES
        .13353320E+00        .59772209E+39        .99926109E+00
        .39233571E+00        .59630209E+00        .99347167E+00
        .39[illegible]15A6E+30        .5992'550E+00        .99833460E+0


$DATA
AM      = .[illegible]2E-01,
AX      = .108E-01,
AY      = .123E-01,
XP      = .354E+0,
YP      = .271E+00,
GM      = .77245E-01, .10332E+00, .11078E+00, .16111E+00, .12944E+00,        .14147E+01, .17511E+00, .14381E+00,
          .15283E+00,
GS      = .4558[illegible]E+05, .1330[illegible]E+06, .16634E+06, .77308E+06, .20848E+06,        .53496E+05, .54730E+06, .4837E+06,
          .85538E+06,
$END
 CONFIGURATION NUMBER =    8

        LOADED PLATE FREQUENCIES
        .39339[illegible]3E+00        .59894292E+00        .99961368E+00
        .39939[illegible]1E+00        .59956146E+00        .39958079E+09
        .39721843E+00        .59884812E+03        .99641[illegible]02E+00


$DATA
AM      = .[illegible]2E-01,
AX      = .1[illegible]9E-01,
AY      = .123E-01,
XP      = .[illegible]32E+00,
YP      = .[illegible]9E+00,
GM      = .[illegible]1E-01, .7[illegible]3E-01, .81283E-01, .1[illegible]102E+00, .10155E+00,        .11237E+03, .1[illegible]52E+00, .12047E+00,
          .13[illegible]E+00,
GS      = .[illegible]35[illegible]E+05, .93795E+05, .117[illegible]3E+16, .72237E+06, .22609E+06,        .20118E+06, .[illegible]974E+06, .40744E+06,
          .72472E+06,
$END
 CONFIGURATION NUMBER =    [illegible]

        LOADED PLATE FREQUENCIES
        .93356072E+00        .9843[illegible]670E+00        .99963925E+00
        .39577329E+00        .59523480E+00        .9976[illegible]2[illegible]E+00
        .99[illegible]590[illegible]9E+00        .9E1[illegible]5428E+00        .96327107E+00
```

PROGRAM SLOAD 74/74 OPT=1 FTN 4.6+ 1/21/77 12.12.

```
      C     THIS PROGRAM CALCULATES THE GENERALIZED MASS(GM) AND GENERALIZED
      C     STIFFNESS(GS) OF EACH MODE FOR AS MANY CONFIGURATIONS AS THE USER
      C     INPUTS DATA.
            PROGRAM SLOAD(INPUT,OUTPUT,TAPE5=INPUT,TAPE6=OUTPUT,PLFILE=0)
            DIMENSION GM(3),GF(3),FSP(9)
      C     NO=9=THE NUMBER OF NATURAL FREQUENCIES BEING EXAMINED.
            DIMENSION COSP(1,2,1),X(5),Y(5),C(4,4),CSFLIN(9,4,4)
      C     COSP(NO,N)(N=THE NUMBER OF GRID POINTS AT WHICH DATA WAS TAKEN.
      C     X(NX),Y(NY)(NX,NY=# GRID POINTS IN X AND Y DIRECTIONS RESPECTIVELY.
            DIMENSION GX(41),GY(41),PHISQ(41,41),WOK(2200)
      C     GX(IX),GY(IY)(IX,IY=#OF POINTS IN X AND Y DIRECTIONS AT WHICH VALUES
      C     OF THE  BICUBIC SPLINE ARE DESIRED.
      C     WOK=WORK VECTOR OF LENGTH((NY+5)*NX+NY-1+MAX(5 NX-4,5*NY-2),FOR
      C     SUBROUTINE DBCQDU.
            DIMENSION WK(250),F(5,5),PDS(6)
      C     WK=WORK VECTOR OF LENGTH(4*MAX(4,NY)+MAX((NX-1)*3,(NY-1)*3+NY),FOR
      C     SUBROUTINE IBCICU.
      C     F=NX BY NY MATRIX OF FUNCTION VALUES.
            DIMENSION WORK(2000)
      C     WORK=WORK VECTOR OF LENGTH(MAX((NX-1)*3,(NY-1) 3+NY),FOR SUBROUTINE
      C     IBCIEU(CALLED BY IBCICU-IS A BICUBIC SPLINE INTERPOLATOR).
            DIMENSION FCN2D(41,41)  ,PSQR(41,41)
            COMMON/PARAM/AM,FX,RY,AA,AB
      C     AA,AB(PANEL DIMENSIONS IN X AND Y DIRECTIONS RESPECTIVELY(METERS)
            COMMON/PARM/E,T,XNU,RHO
      C     E=MODULUS OF ELASTICITY,T=PANEL THICKNESS,XNU=YOUNG'S MODULUS,RHO=
      C     PANEL DENSITY.
            COMMON/MODES/COSP,X,Y,CSPLIN
            NAMELIST/DATA/AA,RX,FY,COREX,COREY,COREM,LLX,LLY
      C     COREX=X LOCATION OF ADDED MASS,COREY=Y LOCATION OF ADDED MASS,COREM=
      C     VALUE OF ADDED MASS,LLX=INTERVAL ON GRID IN X DIRECTION OF LOCATION
      C     OF ADDED MASS,LLY=INTERVAL IN Y DIRECTION OF LOCATION OF ADDED MASS.
            DATA PI,IX,IY,NO,N/3.141592,41,41,9,3/
      C     INPUT VALUES OF UNLOADED NATURAL FREQUENCIES.
            DATA (GS(M),M=1,9)/157.8,180.6,191.3,207.2,237.6,252.1,285.1,292.7
           1,365.0/
            MCON=1
        125 READ(5,DATA)
            IF(EOF(5))135,105
        105 PRINT DATA
            WRITE(6,115) MCON
            MCON=MCON+1
            IFU=5
            NX=5
            NY=5
            DX=AA/40.
            DY=AB/40.
            WRITE(6,130)
            DO 959 M=1,9
            M1=M
            GS(M1)=GS(M1)
            DO 940 II=1,NX
            DO 940 JJ=1,NY
      940   F(II,JJ)=COSP(M1,NY*(II-1)+JJ)
            GX(1)=0.
            LU=LV=.
            DO 910 I=1,IX
```

```
             DO 1000 II=2,NX
             IF(X(II)-GX0)1000,1000,1002
      1002   LX=II-1
             GY0=0.
             GO TO 921
      1000   CONTINUE
      921    DO 920 J=1,IY
             DO 1100 JJ=2,NY
             IF(Y(JJ)-GY0)1100,1100,1102
      1102   LY=JJ-1
             GO TO 922
      1100   CONTINUE
      922    CONTINUE
             IF(LU.EQ.LX.AND.LV.EQ.LY)GO TO 71
             LU=LX
             LV=LY
      C      CALCULATE 2-D BICUBIC SPLINE COEFFICIENTS.
             CALL IBCICU(F,IFD,X,NX,Y,NY,LX,LY,C,VR,IER)
      C      CALCULATE MIXED PARTIAL DERIVATIVES OF BICUBIC SPLINE FOR LUMPED
      C      MASS AND PANEL.
             CALL DBCEVU(X,NX,Y,NY,ILX,ILY,C,COREX,COREY,PDS,IER)
      C      C=4 X4 MATRIX CONTAINING SPLINE COEFFICIENTS.
      C      PDS IS A VECTOR OF LENGTH 6 CONTAINING THE EVALUATED BICUBIC SPLINE
      C      S(U,V) AND ITS MIXED PARTIAL DERIVATIVES(PDS(1)=S(XL,YL),PDS(2)=
      C      DS/DX,PDS(3)=DS/DY,PDS(4)=D(DS/DX)/DY,PDS(5)=D(DS/DX)/DX,PDS(6)=
      C      D(DS/DY)/DY.
             CORE=LUMCM*PDS(1)**2
      71     CALL DBCEVU(X,NX,Y,NY,LX,LY,C,GX1,GY0,PDS,IER)
             PHISQ(I,J)=PDS(1)**2
             FCN2C(I,J)=PDS(1)
             GY(J)=GY0
      920    GY0=GY0+DY
             GX(I)=GX0
      910    GX1=GX0+DX
             ILX=COREX/DX+1
             ILY=COREY/DY+1
             PSQ(ILX,ILY)=CORE/(DX*DY)
      C      CALCULATE BICUBIC SPLINE QUADRATURE-COMPUTE DOUBLE INTEGRAL USING
      C      NATURAL BICUBIC SPLINE INTERPOLANT OVER RECTANGLE (X(1),X(NX))BY(Y(1),Y(NY))
      C      -ONCE FOR THE PANEL ,ONCE FOR THE LUMPED MASS.LATTER RESULTS IN EVALUATION
      C      AT A SINGLE POINT(COREX,COREY).
             CALL DBCQDU(PSQ,IX,GX,IX,GY,IY,GX(1),GX(IX),GY(1),GY(IY),CORR,WOK
            *,IER)
             CALL DBCQDU(PHISQ,IX,GX,IX,GY,IY,GX(1),GX(IX),GY(1),GY(IY),QM,WOK,
            *IER)
      C      COMPUTE GENERALIZED MASS.
             GM(M1)=RHO*T*QM    +CORR
      C      COMPUTE GENERALIZED STIFFNESS.
             GSP(M1)=GM(M1)*(2.*PI*FSP(M1))**2.
             WRITE(6,1401)GM(M1),GSP(M1)
      C      THIS PORTION OF THE PROGRAM PLOTS THE CONTINUOUS MODE SHAPES IN 3-D.
             IXDIM=41
             IYDIM=41
             ZMIN=-1.00
             ZMAX=1.00
             YMIN=0.
             YMAX=6.941
```

```
                XMIN=0.
                XMAX=8.500
                X3D=Y3D=1.0
                Z3D=1.0
                X3DMAX=.500
                Y3DMAX=.541
                CALL COMPRS
                CALL BGNPL(1)
                CALL BASALF("STANDARD")
                CALL MIXALF("L/CSTD")
                CALL PAGE(14.25,10.25)
                CALL TITL 3D(44HRIB STIFFENED PANEL MODE SHAPE:CONFIGURATION ,39,
               *11.4,8.14)
C               LABEL AXES.
                CALL AXES 3D(1HX,1,1HY,1,1HZ,1,X3D,Y3D,Z3D)
C               CHOOSE VIEW POINT FROM WHICH WISH VIEW PLOT.
                CALL VIEW(1.1,-.23,.6)
C               SCALE AXES AS DESIRED.
                CALL GRAF 3D(XMIN,5HSCALE,XMAX,YMIN,5HSCALE,YMAX,ZMIN,5HSCALE,ZMAX
               *)
C               PLOT MODE SHAPE-"1"CALLS FOR FINEST MESH POSSIBLE IN DRAWING THE PLOT.
                CALL SURMAT(FCN2),1,41,1,41,WORK)
                CALL ENDPL(1)
          999   CONTINUE
                CALL DONEPL
                GO TO 125
          100   FORMAT(2X,3E20.8)
            115 FORMAT(4X,"***THIS IS CONFIGURATION NUMBER",I2,1X,"****")
            130 FORMAT(/,9X,*GENERALIZED MASS*,5X,*GENERALIZED STIFFNESS*)
            140 FORMAT(2(8X,E15.5))
          160   FORMAT(2X,*X=*,E12.5)
          170   FORMAT(2X,*Y=*,E12.5)
            195 STOP
                END
```

BLOCK DATA BLKDAT1.   74/74   OPT=1   FTN 4.7+476   10/13/79 12.12.54

```
      BLOCK DATA
      COMMON/MODES/COSP,X,Y,CSPLIN
      DIMENSION COSP(9,25),X(5),Y(5),CSPLIN(3,4,5)
      COMMON/PARAM/AM,RX,RY,AA,AB
      COMMON/PARM/L,T,XNU,RHO
      DATA AA,AB/.008,.01/
      DATA L,T,XNU,RHO/5.9E1,2.36E-3,.33,3.32E3/
      DATA (X(I),I=1,5)/0.,.127,.254,.381,.508/
      DATA (Y(I),I=1,5)/0.,.135,.270,.405,.541/
      DATA (COSP(1,I),I=1,5)/1.00,-.165,.359,-.302,.259/
      DATA (COSP(1,I),I=6,10)/.016,-.335,.040,-.015,-.130/
      DATA (COSP(1,I),I=11,15)/.231,-.106,.006,-.011,-.027/
      DATA (COSP(1,I),I=16,20)/.049,-.109,.008,-.019,-.039/
      DATA (COSP(1,I),I=21,25)/-.697,-.033,.351,.224,.221/
      DATA (COSP(2,I),I=1,5)/.773,.103,.146,.205,1.0./
      DATA (COSP(2,I),I=6,10)/-.117,.911,.077,.223,-.121/
      DATA (COSP(2,I),I=11,15)/-.185,.379,.064,.255,-.191/
      DATA (COSP(2,I),I=16,20)/-.120,.396,.071,.195,-.132/
      DATA (COSP(2,I),I=21,25)/.153,.155,.132,.197,.193/
      DATA (COSP(3,I),I=1,5)/.759,.561,-1.00,-.127,-.948/
      DATA (COSP(3,I),I=6,10)/-.008,.018,.60,-.656,.021/
      DATA (COSP(3,I),I=11,15)/.025,-.180,-.008,.044,-.030/
      DATA (COSP(3,I),I=16,20)/-.025,.104,.013,-.006,.100/
      DATA (COSP(3,I),I=21,25)/.464,.211,.312,.127,-.253/
      DATA (COSP(4,I),I=1,5)/-.342,-.531,1.00,.379,.446/
      DATA (COSP(4,I),I=6,10)/-.192,-.123,.136,.116,-.200/
      DATA (COSP(4,I),I=11,15)/-.161,-.135,.094,.083,-.179/
      DATA (COSP(4,I),I=16,20)/-.220,-.122,.129,.165,-.339/
      DATA (COSP(4,I),I=21,25)/-.136,-.454,.530,.317,.354/
      DATA (COSP(5,I),I=1,5)/.365,.309,-.883,1.00,-.135/
      DATA (COSP(5,I),I=6,10)/-.235,.125,-.056,.126,-.165/
      DATA (COSP(5,I),I=11,15)/-.150,.105,-.063,.021,-.056/
      DATA (COSP(5,I),I=16,20)/-.274,.131,-.063,.029,-.060/
      DATA (COSP(5,I),I=21,25)/.317,.513,-.460,.219,-.172/
      DATA (COSP(6,I),I=1,5)/-.129,-1.00,-.062,.253,.130/
      DATA (COSP(6,I),I=6,10)/-.179,.050,-.059,-.125,-.525/
      DATA (COSP(6,I),I=11,15)/-.193,.122,-.035,-.070,-.254/
      DATA (COSP(6,I),I=16,20)/-.090,.131,-.051,-.12[illegible],-.398/
      DATA (COSP(6,I),I=21,25)/-.137,-.289,-.229,.310,.132/
      DATA (COSP(7,I),I=1,5)/.730,.379,.529,-1.0[illegible],-.710/
      DATA (COSP(7,I),I=6,10)/-.232,.220,-.169,-.142,.108/
      DATA (COSP(7,I),I=11,15)/-.204,.106,-.109,-.077,.056/
      DATA (COSP(7,I),I=16,20)/-.272,.130,-.140,-.60[illegible],.103/
      DATA (COSP(7,I),I=21,25)/.302,.313,-.630,-.317,-.231/
      DATA (COSP(8,I),I=1,5)/.295,.217,-.012,-.527,.[illegible]93/
      DATA (COSP(8,I),I=6,10)/.125,-.100,-.040,-.126,.174/
      DATA (COSP(8,I),I=11,15)/-.182,-.042,-.311,.37[illegible],.161/
      DATA (COSP(8,I),I=16,20)/.123,-.13[illegible],-.[illegible]62,-.13[illegible],.169/
      DATA (COSP(8,I),I=21,25)/.259,.1[illegible],.172,1.00,.[illegible]51/
      DATA (COSP(9,I),I=1,5)/-.[illegible]07,.235,.212,-.507,-.356/
      DATA (COSP(9,I),I=6,10)/-.109,.115,-.425,-.6[illegible]3,.126/
      DATA (COSP(9,I),I=11,15)/-.125,-.063,-.211,.25[illegible],.12[illegible]/
      DATA (COSP(9,I),I=16,20)/-.23[illegible],-.043,-.124,.63[illegible],.257/
      DATA (COSP(9,I),I=21,25)/.252,-.232,-.21[illegible],-1.0[illegible],-.[illegible]06/
      END
```

Appendix E

Miscellaneous Information

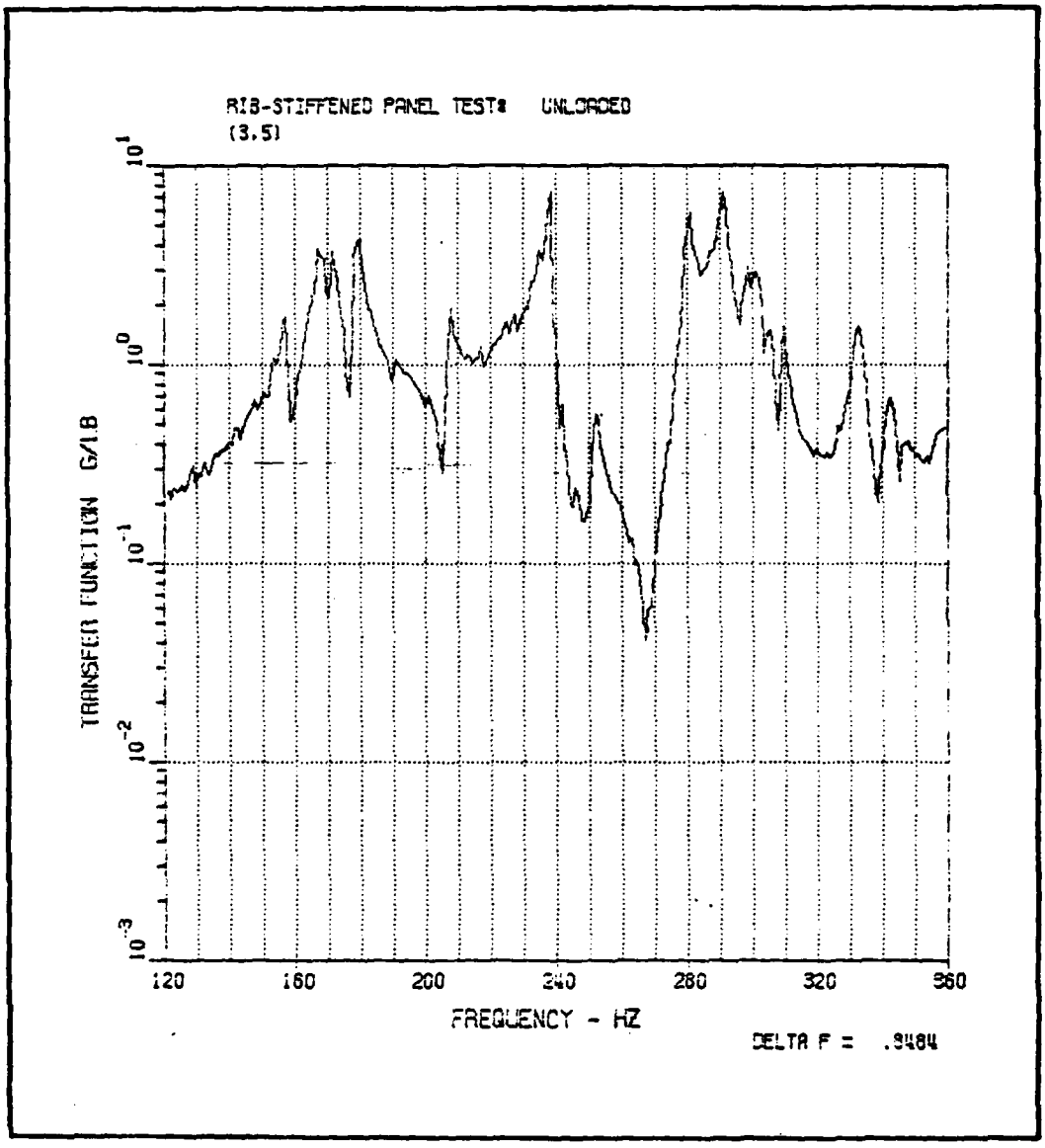

Fig. E-1 Sample Transfer Function Plot - Method 1

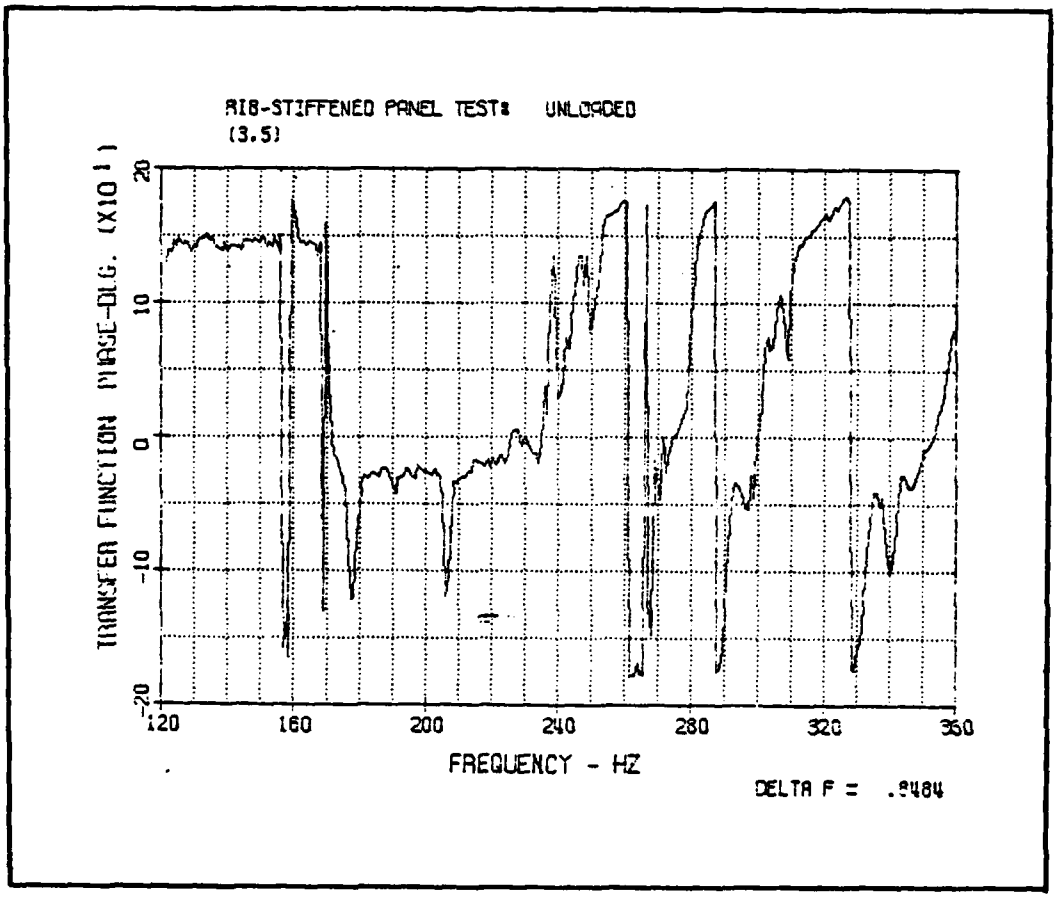

Fig. E-2 Sample Phase Plot - Method 1

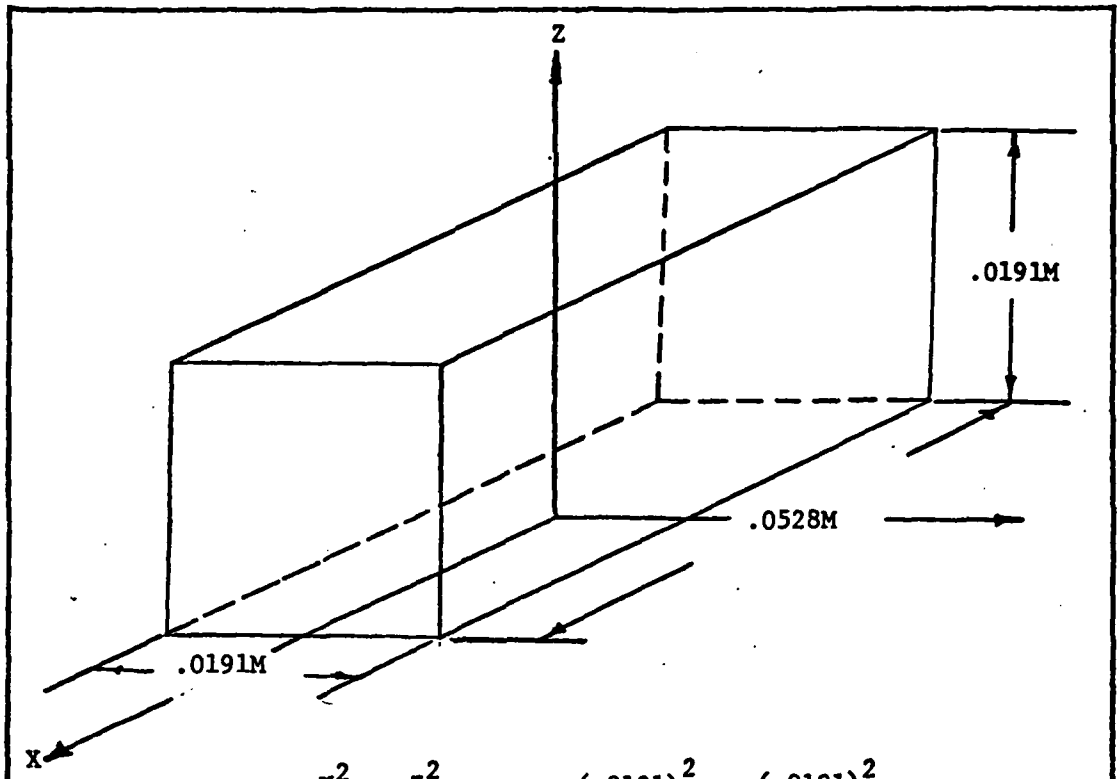

$$I_x = M_o \left(\frac{Y^2}{12} + \frac{Z^2}{3}\right) = .052\left(\frac{(.0191)^2}{12} + \frac{(.0191)^2}{3}\right)$$

$$= 7.904 \times 10^{-6}$$

$$I_y = M_o \left(\frac{X^2}{12} + \frac{Z^2}{3}\right) = .052 \left(\frac{(.0528)^2}{12} + \frac{(.0191)^2}{3}\right.$$

$$= 1.840 \times 10^{-5}$$

$$R_x = \sqrt{\frac{I_x}{M_o}} = \left(\frac{7.904 \times 10^{-6}}{.052}\right)^{\frac{1}{2}} = .0123$$

$$R_y = \sqrt{\frac{I_y}{M_o}} = \left(\frac{1.840 \times 10^{-5}}{.052}\right)^{\frac{1}{2}} = .0188$$

Fig. E-3 Sample Radii of Gyration Calculation

Appendix F

Recommended Future Test Procedures

Appendix F

Recommended Testing Procedures

There are two test methods that would lend themselves well to a study seeking to determine both the accuracy of the algorithm in predicting loaded natural frequencies, and the mass loaded forced response. The choice of methods is largely the user's, but will also be dependent upon the capabilities of the data processing unit, as the second method covered here requires knowledge of a very new procedure.

Procedure 1

This one is a very classical approach, but supplies the exact information required, and is simple to set up and use. The test specimen could be configured as desired and as fine a grid as is judged necessary must be laid out on the panel surface. Then, with accelerometers in the proper locations, the panel is excited by striking it with a hammer at a single point. The inputs to the HP 5451B (which is capable of performing all necessary data processing), are the amplified output of one of the accelerometers, and the amplified output of a force gauge which is attached to the hammer. This must be carried out for each point at which data is desired. The fourier analyzer would have computed and stored the input force power spectrum, the output response power spectrum (from which can be found natural frequency and mode shape data), and the system transfer function for each point. This is all the data required for computation of the forced response.

Procedure 2

This method is just a repeat of Test Method 1 described in Chapter III. The set up can be exactly the same and the input force can again be a broadband random force input. What allows one to now use such a method and avoid the problems described earlier, is a new data processing procedure called Overlap Processing, (Ref. 15). It removes the limitation on total recorded data time, and on the length of the time window over which each transform is taken. Each frequency response function is computed by taking many overlapping transforms and averaging them all to yield the desired result. In such a manner sufficient time may be allowed that the response signal to a given excitation can decay away to zero. Also, sufficient numbers of the input and output spectrum can always be computed to allow adequate reduction of system statistical fluctuation, through ensemble averaging. It should be noted here that this technique is new, that AFFDL did not learn of it until approximately two weeks prior to this writing, and it still had not been implemented at the time of this writing.

Vita

Larry Blake Glenesk was born on 10 December 1953 in Winnipeg, Manitoba, Canada to Sydney B. and A. Lorraine Glenesk. After graduating from Vincent Massey High School in 1971, he entered Royal Roads Military College (RRMC) in Victoria, British Columbia. He graduated from RRMC in 1973, and went on to the Royal Military College (RMC) in Kingston, Ontario. He graduated from RMC in 1975 with a degree of Bachelor of Science in Electrical Engineering, and a commission in the Canadian Armed Forces. After graduating from the Canadian Forces School of Aerospace and Ordinance Engineering at CFB Borden with a certificate in Aerospace Engineering, he was assigned a tour of duty at 408 Tactical Helicopter Squadron at CFB Edmonton, as the Squadron Aircraft Maintenance and Engineering Officer. Capt. Glenesk was assigned to the United States Air Force Institute of Technology in June 1978 in the Graduate Aeronautical Engineering Program.

Mailing Address: P. O. Box 1678
Medley, Alberta
TOA 2MO
Canada

UNCLASSIFIED

SECURITY CLASSIFICATION OF THIS PAGE *(When Data Entered)*

REPORT DOCUMENTATION PAGE		READ INSTRUCTIONS BEFORE COMPLETING FORM
1. REPORT NUMBER AFIT/GAE/AA/79-5	2. GOVT ACCESSION NO.	3. RECIPIENT'S CATALOG NUMBER
4. TITLE *(and Subtitle)* The Prediction of Mass Loaded Natural Frequencies and Forced Response of Complex Structures		5. TYPE OF REPORT & PERIOD COVERED MS Thesis 6. PERFORMING ORG. REPORT NUMBER
7. AUTHOR*(s)*		8. CONTRACT OR GRANT NUMBER*(s)*
9. PERFORMING ORGANIZATION NAME AND ADDRESS Air Force Institute of Technology (AFIT-EN) Wright-Patterson AFB, Ohio 45433		10. PROGRAM ELEMENT, PROJECT, TASK AREA & WORK UNIT NUMBERS
11. CONTROLLING OFFICE NAME AND ADDRESS		12. REPORT DATE December 1979 13. NUMBER OF PAGES 136
14. MONITORING AGENCY NAME & ADDRESS*(if different from Controlling Office)*		15. SECURITY CLASS. *(of this report)* Unclassified 15a. DECLASSIFICATION/DOWNGRADING SCHEDULE

16. DISTRIBUTION STATEMENT *(of this Report)*

Approved for public release; distribution unlimited

17. DISTRIBUTION STATEMENT *(of the abstract entered in Block 20, if different from Report)*

18. SUPPLEMENTARY NOTES

Approved for public release; IAW AFR 190-17

Joseph P. Hipps, Major, USAF
Director of Information

19. KEY WORDS *(Continue on reverse side if necessary and identify by block number)*

Complex Structure
Modification by Mass Loading
Modal Analysis
Natural Frequency Prediction
Forced Response Prediction

20. ABSTRACT *(Continue on reverse side if necessary and identify by block number)*

An experimental investigation was conducted to determine the validity of an algorithm developed by Whaley (Ref 14) to approximate the natural frequencies of a complex structure under arbitrary mass loading conditions, when only the unloaded natural frequency and mode shape data is known. The chosen test specimen was a curved, rib-stiffened panel from a C-141 Starlifter, aircraft. The panel was suspended from the ceiling by bungy cords and tested in an unloaded configuration and nine separate mass loaded configurations. Then using only unloaded data the generalized mass and generalized stiffness for each mass loaded configuration

DD FORM 1 JAN 73 1473 EDITION OF 1 NOV 65 IS OBSOLETE

UNCLASSIFIED

SECURITY CLASSIFICATION OF THIS PAGE *(When Data Entered)*

Block 20 (cont)

were computed, and the natural frequencies for each configuration were computationally predicted using the aforementioned algorithm. The theoretical and experimental results were then compared to determine the amount of error incurred in the approximation technique. The theory of how to ultimately determine the overall forced response of the specimen was discussed and an error model was developed to enable an examination of the reliability of the algorithm in predicting forced response. Recommendations concerning future test procedures, areas requiring further study, and the use of the algorithm were made.